ESC-TR-99-058

Technical Report
1061

EO-1 Advanced Land Imager Modulation Transfer Functions

D.R. Hearn

NMP 00661

22 March 2000

MIT LINCOLN LABORATORY
COPY 0028
G18D143154G

Lincoln Laboratory
MASSACHUSETTS INSTITUTE OF TECHNOLOGY
LEXINGTON, MASSACHUSETTS

Prepared for the National Aeronautics and Space Administration under Air Force Contract F19628-95-C-0002.

Distribution authorized to U.S. Government agencies and their contractors; test and evaluation, 7 March 2000. Other requests for this document shall be referred to NASA/GSFC, Greenbelt, MD 20771.

This report is based on studies performed at Lincoln Laboratory, a center for research operated by Massachusetts Institute of Technology. This work was sponsored by NASA under Air Force Contract F19628-95-C-0002.

This report may be reproduced to satisfy needs of U.S. Government agencies.

This technical report has been reviewed and is approved for publication.

FOR THE COMMANDER

Gary Tutungian
Administrative Contracting Officer
Plans and Programs Directorate
Contracted Support Management

Non-Lincoln Recipients

PLEASE DO NOT RETURN

Permission has been granted by the Contracting Officer to destory this document, when it is no longer required by the using agency, according to applicable security regulations.

MASSACHUSETTS INSTITUTE OF TECHNOLOGY
LINCOLN LABORATORY

EO-1 ADVANCED LAND IMAGER MODULATION TRANSFER FUNCTIONS

D.R. HEARN
Group 99

TECHNICAL REPORT 1061

22 MARCH 2000

Distribution authorized to U.S. Government agencies and their contracts; test and evaluation, 7 March 2000. Other requests for this document shall be referred to NASA/GSFC, Greenbelt, MD 20771.

LEXINGTON MASSACHUSETTS

ABSTRACT

This report presents results of laboratory calibrations of the EO-1 Advanced Land Imager (ALI) instrument. Specifically, it is concerned with the estimated spatial modulation transfer function, or MTF. A combination of design data for the detectors, measurements on the optical subsystem, and laboratory measurements of the complete instrument are used to construct a model of the system spatial transfer function (STF) of the ALI. The optical subsystem measurements, done by the telescope builder, SSG, consisted of interferograms, which they analyzed with Zernike polynomials. Those polynomials were used to model the optical transfer function. The system measurements were scans of a knife-edge, viewed through an imaging collimator. The parameters of the STF model, in particular focus error and carrier diffusion in the detectors, were adjusted to obtain the best agreement with the system measurements. The full, two-dimensional STFs for the ten spectral bands of the instrument are presented.

TABLE OF CONTENTS

1 INTRODUCTION 1
2 KNIFE-EDGE SCANS PERFORMED 3
3 DATA PROCESSING 5
3.1 Pre-processing 5
3.2 Full data analysis 5
3.3 Typical MTF scan and analysis 6
3.4 Equipment defects and artifacts 6
4 MTF MODEL 9
4.1 Optical MTF 9
4.1.1 ALI telescope 9
4.1.2 Collimator 10
4.1.3 Mirror scatter 10
4.2 Detector MTF 11
4.3 Scan motion MTF 15
4.4 Uncertainties in the model 15
4.4.1 Focus error 15
4.4.2 Collimator aberrations & alignment 15
4.4.3 Collimator ghosts 15
4.4.4 Scattered light effects 16
5 NUMERICAL RESULTS 17
5.1 Wavefront error of the ALI 17
5.2 Panchromatic MTF 20
5.3 Multispectral MTFs 26
5.4 Point-spread functions 32
6 REFERENCES 39
APPENDIX A 41
APPENDIX B 53

LIST OF ILLUSTRATIONS

Figure No.		Page
1	Edge-spread functions of SCA2, Band 4 in the cross-track direction.	7
2	Average line-spread function derived from the data shown in Figure 1.	7
3	Normalized transfer functions derived from the data shown in Figure 1.	8
4	Average normalized transfer function derived from the data shown in Figure 1.	8
5	ALI focus figure of merit vs. Z Offset.	10
6	Modulation transfer function of the Pan detectors.	12
7	Point-spread function of the Pan detectors.	12
8	Modulation transfer function of the VNIR multispectral detectors.	13
9	Point-spread function of the VNIR multispectral detectors.	13
10	Modulation transfer function of the SWIR multispectral detectors.	14
11	Point-spread function of the SWIR multispectral detectors.	14
12	Surface plot of the wavefront error near the middle of the MS/Pan array.	17
13	Contour plots of the wavefront error at the centers of the Pan arrays.	18
14	Optical point-spread function of the Pan band.	19
15	Optical transfer function of the Pan band (real part).	19
16	Measured and modeled Average MTFs for the Pan band	20
17	Measured and modeled MTF for the Pan band, SCA 1, pixel 480.	21
18	Measured and modeled MTF for the Pan band, SCA 2, pixel 1440.	21
19	Measured and modeled MTF for the Pan band, SCA 3, pixel 2400.	22
20	Measured and modeled MTF for the Pan band, SCA 4, pixel 3360.	22
21	System MTF of the Panchromatic band near the center of the detector array.	23
22	System PSF of the Panchromatic band near the center of the detector array.	24
23	System PSF of the Panchromatic band near the center of the detector array.	25
24	System PSF of the Panchromatic band near the center of the detector array.	25
25	Measured and modeled Average MTFs for band 1'.	26
26	Measured and modeled Average MTFs for band 1.	27
27	Measured and modeled Average MTFs for band 2.	27
28	Measured and modeled Average MTFs for band 3.	28
29	Measured and modeled Average MTFs for band 4.	28
30	Measured and modeled Average MTFs for band 4'.	29
31	Measured and modeled Average MTFs for band 5'.	29
32	Measured and modeled Average MTFs for band 5.	30

LIST OF TABLES

Table No.		Page
A-1	Spatial Transfer Function of the Panchromatic Band	42
A-2	Spatial Transfer Function of Band 1'	43
A-3	Spatial Transfer Function of Band 1	44
A-4	Spatial Transfer Function of Band 2	45
A-5	Spatial Transfer Function of Band 3	46
A-6	Spatial Transfer Function of Band 4	47
A-7	Spatial Transfer Function of Band 4'	48
A-8	Spatial Transfer Function of Band 5'	49
A-9	Spatial Transfer Function of Band 5	50
A-10	Spatial Transfer Function of Band 7	51
B-1	Measurement Positions in the Focal Plane	53
B-2	Zernike Polynomial Definitions	54
B-3	Estimated Zernike Polynomial Coefficients	55

1 INTRODUCTION

The Advanced Land Imager (ALI) is the primary instrument on the Earth Observing-1 (EO-1) spacecraft of the NASA New Millennium program. A general description of the ALI has been given by Bicknell, et al.[1] For an overview of the instrument's calibration, see Lencioni, et al.[2] The spatial response of the ALI instrument was calibrated in the laboratory during the period July to December, 1998, prior to its integration with the spacecraft. Hearn, Mendenhall, and Willard[3] described techniques used for those calibrations. This document presents the final results for the calibrations of the Modulation Transfer Function (MTF). In the following sections, the measurements made in the laboratory are first summarized, then the steps in processing and analyzing those measurements are outlined. Details of the MTF model developed for the instrument are then presented. Finally, results for the various bands are shown graphically. Numerical values of the MTFs are presented in Appendix A.

Spatial response is fully characterized by a spatial transfer function (STF). The full STF of the instrument is a two-dimensional complex function, which depends on the wavelength band, and to a lesser degree, on the position within the field of view. The STF is the Fourier transform of the point-spread function (PSF). The modulation transfer function is normally defined as the magnitude of the STF, a real, non-negative quantity. An additional phase transfer function (PTF) is then required to describe the spatial response completely.

In the ALI, as in most good imaging instruments, the PSF is essentially symmetrical. As a result, the imaginary part of the STF (Im(STF)) is very small, compared to the real part (Re(STF)). The conventional MTF then looks like the absolute value of Re(STF). For simplicity, we prefer to work with the STF, rather than the MTF and a PTF which goes through sudden swings of 180° where Re(STF) changes sign. We have habitually called the STF the "complex MTF," or simply the MTF while working on the ALI calibration. In the rest of this document, the terms have been used interchangeably. The reader should simply be aware that we are not following the conventional terminology.

2 KNIFE-EDGE SCANS PERFORMED

The approach we used to measure the MTFs of the ALI was to project the image of a knife-edge into the instrument, and scan the edge slowly across a selected set of detectors while the instrument records the image data at its nominal rates. The knife-edge was physically located at the focus of a collimator and the scan was performed by translating its support stage slowly in the plane of best focus. For each pixel in the set, the detected signal vs. time, after normalization, yields an edge-spread function (ESF). Differentiation of the ESF gives the line-spread function (LSF). Fourier transformation of the LSF results in the STF, or complex MTF, along one axis.

All measurements reported here were made while the instrument was in a thermal vacuum chamber, at its normal operating temperatures. For each of the four sensor chip assemblies (SCAs), the knife-edge was scanned across a set of pixels near the middle of that SCA, for each band. Scans were performed in both the cross-track and in-track directions of the instrument by using two sides of the 9 mm open square in a negative "USAF 1951" target as our knife-edges. (The rest of the target was covered by black plastic.) When switching from one SCA to the next, the instrument was re-positioned on an azimuthal rotation stage in the vacuum chamber in order to scan each SCA with the knife-edge within ~0.5° of the collimator axis.

The knife-edge was moved at 200 μm/s, which translates to 127.4μm/s at the ALI focal plane. The frame rates were 226 s^{-1} for the multispectral (MS) bands, and 678 s^{-1} for the panchromatic (Pan) band. The spatial sampling intervals were 0.564 μm and 0.188 μm for the MS and Pan bands, respectively, or approximately 70 samples per pixel width in all cases.

The recorded data files contained 10, 20, or 30 seconds of data each, from the entire focal plane. As many as six of the MS bands could be scanned at once in the cross-track direction. No more than three bands could be scanned in one pass in the in-track direction. Approximately four dozen scan data files were ultimately recorded, once the measurement system was deemed to be working correctly.

3 DATA PROCESSING

Analysis of the data from the knife-edge scans proceeded in several steps. While the scans were being performed in the thermal vacuum chamber in the clean room, a portion of the data was analyzed and graphically displayed on a monitor next to the control computer. This Quick-Look analysis was a necessary check that the equipment was set up and working properly. The data files were stored on the hard drives of a Silicon Graphics R-10000 workstation (called the Performance Assessment Machine (PAM)), and periodically backed up on DLT cartridges.

3.1 PRE-PROCESSING

After all of the knife-edge scan files were recorded, preliminary processing was done on the PAM. A program was run to de-scramble the raw data ("mandescram," written in C). Next, running under IDL♦, the "get_knife_scan" procedure read the full MS or Pan data file and wrote a much more compact file (*.kes)†, containing only the data from the SCA and bands of that particular scan.

For convenience, further analysis under IDL was performed after copying the *.kes files to a 180 MHz Power Macintosh. (It was found to be just as fast as the PAM for running IDL procedures, since its clock rate is the same. It simply lacked the massive storage capability of the PAM.)

The next step was to analyze the signal from each detector to derive its edge-spread function. A sigmoid curve (hyperbolic tangent) was fitted to each pixel's ESF, in order to resample the ESFs to co-align all of the edge-crossing times. In the process, automatic selection criteria were applied to reject pixels that had data artifacts or incomplete scans. An intermediate file (*.kes.fit) was written to facilitate the further processing steps. All of these steps were performed by IDL procedure "MTF_process1.pro"

3.2 FULL DATA ANALYSIS

To transform the ESFs to MTFs, another procedure ("MTF_process8.pro") was developed to read the *.kes and *.kes.fit files, then derive the LSF and MTF functions from them. For each SCA and band combination, the complex MTF was computed on a pixel-by-pixel basis, then the mean and standard deviation was derived. These are written to an IDL data file (*.mtf) for further reference, and plots are generated to display the results of each step in the analysis.

Finally, for each band the complex MTFs for the individual SCAs are averaged and plotted together, along with a curve representing the MTF model. Again, the results are written to an IDL data file.

♦ Interactive Data Language, from Research Systems, Inc., 4990 Pearl East Circle, Boulder, CO 80301, (see www.rsinc.com).

† In this context, * represents a "wildcard," substituting for the root name of the data file.

3.3 TYPICAL MTF SCAN AND ANALYSIS

A typical page of plots generated in the analysis of one scan file is shown in Figures 1 to 4. In all plots of this sort, the independent variable is spatial position at the focal plane (in μm) or frequency in image space (in cycles/mm). These are convertible to object space by dividing or multiplying by the ALI focal length (0.946 m) to obtain units of microradians or cycles/mrad, respectively.

3.4 EQUIPMENT DEFECTS AND ARTIFACTS

Not all of the scans produced data as clean as that seen in Figures 1 to 4. Artifacts were sometimes seen in the data, particularly from in-track scans, wherein the knife-edge moved vertically. They included occasional jitter, with amplitude on the order of a micrometer, and apparent errors in translation speed. It was later discovered that the vertical Newport slide was not properly adjusted. Fortunately, there is enough redundancy in the set of scans performed that those that have obvious artifacts could simply be omitted from the MTF averages.

There are two "leaky" pixels among the 11,520 MS pixels. Their signals are cross-coupled to all of the other pixels in the same row of their particular SCA. Fortunately, they affect only the even- or odd-numbered pixels of that band/SCA combination. It was an easy matter to exclude the contaminated pixels from the MTF analyses.

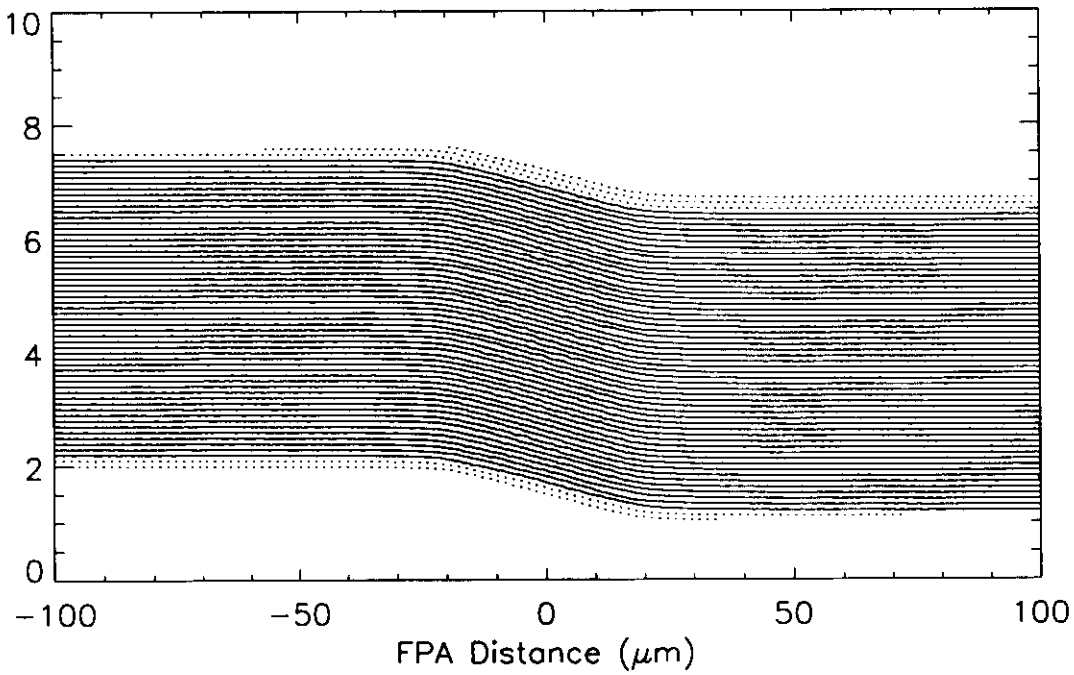

Figure 1. Edge-spread functions of SCA2, Band 4 pixels scanned in the cross-track direction, from file no. 16638. Pixels not used in further analysis are shown with dotted lines.

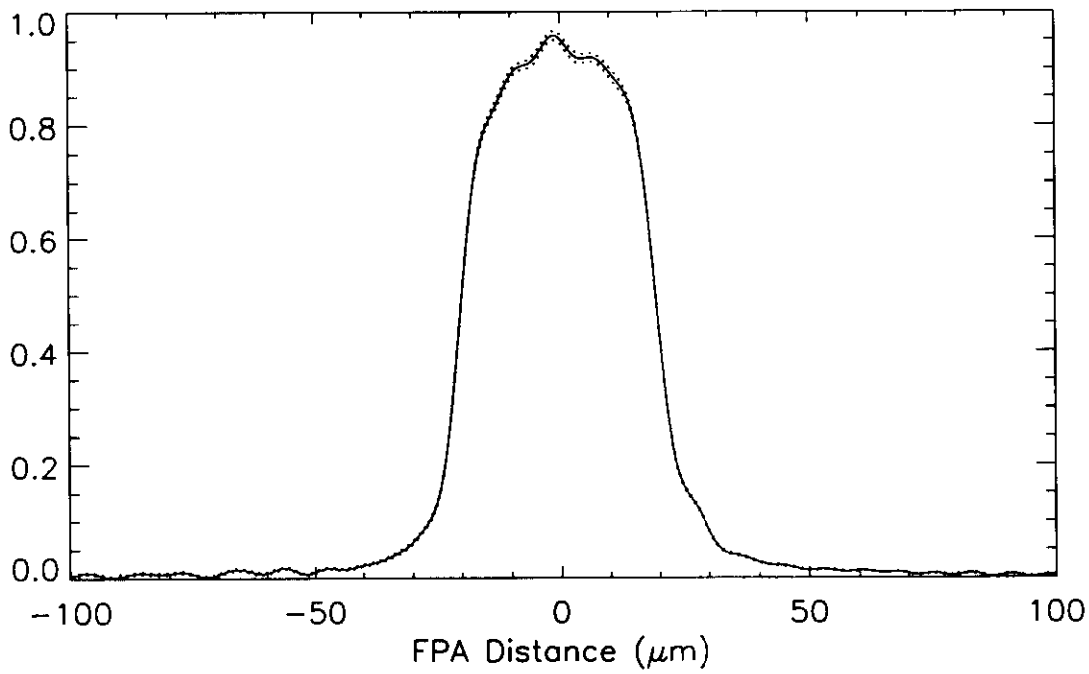

Figure 2. Average line-spread function derived from the data shown in Figure 1. The dotted lines are one standard deviation above and below the mean.

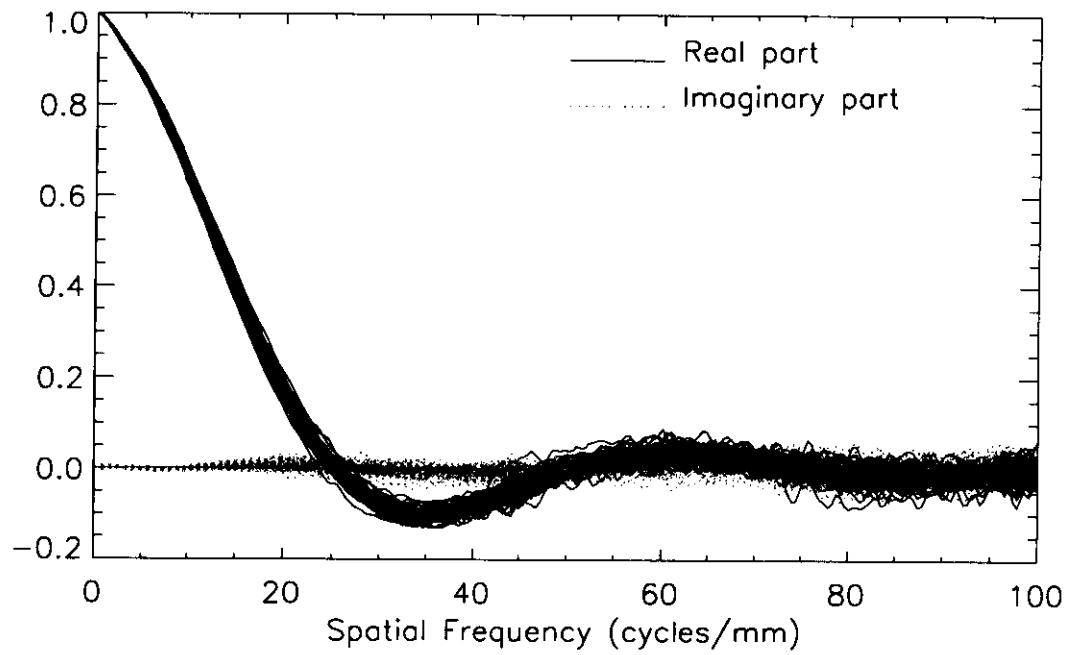

Figure 3. Normalized transfer functions derived from the data shown in Figure 1.

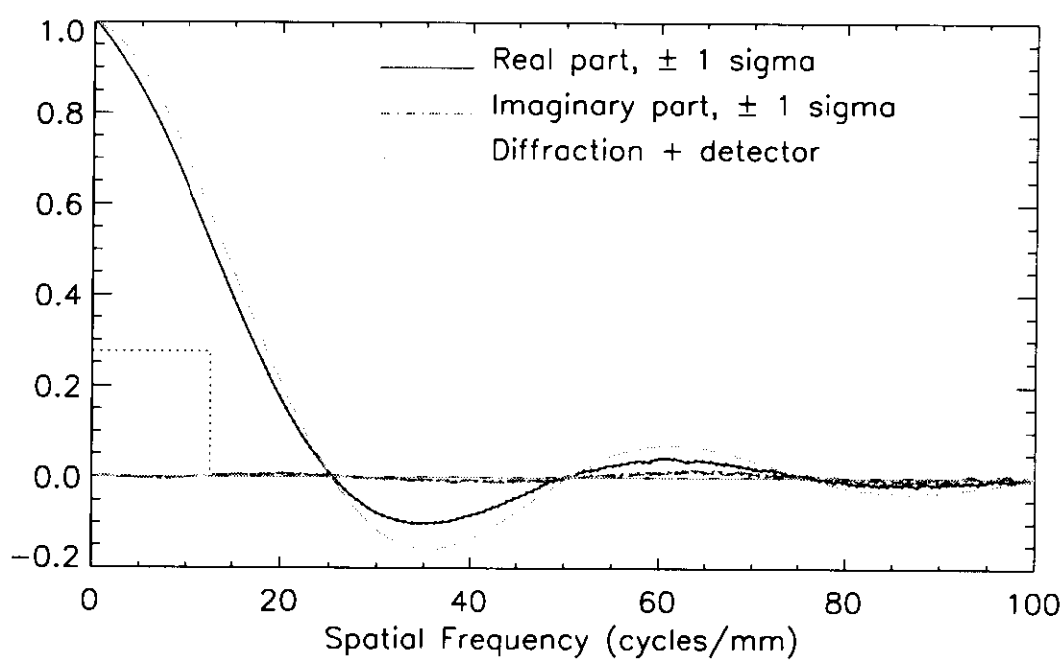

Figure 4. Average normalized transfer function derived from the data shown in Figure 1. The dotted lines are one standard deviation above and below the mean. The curve labeled "Diffraction + detector" is computed from the simplest model of diffraction by a circular aperture and a sharp-edged detector response. The specified MTF at the Nyquist frequency is indicated with dotted lines.

4 MTF MODEL

Our goal is to describe the MTF of the instrument with a model which contains only enough parameters to fit the measurement data within the experimental uncertainties, and which will enable other investigators to compute the MTF for their own needs. It is important to have a model for the MTF, since the knife-edge scan measurements can only produce one-dimensional cross-sections of the MTF, which is a two-dimensional function. The following subsections describe the various factors which, when multiplied together, yield the system MTF of the ALI instrument. These are the optical system MTF, the detector MTF, and the MTF of the scan motion of the instrument as it collects images on orbit. Uncertainties in the model are summarized at the end of this section.

4.1 OPTICAL MTF

The optical MTF estimated from our laboratory measurements results from the combined optical transfer functions (OTFs) of the ALI telescope and the collimator. It is modified by the effects of light scattering from the imperfect surfaces of the ALI mirrors.

4.1.1 ALI telescope

The OTF of an optical system can be obtained from the autocorrelation of the total wavefront error (WFE) over the pupil of the system. SSG, Inc., the builder of the ALI optical system, has used a laser unequal-path interferometer (LUPI) to characterize the WFE of the ALI. They obtained interferograms at a dozen points distributed over the 1.26°x15° field of view of the optical system. The interferograms were referenced to a fixture representing the focal plane. The WFE derived from each interferogram was fitted with a set of 37 Zernike polynomials. The resulting coefficients encapsulate the WFE estimate. The first three Zernike polynomials, representing piston, tip, and tilt, are set to zero. The fourth coefficient represents a focus error.

We use the Zernike coefficients from SSG to obtain an interpolated set of coefficients for any given point within the MS/Pan array of the ALI. Since the focal plane fixture used by SSG was not at the correct focus of the system, the focus terms have to be modified to represent the position of the ALI focal plane array (FPA) after final shimming. Three parameters, consisting of the axial shift (piston), and two tilt angles control this correction.

To ascertain the amount of focus error in the integrated system, MTF scans were performed with varying amounts of defocus applied at the collimator, as described in Reference 1. The figure of merit (FoM) chosen to test the defocus was the integral of the MTF from zero to the detector sampling frequency of the FPA. A plot of this FoM as a function of the axial displacement of the knife-edge from the collimator focus is shown in Figure 5. The plot also shows a parabola fitted to the highest values, to derive the focus error. These results indicate that the ALI FPA, at operating temperature, is approximately 75±20 μm away from the optimum focus position. This does not seriously degrade the optical resolution, but must be taken into account when modeling the system MTF.

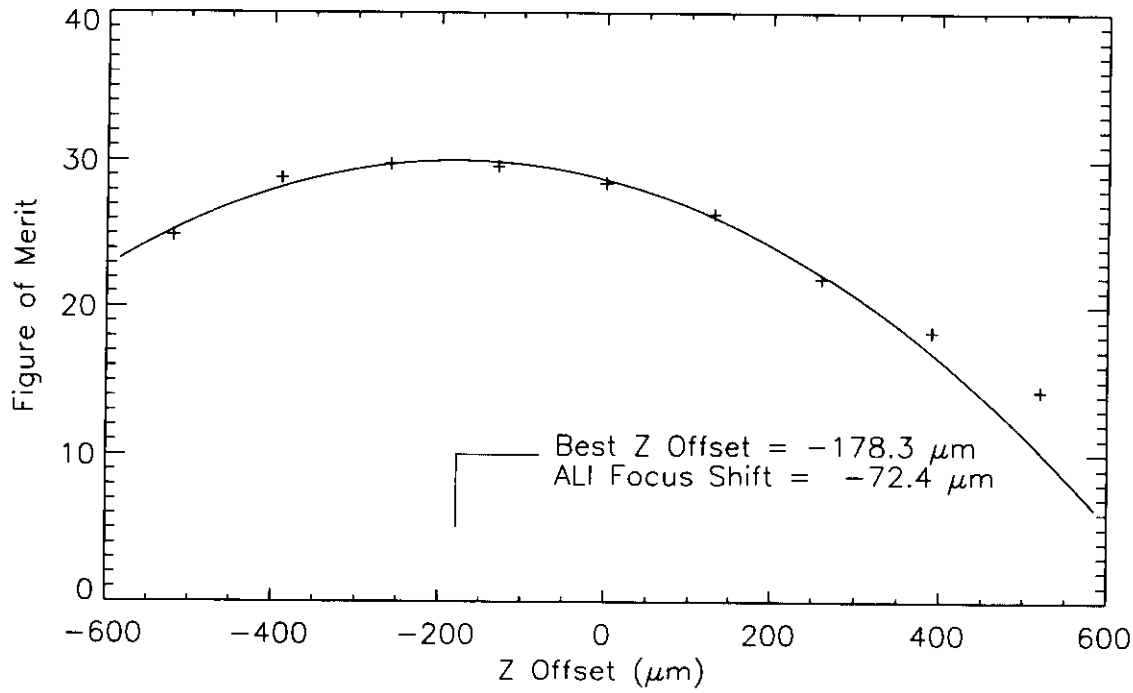

Figure 5. ALI focus figure of merit vs. axial displacement of the knife-edge from the collimator focus (Z Offset). Data symbols represent individual MTF scans. The curve is a parabola fitted to the points within 500 μm of the peak.

4.1.2 Collimator

Wavefront error introduced by the collimator should be added to the WFE of the ALI optics before the PSF or MTF is calculated. The collimator, and the methods used to set it to best focus, are described in a paper by Willard.[4] The spherical aberration of the collimator is calculated to be 0.007 μm rms, when the collimator and ALI pupils are correctly aligned. The remaining rms WFE, caused mainly by the beamsplitter, is approximately 0.032 μm. Though the spherical aberration is easily evaluated, we lack a full description of the collimator WFE.

4.1.3 Mirror scatter

Microscopic roughness of the surfaces of some of the ALI mirrors produces a large-angle scatter of a fraction of the incident light.[5] The MTF of this scattered light is a very narrow peak around zero spatial frequency. The total optical MTF is the sum of this narrow scattering peak and the specularly-reflected, normal MTF. The fractional division between the scattered and specular light varies inversely with the fourth power of the wavelength. Our MTF model includes a parameter to allow for this scattering MTF. It is adjusted to match the MTF measurements, though since the knife-edge scans cover a limited angular range, they are not sufficient to determine the fullest extent of the scattering. Scattering accounts for ~5% of the light at the shortest ALI wavelengths (band 1', 433-453 nm).

4.2 DETECTOR MTF

The spatial response of the detectors was initially modeled as unity within a defining rectangular mask (39.6 μm x 40 μm for the MS pixels, and 13.2 μm square for the Pan pixels), and zero outside of that area. The corresponding pixel MTF is a product of two sinc functions:

$$MTF_{PIX}(f_x, f_y) = \mathrm{sinc}(wf_x)\,\mathrm{sinc}(hf_y)$$

where w and h are the width and height of the detector mask, respectively, and (f_x, f_y) are the components of the spatial frequency.

Measured values of the ALI system MTF tended to decrease approximately linearly, in comparison with the system MTF computed using this simple detector model, after adjustment of the free optical parameters. Good fits between measured and modeled MTFs are only obtained when a *carrier diffusion MTF* is included in the model[6]:

$$MTF_{DET} = MTF_{PIX} \cdot MTF_{CD} \quad ,$$

$$MTF_{CD} = \exp\left(-\left|f/f_0\right|^g\right) \quad ,$$

$$f^2 = f_x^{\,2} + f_y^{\,2} \quad ,$$

where f_0 and g are constants.

The VNIR detectors (bands 1' through 4' and Pan) are Si PIN photodiodes, formed within the readout circuit (ROIC). Good MTF fits were obtained with $g = 1$, $f_0 = 200 \pm 50$ cycles/mm, and the nominal geometric size of the mask regions. Thus the spatial response of the VNIR detectors is a convolution of the nominal mask rectangle with a Lorentzian function having a full width at half-maximum (FWHM) of approximately 0.8 μm.

The HgCdTe SWIR detectors (bands 5', 5, and 7) are on a chip bump-bonded to the ROIC. Best MTF fits were obtained in this case with $g = 1.5$, $f_0 = 35$ cycles/mm, and the geometric size reduced to 36.8 μm square.

A plot of the two-dimensional MTF of the Pan detectors is shown in Figure 6. Figure 7 shows the Pan detector spatial response (point-spread function). The corresponding MTF and PSF for the VNIR and SWIR multispectral detectors appear in Figures 8 through 11.

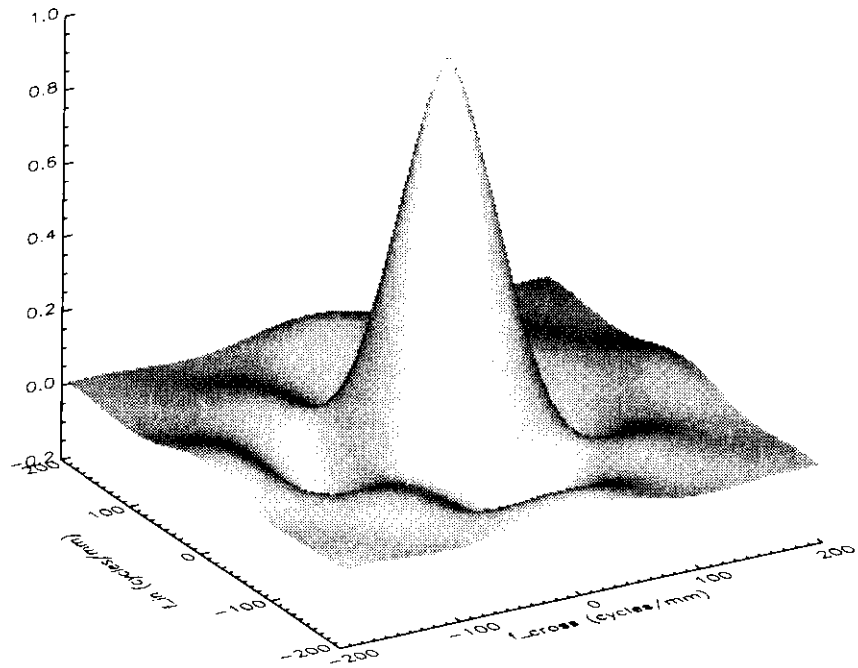

Figure 6. Modulation transfer function of the Pan detectors.

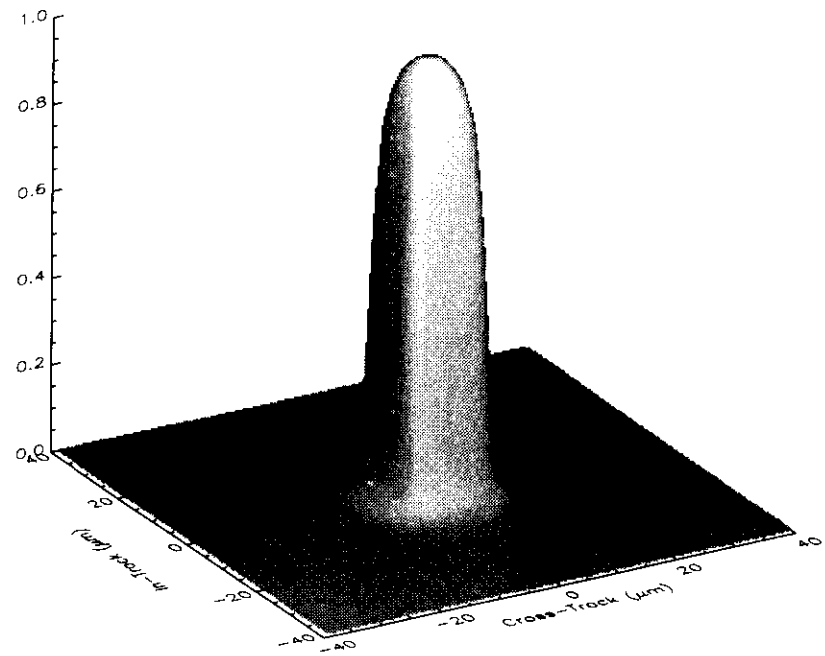

Figure 7. Point-spread function of the Pan detectors.

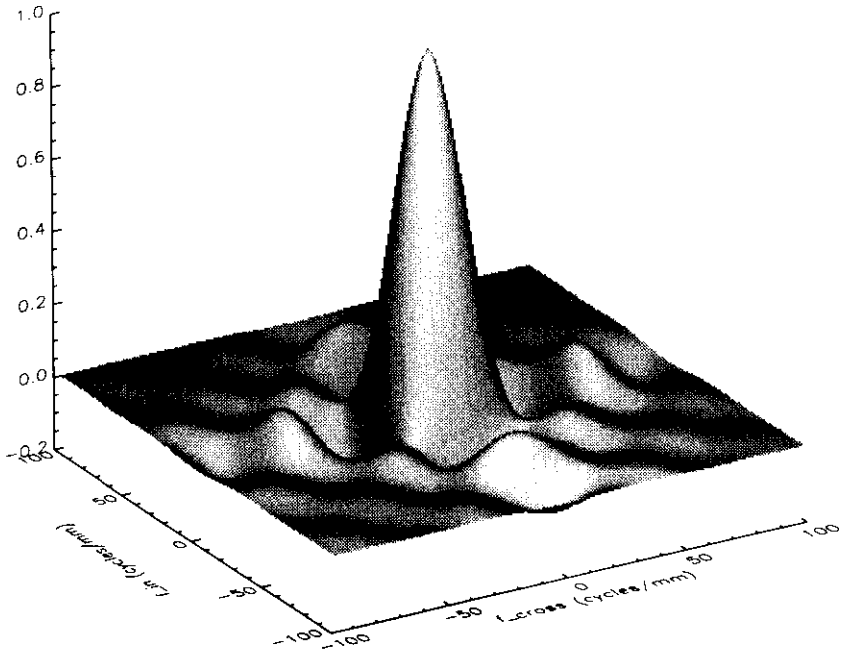

Figure 8. Modulation transfer function of the VNIR multispectral detectors.

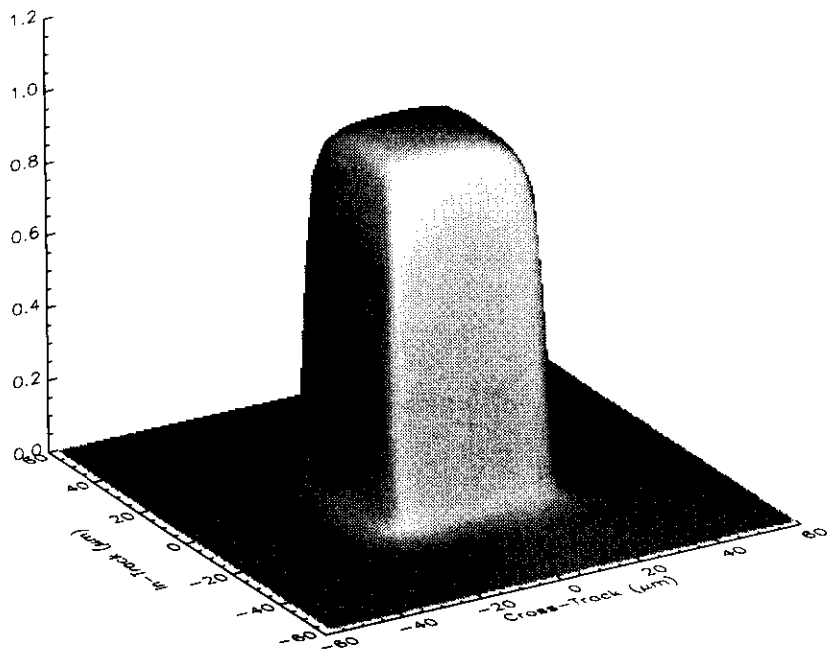

Figure 9. Point-spread function of the VNIR multispectral detectors.

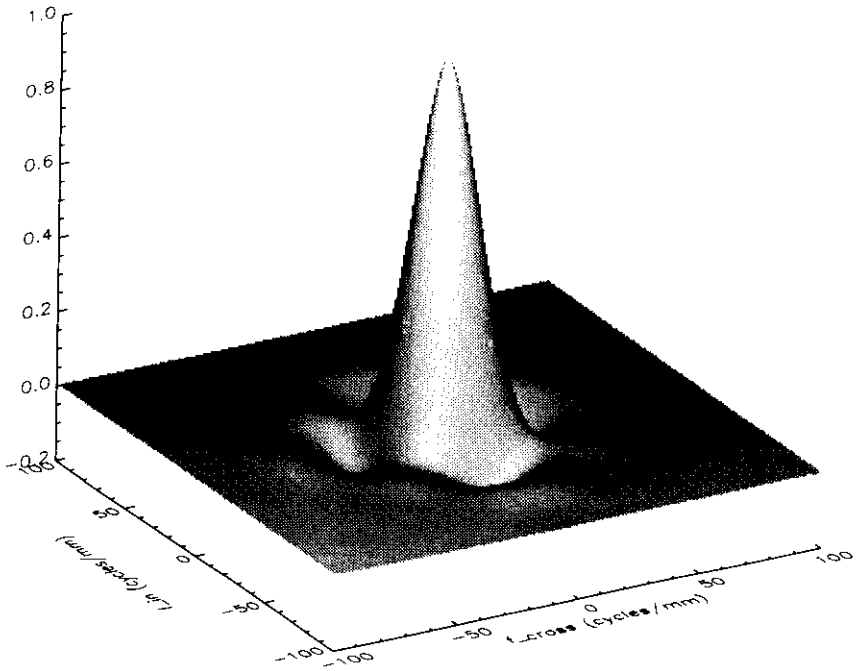

Figure 10. Modulation transfer function of the SWIR multispectral detectors.

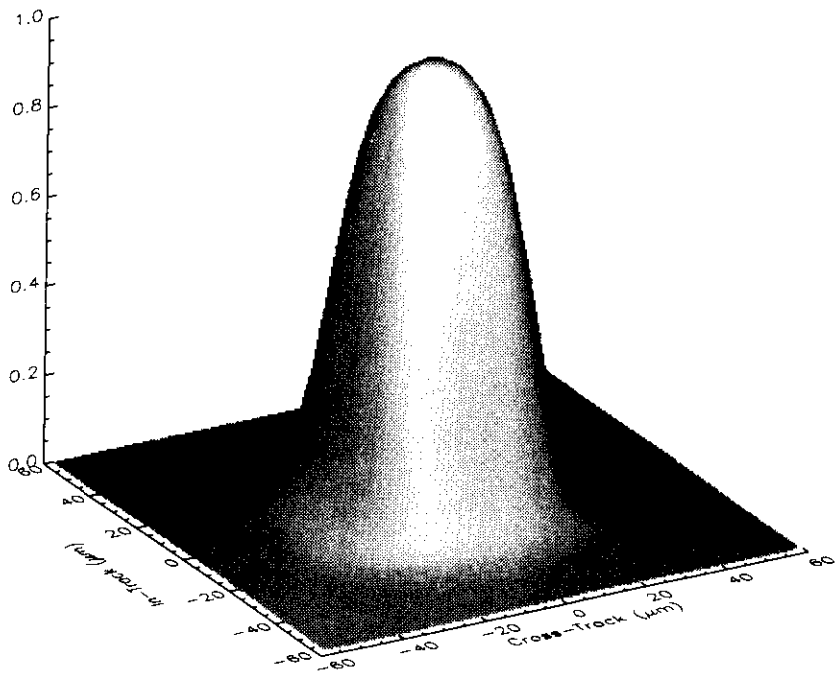

Figure 11. Point-spread function of the SWIR multispectral detectors.

4.3 SCAN MOTION MTF

Motion of the satellite as it collects image data in push-broom mode causes a slight smearing of the image in the in-track direction. The geometric footprint of each pixel on the ground is convolved with a vector representing the motion of the view axis during the integration time of a single frame. The MTF of this motion is another sinc function in the in-track direction only:

$$MTF_{INT} = \mathrm{sinc}(\alpha v) \quad ,$$

where v is the angular frequency and α is the angle subtended by the ground motion vector.

The nominal ground speed of the sub-satellite point is 6.75 km/s. The nominal integration times are 4 ms and 1.33 ms for the MS and Pan bands, respectively. (Alternative integration times can be set by ground command.) The nominal motions during integration are thus 27.0 and 8.9 meters, respectively. At the EO-1 altitude of 705 km, the corresponding values of α are 38.28 and 12.76 μrad.

4.4 UNCERTAINTIES IN THE MODEL

The differences between the modeled MTF and the measured MTF may be attributable to a number of causes. In this section, we mention several areas of uncertainty remaining in the MTF model after we have adjusted it to fit the measurements.

4.4.1 Focus Error

The necessity of setting and measuring the focus of the instrument in a clean room prevents us from testing it directly by observing a distant object. The imaging collimator had to be employed, and the estimated error in setting its focus is 0.145 μm p-v, over the 12.5 cm aperture.

It was necessary to compensate for optical power induced in the vacuum chamber window when the chamber interior was cooled.[7] Typically, the required focus correction was found to change over the course of five hours by 0.008 μm p-v.

The focus error of the ALI was measured for one location on the FPA. An error in cutting the focus shim at the correct wedge angle (if any) would cause a different focus error at other points on the FPA.

4.4.2 Collimator Aberrations and Alignment

We lack a precise description of the random aberrations of the collimator sufficient to reconstruct its actual WFE, as was done for the ALI. Thus those aberrations could not be incorporated in the model which was fitted to the measured MTFs. The spherical aberration of the collimator was included, but it increases rapidly as the collimator exit pupil is moved away from its correct registration with the entrance pupil of the ALI. At the time most of these measurements were performed, the pupil registration was uncertain by ~±5 mm.

4.4.3 Collimator Ghosts

Unwanted reflections at surfaces of the transmissive elements of the collimator give rise to ghost images. The most noticeable of these is caused by light reflected from the back face of the

beamsplitter, instead of its coated, front face. This displaced, out-of-focus ghost has an intensity ~1.2% of the main image. We believe, without doing an exhaustive analysis, that these ghost images did not interfere with images of the knife edge sufficiently to compromise the MTF measurements.

4.4.4 Scattered Light Effects

Scattered light appears to have reduced the main portion of the MTF we measure by as much as a few percent. The sources of this scattering are the ALI mirrors, as mentioned above, and a contamination of the focal plane. The exact magnitude of the scattering fraction as well as the true shape of the scattering MTF at angular frequencies less than ~ 5 cycles/mrad, is somewhat uncertain.

4.4.4.1 Mirrors

The knife-edge scans in the cross-track direction moved the image of the edge approximately 1.2 mm across the focal plane of the ALI. This is not sufficient to delineate fully the effects of wide-angle scattering of the light. Thus the reduction of the specular MTF caused by light scattering at the mirror surfaces was underestimated in our data analysis.

4.4.4.2 Contamination on filters

Following the series of MTF measurements performed during December, 1998, we discovered that an unknown contaminant had gradually accumulated on the top surfaces of the filters which are situated just above the FPA detectors. The contamination was manifested by a spatial modulation of the light from the internal calibration lamps, amounting to several percent. We obtained images of the contaminant by placing a CCD camera at the focus of the collimator and illuminating the FPA of the ALI with flashlights. It had the appearance of condensation on a window in winter. The modulation, or spatial noise, was smaller for the normal *f*/7.5 illumination from external sources. Nevertheless, it is probable that this contaminant caused some amount of wide-angle scattering, which because of its proximity to the detectors, would appear to extend only a few milliradians in angle.

The contaminant left the focal plane when it was warmed above ~-5° C. Upon re-cooling, it reappeared, but not so strongly as before. Evidence of similar contamination was seen during thermal vacuum tests following integration of the ALI with the spacecraft bus. It is not known where the contaminant(s) originates, or whether it will reappear on orbit. Provisions have been made to warm the focal plane periodically on orbit, to outgas it if the contamination does appear. Thus the effects of this scattering on the MTF is not only uncertain by a few percent, but could be variable while on orbit.

5 NUMERICAL RESULTS

5.1 WAVEFRONT ERROR OF THE ALI

Procedures written in IDL are used to construct the ALI WFE from the adjusted set of Zernike coefficients derived from interferograms by SSG. From the WFE, the optical point-spread function (PSF) and MTF of the ALI telescope are obtained, by use of the Fourier transform procedure in IDL.

A surface plot of the WFE near the middle of the MS/Pan array, excluding tip, tilt, and focus, is shown in Figure 12. Contour plots of the WFE at the Pan arrays of SCAs 1 through 4 are shown for comparison in Figure 13. There are small differences caused by the fact that the beam footprint covers different parts of the M1 and M3 mirrors for different points in the field of view.

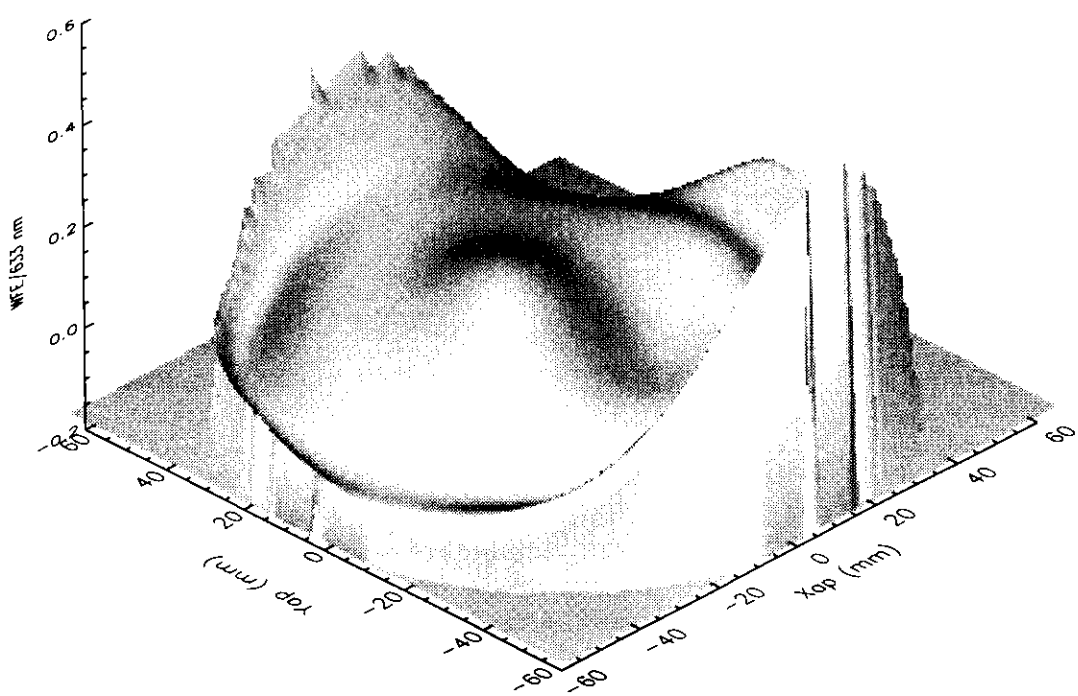

Figure 12. Surface plot of the wavefront error near the middle of the MS/Pan array. The focus term is not included here.

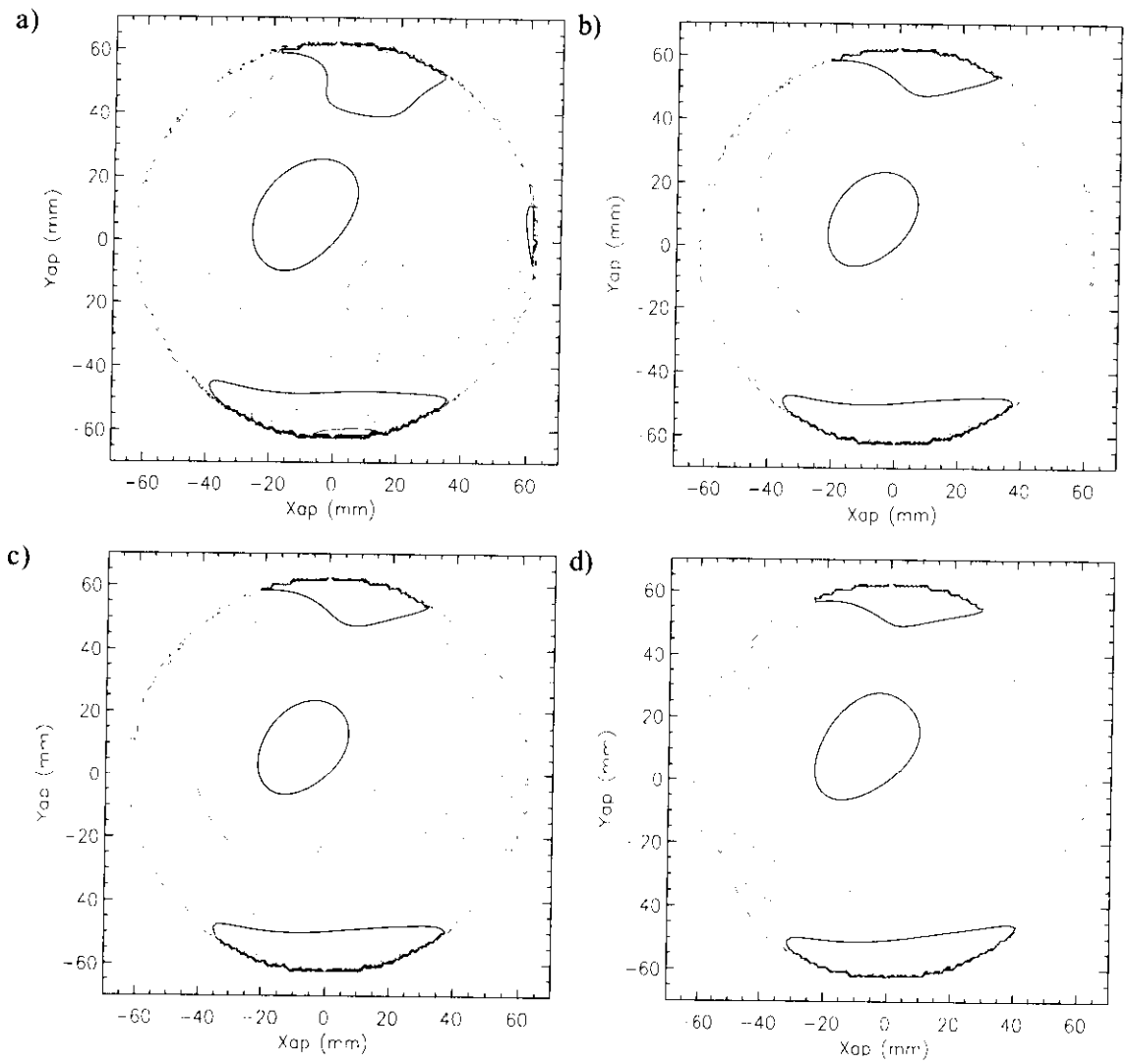

Figure 13. Contour plots of the wavefront error at the centers of the Pan arrays. Plots a), b), c), and d) represent SCAs 1, 2, 3, and 4, respectively. The interval between contours is 63.3 nm (1/10 HeNe wave).

When the modeled MTF was compared to the measured Pan MTFs in the cross-track and in-track directions, an apparent inconsistency was found. Much better fits were obtained by rotating the WFE array by 90°. On consulting SSG, we learned that the orientation of the interferogram data was ambiguous. It was not recorded, because the interferograms were originally taken only for the purpose of obtaining an rms wavefront error and MTF magnitude at a specific frequency. Subsequently, we used the rotated WFE for our MTF model.

The optical point-spread function of the Pan band, computed from the WFE, is shown in Figure 14. The real part of the corresponding OTF is shown in Figure 15.

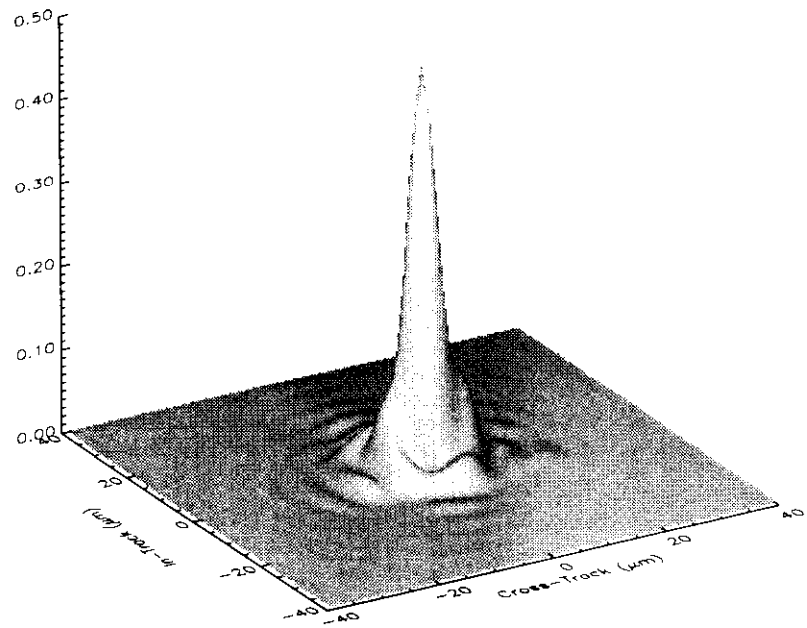

Figure 14. Optical point-spread function of the Pan band, computed from the full wavefront error, including the focus term.

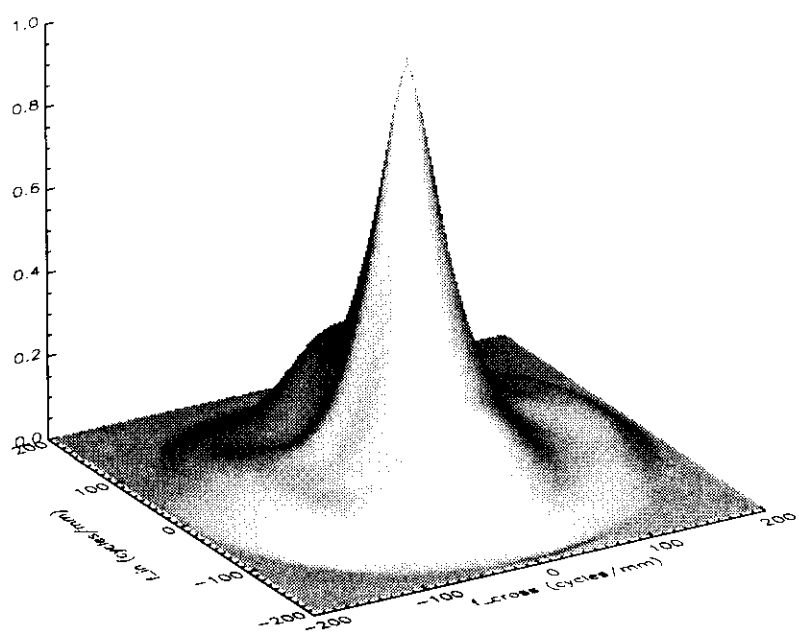

Figure 15. Optical transfer function of the Pan band (real part), computed from the wavefront error, including the focus term.

5.2 PANCHROMATIC MTF

Figure 16 shows the MTF curves derived from scans of the four Pan arrays, along with the average, modeled MTF curve. The measured MTF curves, and corresponding modeled MTF for the four individual SCAs, are plotted in Figures 17 to 20.

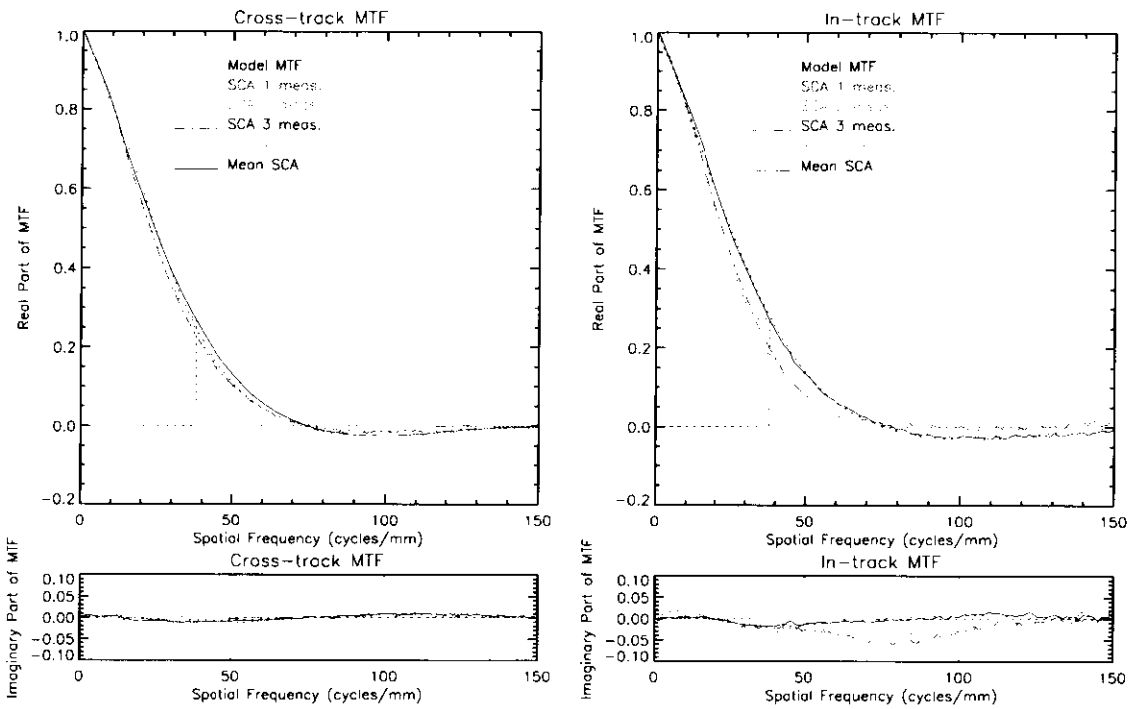

Figure 16. Measured and modeled Average MTFs for the Pan band, and measured MTFs for the individual SCAs.

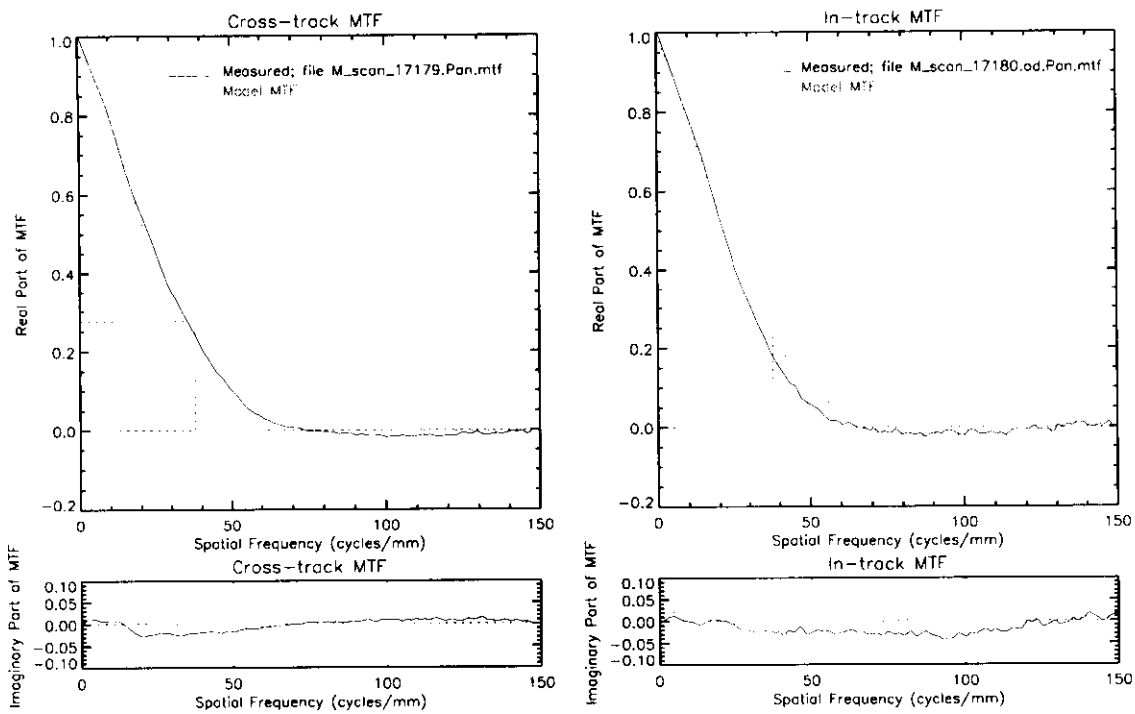

Figure 17. Measured and modeled MTF for the Pan band, SCA 1, pixel 480.

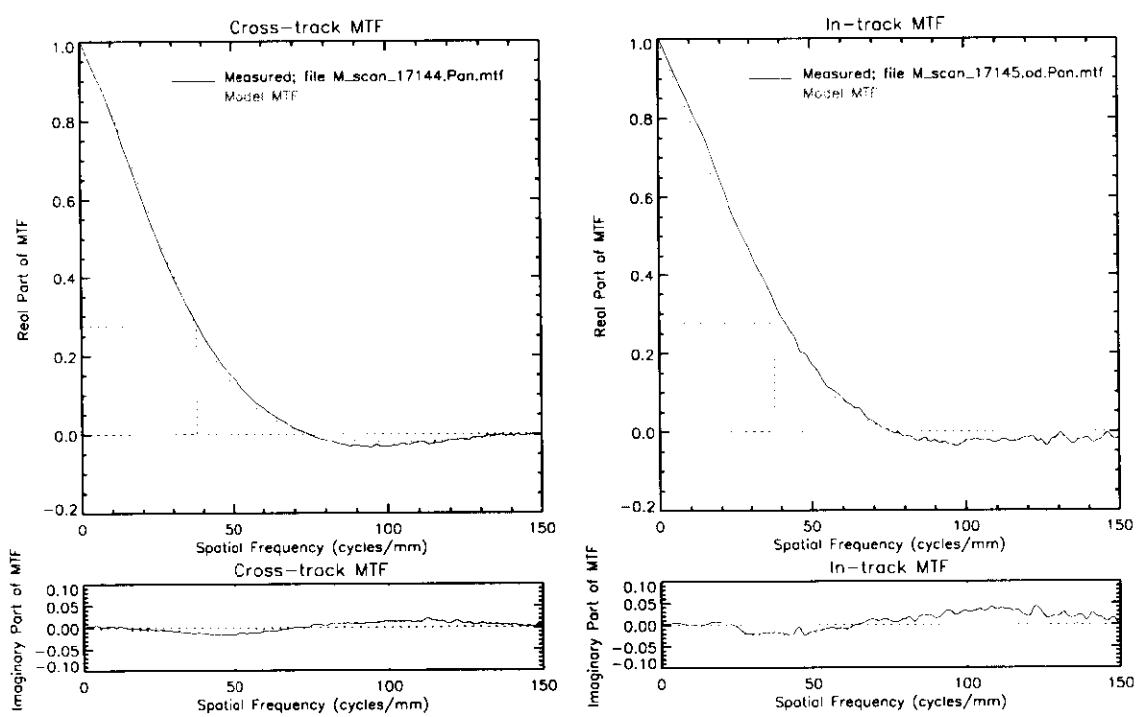

Figure 18. Measured and modeled MTF for the Pan band, SCA 2, pixel 1440.

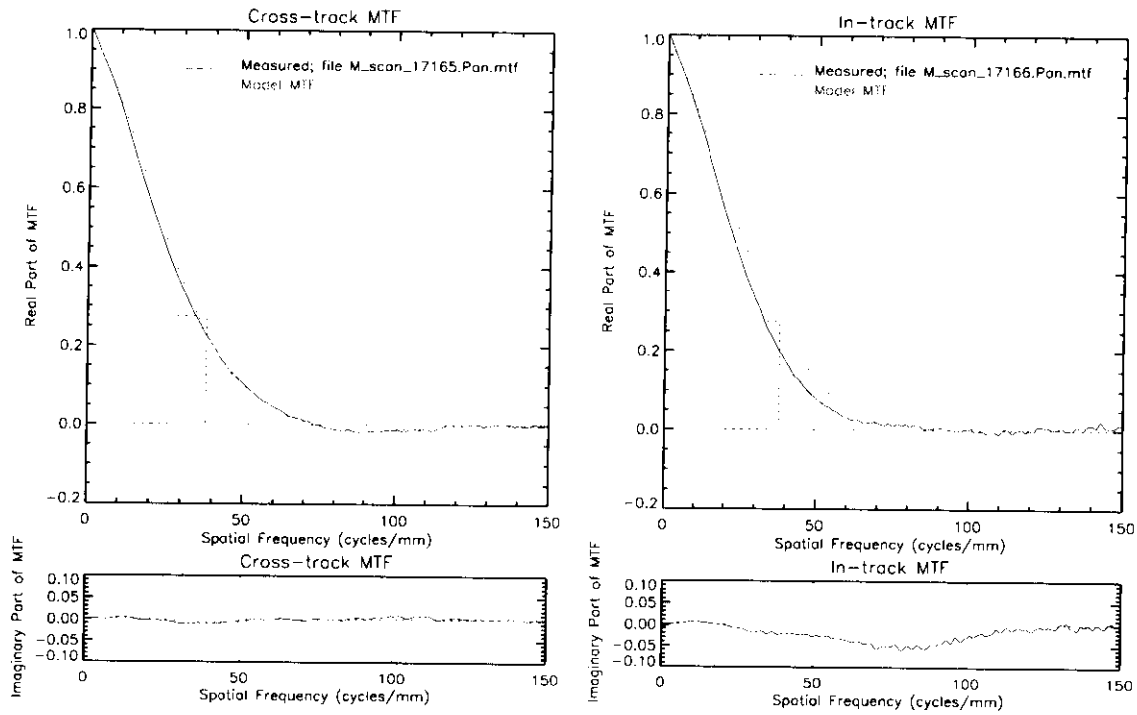

Figure 19. Measured and modeled MTF for the Pan band, SCA 3, pixel 2400.

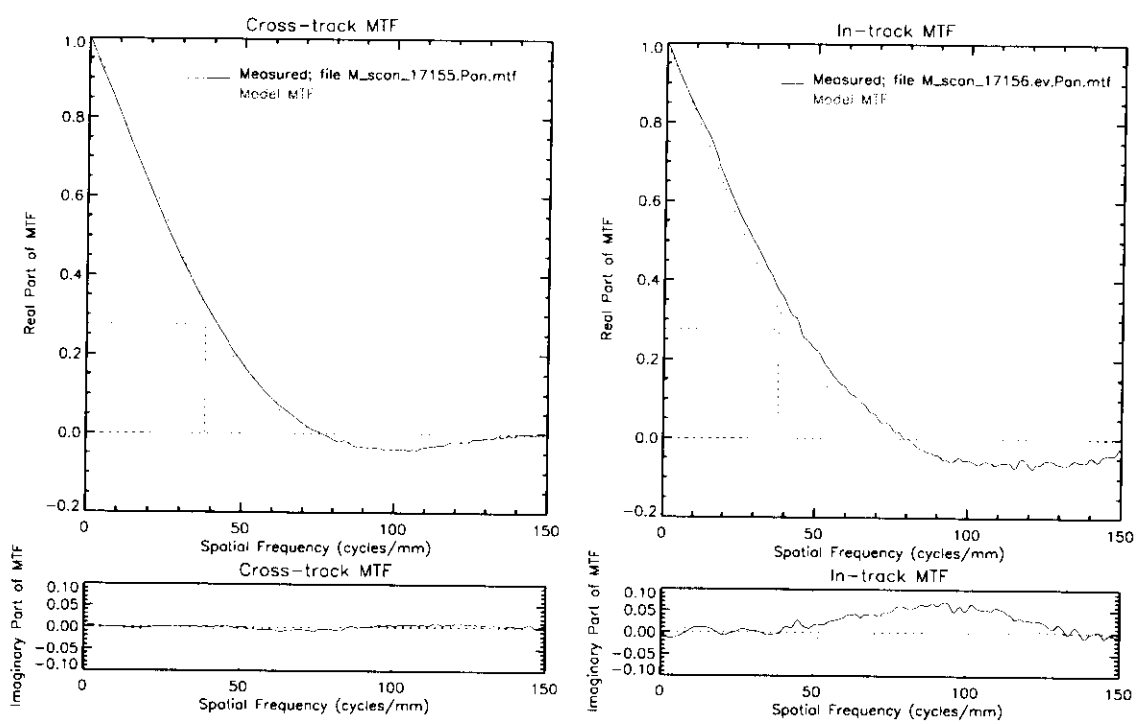

Figure 20. Measured and modeled MTF for the Pan band, SCA 4, pixel 3360.

The real part of the two-dimensional Pan MTF at the center of the array computed from our model is shown in Figure 21. The small imaginary part can be neglected, given the uncertainties in our fitting of the model to the measurements. The real part of the MTF is symmetric in both axes, the imaginary part anti-symmetric. MTF values over one quadrant are tabulated at reduced resolution in Appendix A.

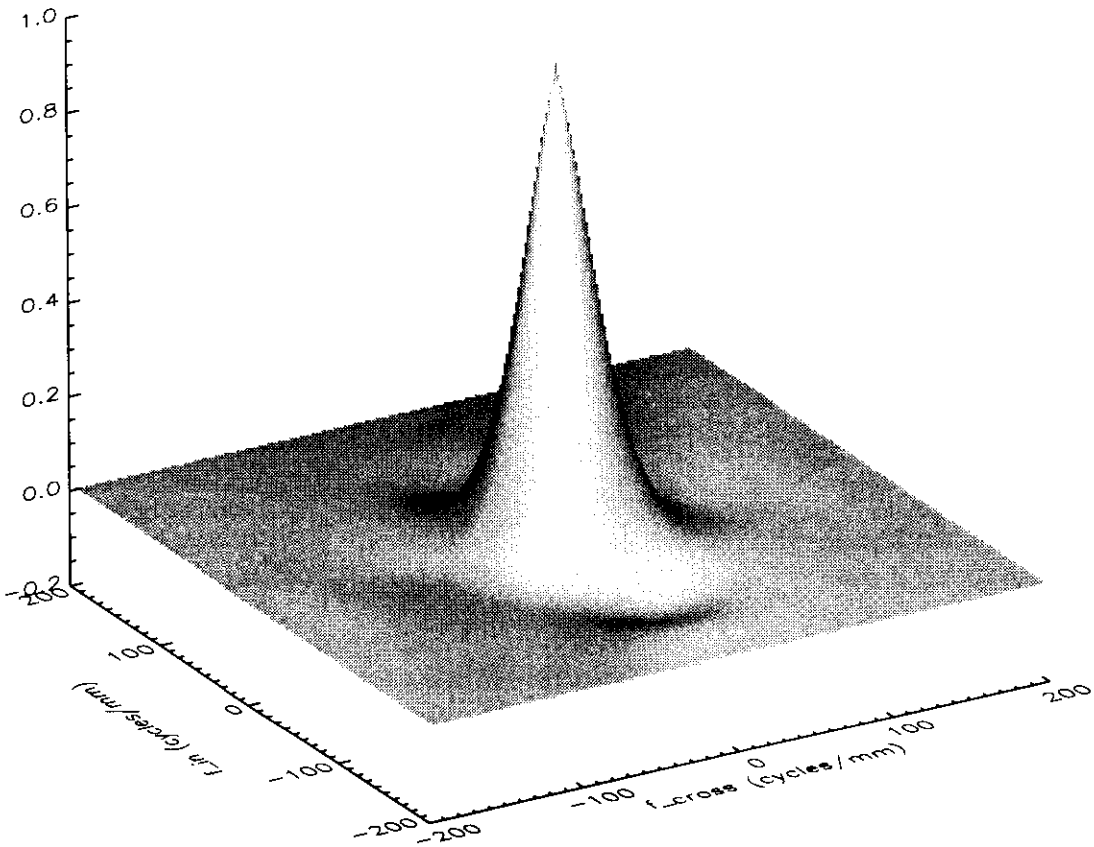

Figure 21. System MTF of the Panchromatic band near the center of the detector array.

Figures 22 to 24 give several representations of the Panchromatic system point-spread function (PSF), not including scan motion spreading.

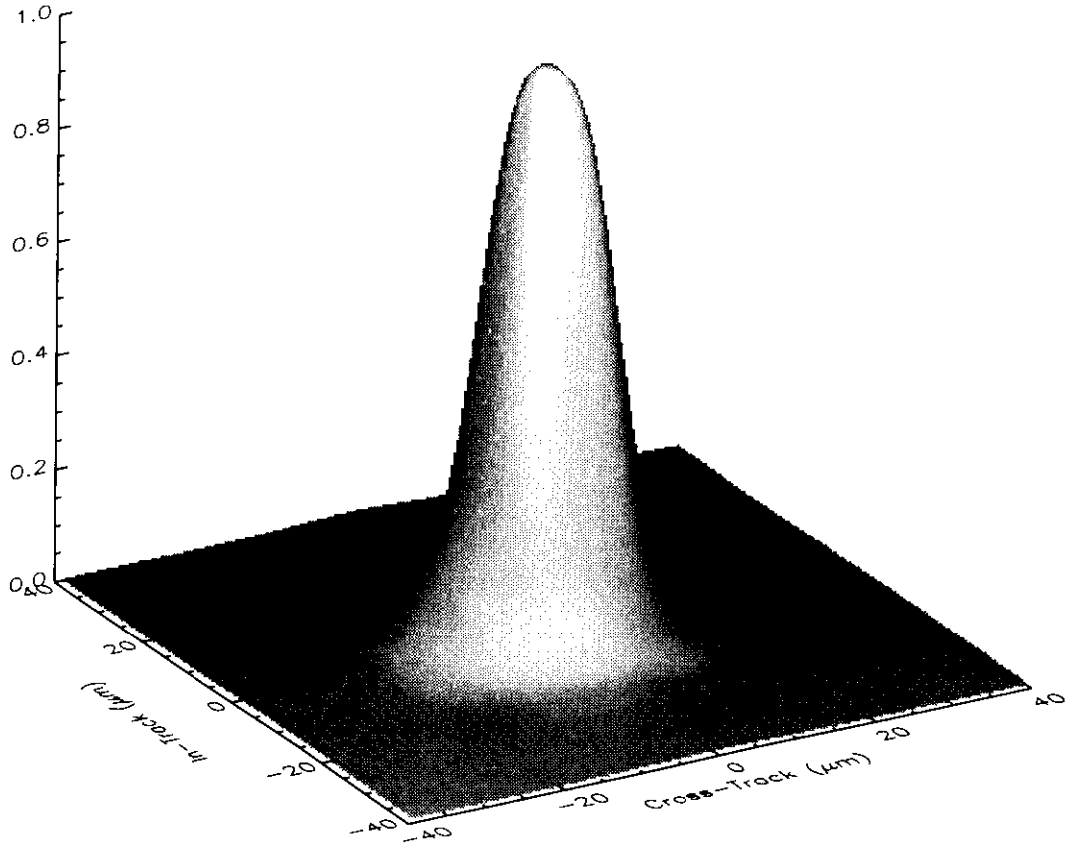

Figure 22. System PSF of the Panchromatic band near the center of the detector array.

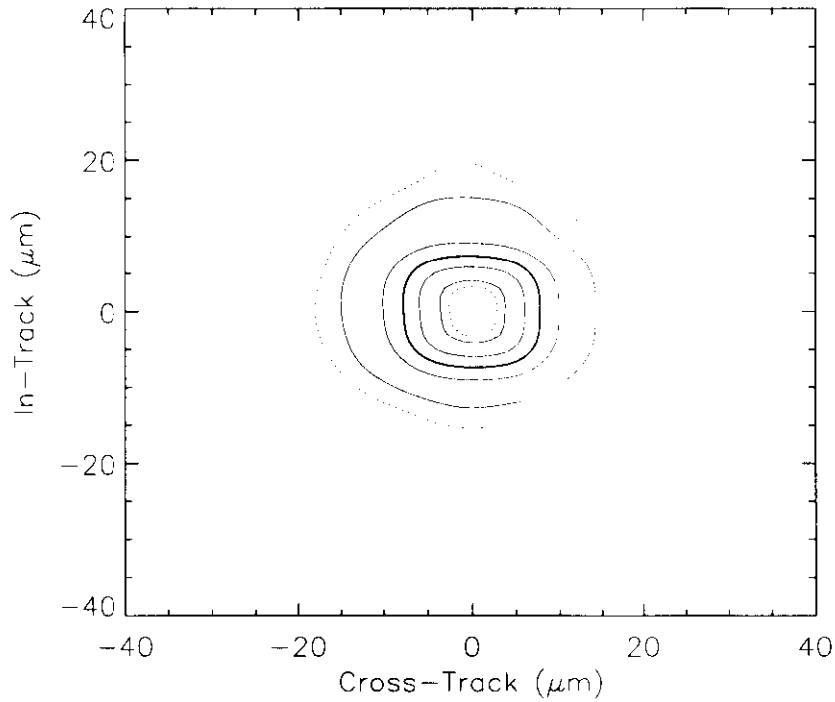

Figure 23. System PSF of the Panchromatic band near the center of the detector array. The contour levels are at 5, 10, 30, 50, 70, 90 and 95% of the peak.

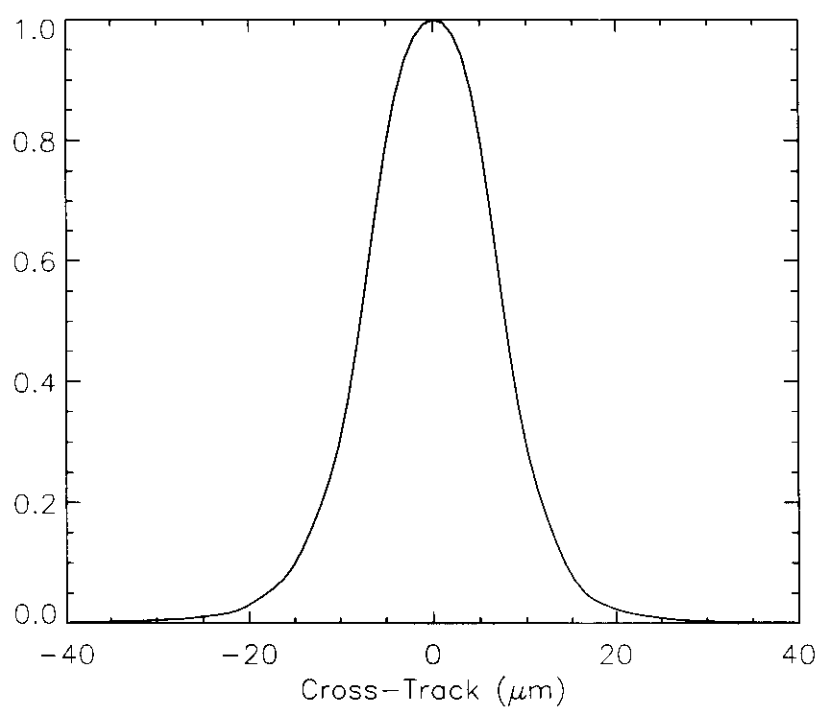

Figure 24. System PSF of the Panchromatic band near the center of the detector array.

5.3 MULTISPECTRAL MTFs

Summary plots, similar to Figure 16, of the MTFs of each of the multispectral bands are shown in Figures 25 to 33. The real part of the two-dimensional average MTFs for bands 1', 4', and 7 are plotted in Figures 34 to 36. Appendix A contains the tabulated values.

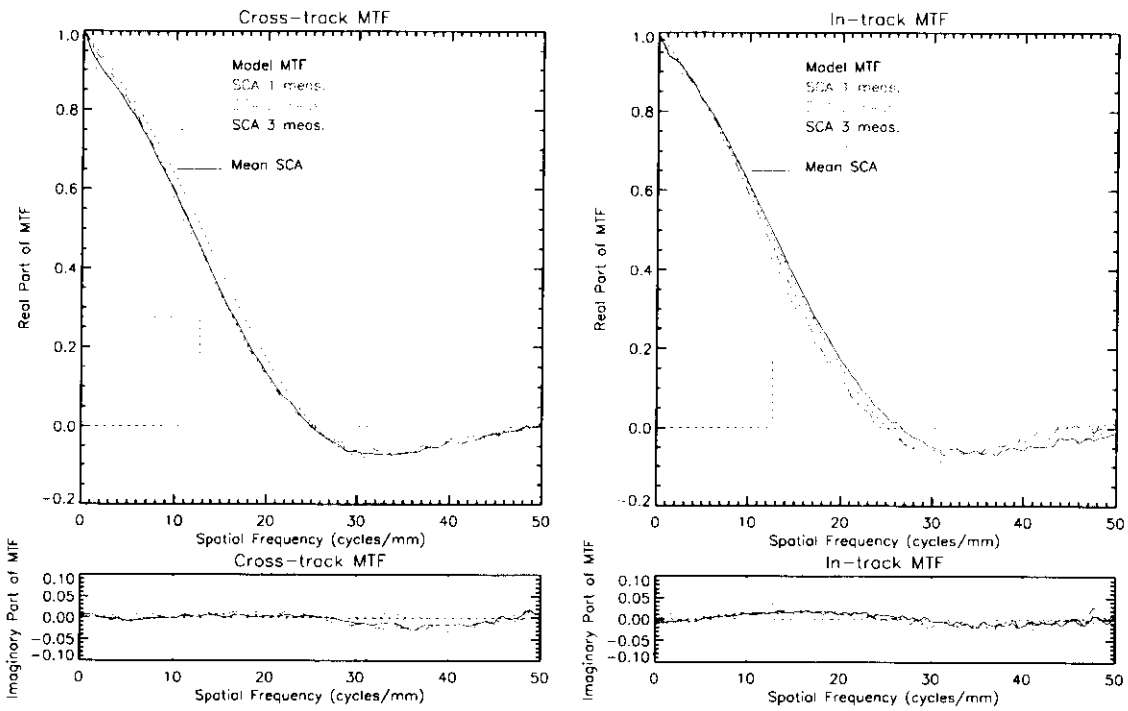

Figure 25. Measured and modeled Average MTFs for band 1', and measured MT's for the individual SCAs.

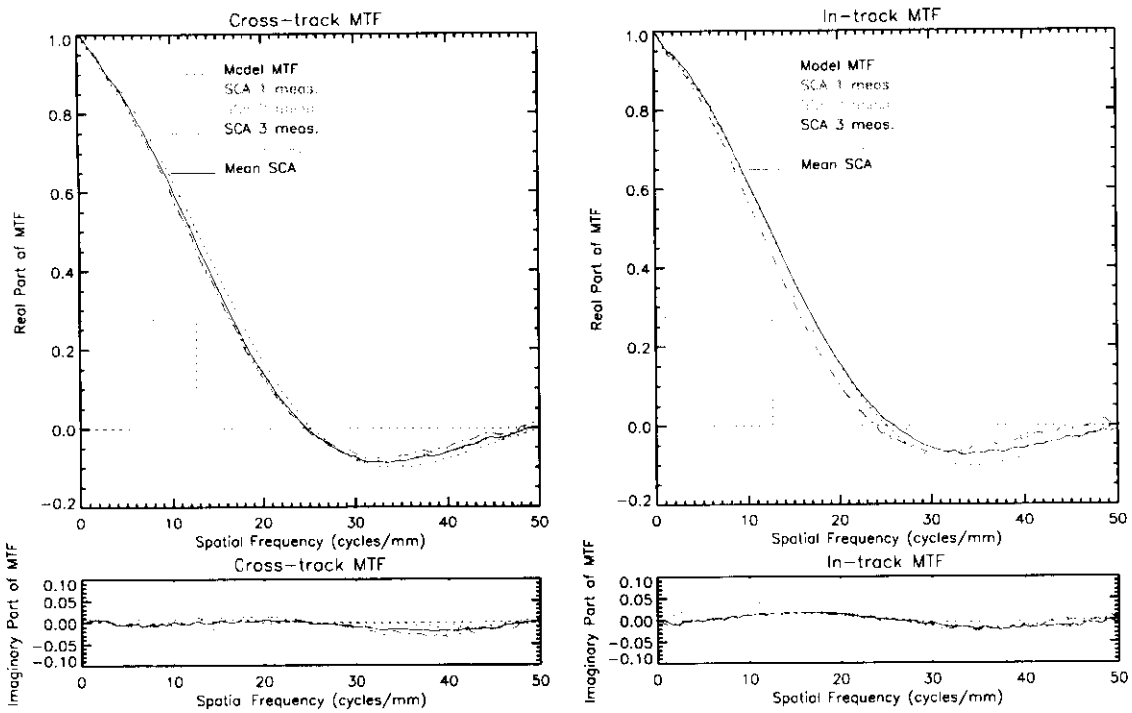

Figure 26. Measured and modeled Average MTFs for band 1, and measured MTFs for the individual SCAs.

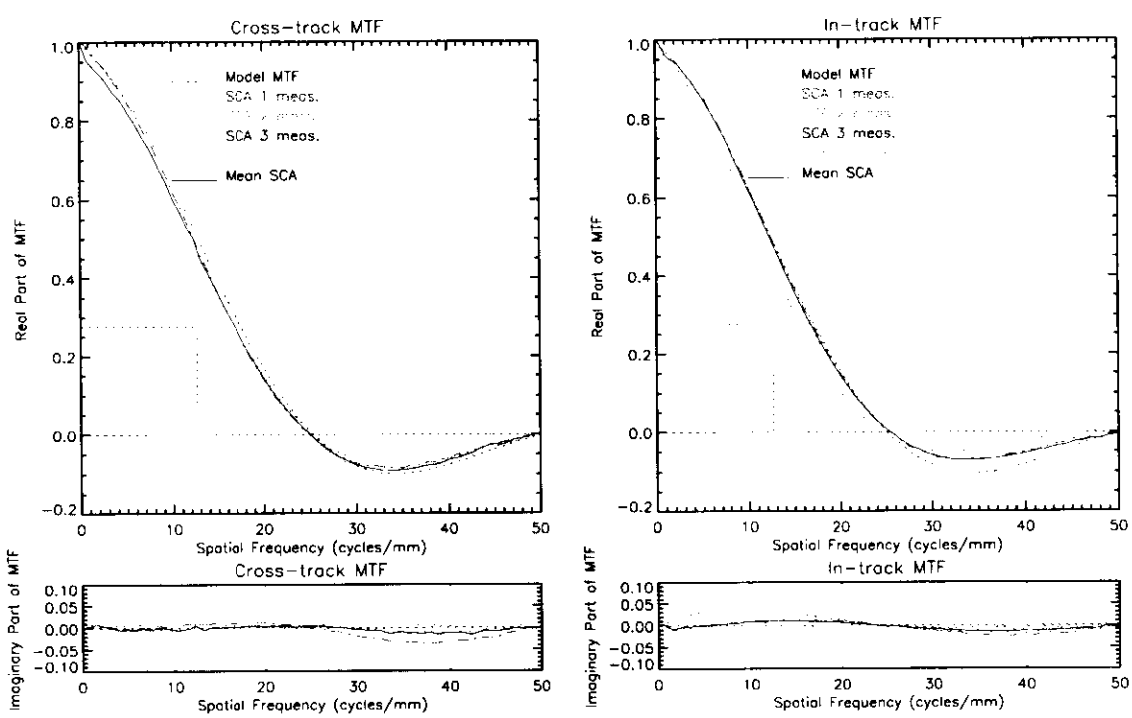

Figure 27. Measured and modeled Average MTFs for band 2, and measured MTFs for the individual SCAs.

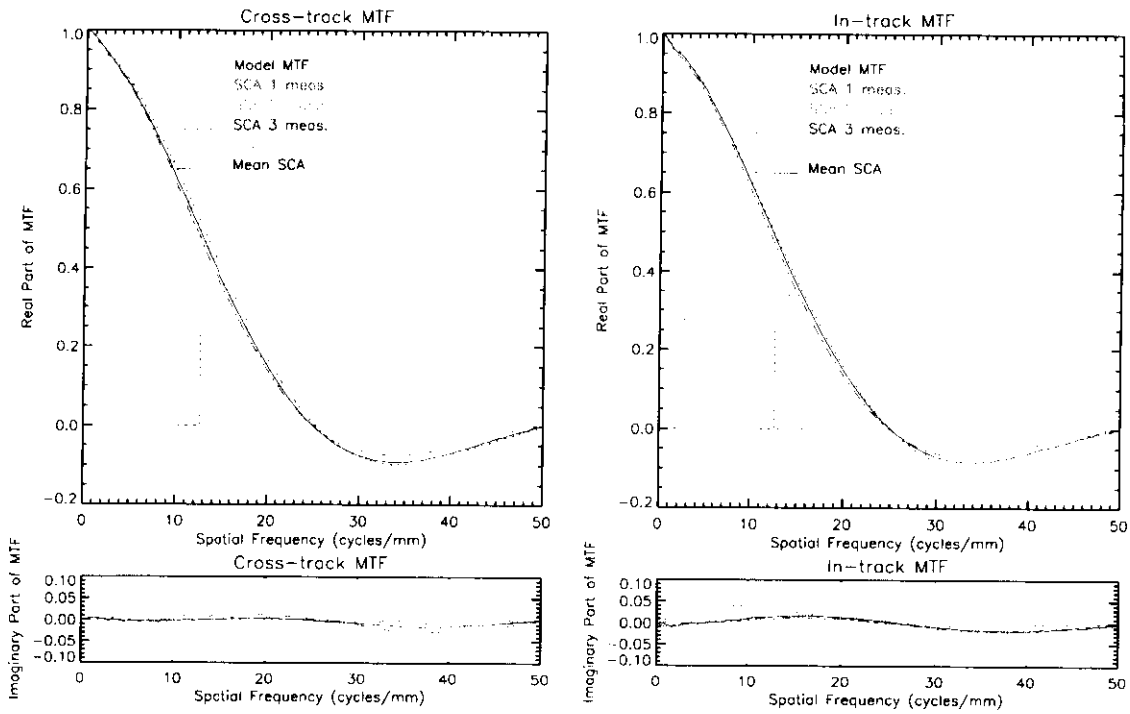

Figure 28. Measured and modeled Average MTFs for band 3, and measured MTFs for the individual SCAs.

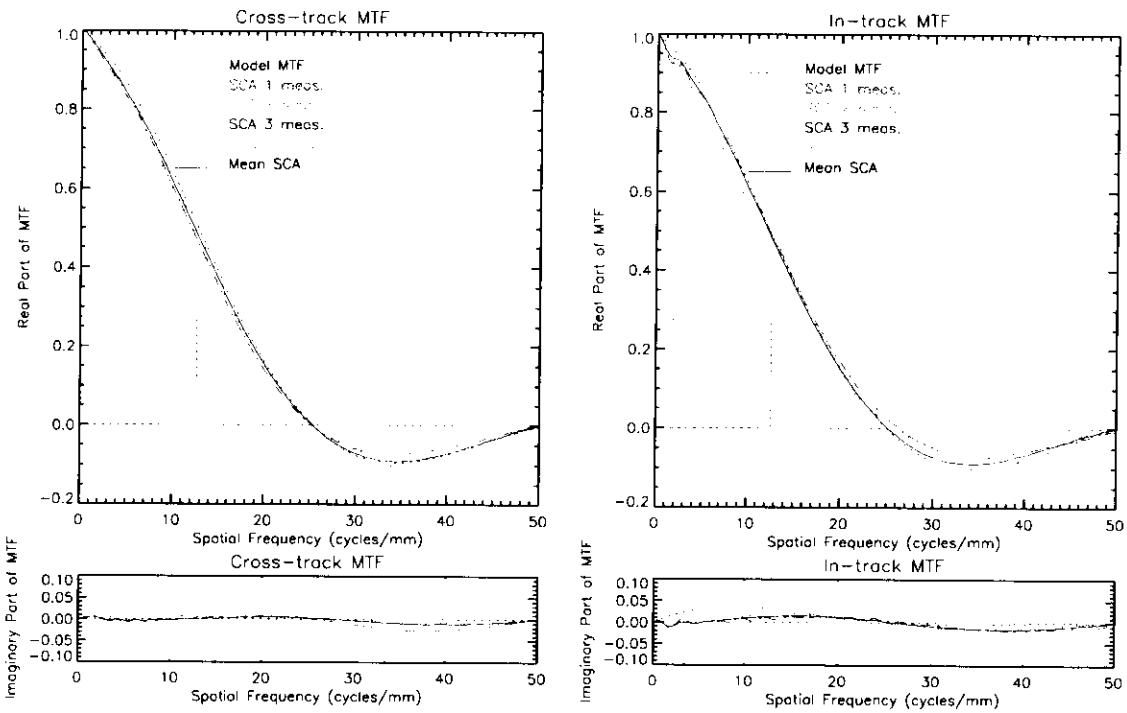

Figure 29. Measured and modeled Average MTFs for band 4, and measured MTFs for the individual SCAs.

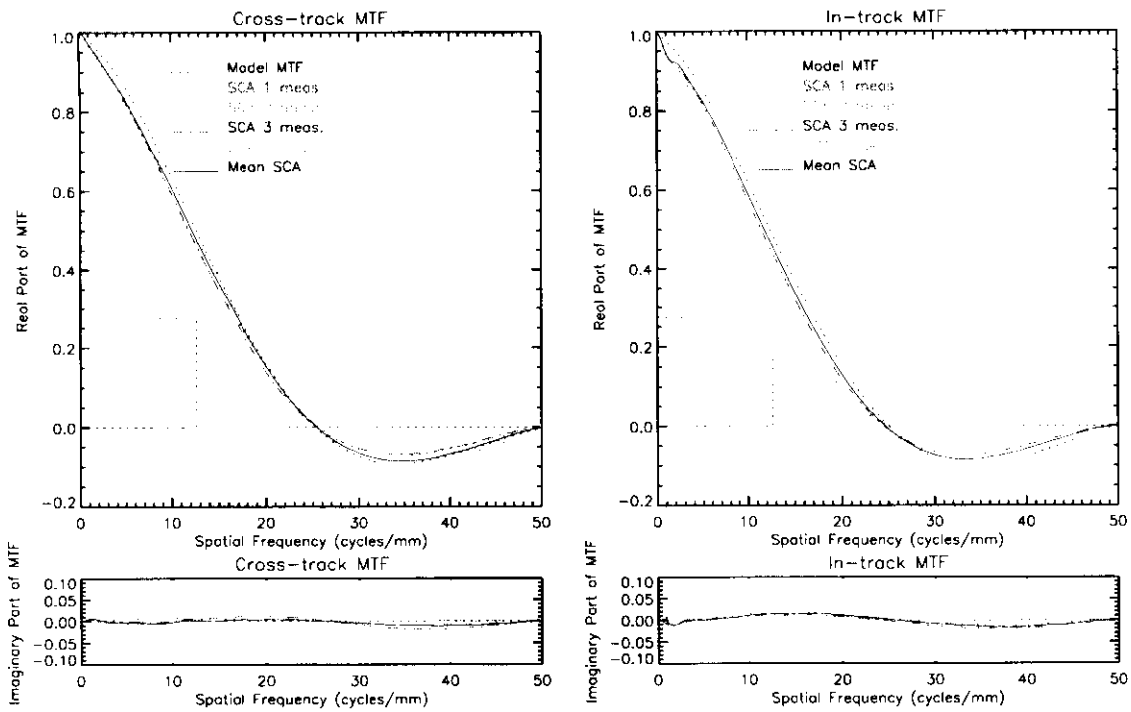

Figure 30. Measured and modeled Average MTFs for band 4', and measured MTFs for the individual SCAs.

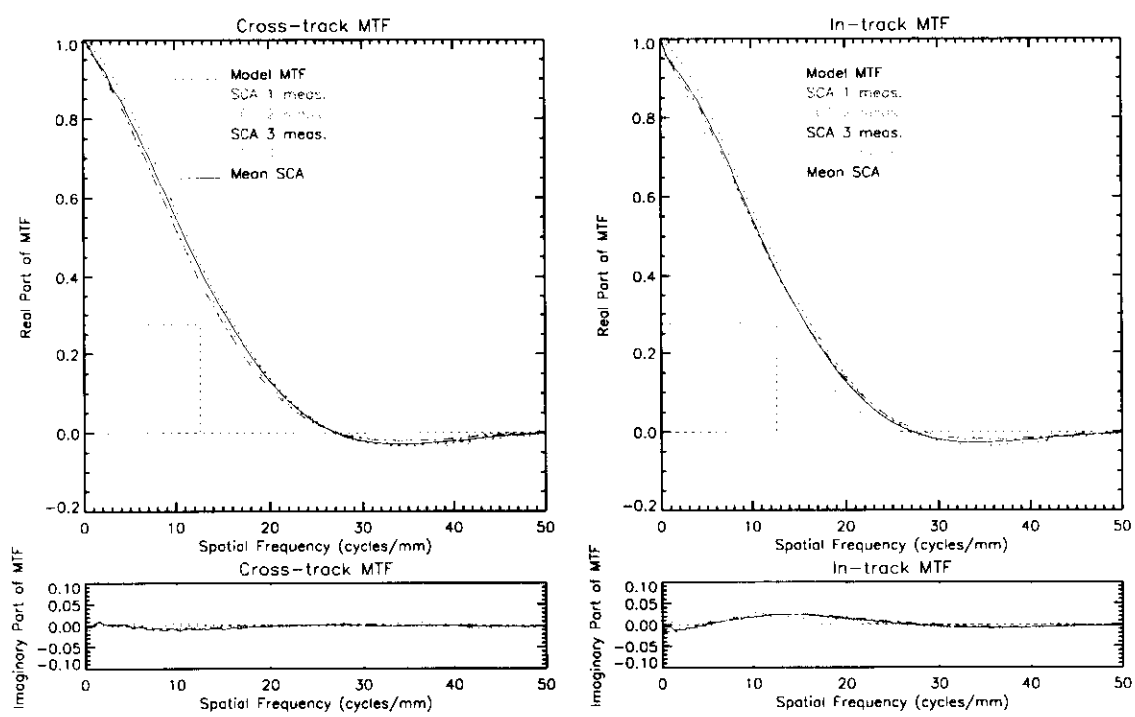

Figure 31. Measured and modeled Average MTFs for band 5', and measured MTFs for the individual SCAs.

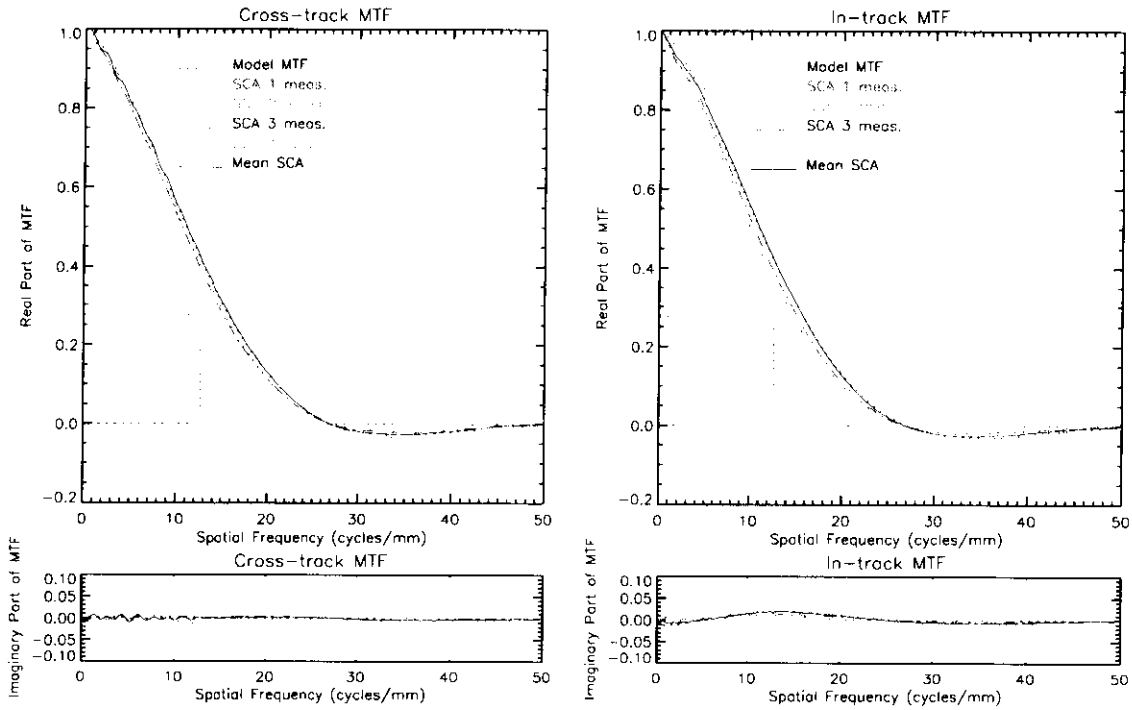

Figure 32. Measured and modeled Average MTFs for band 5, and measured MTFs for the individual SCAs.

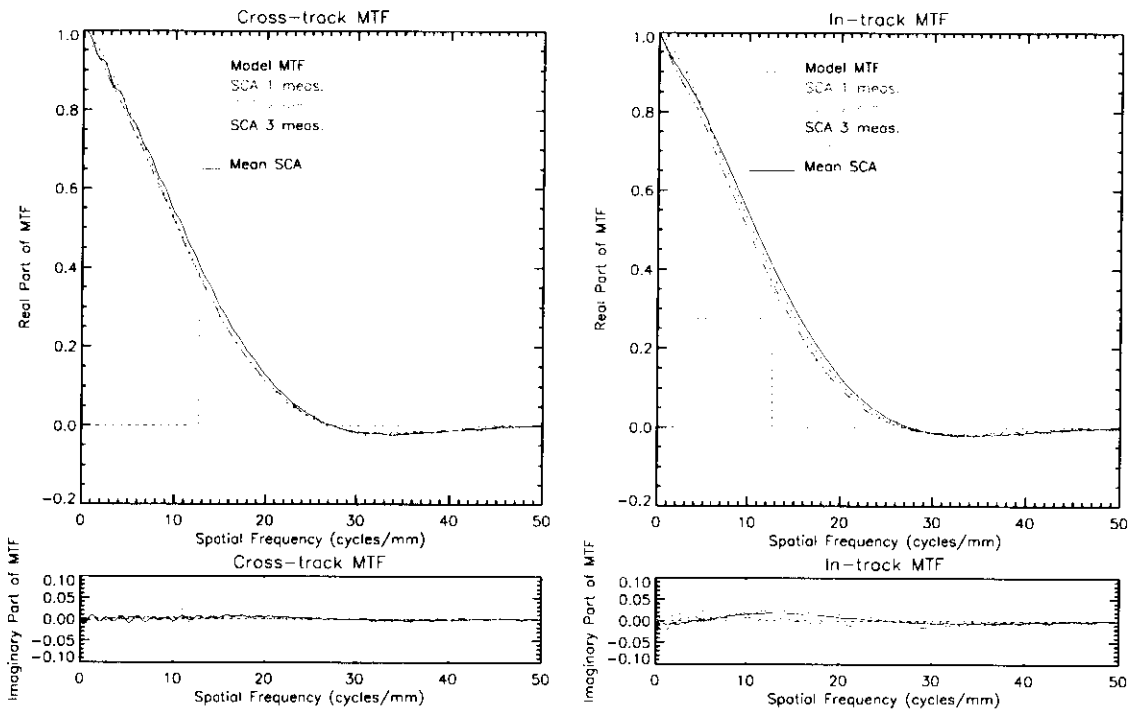

Figure 33. Measured and modeled Average MTFs for band 7, and measured MTFs for the individual SCAs.

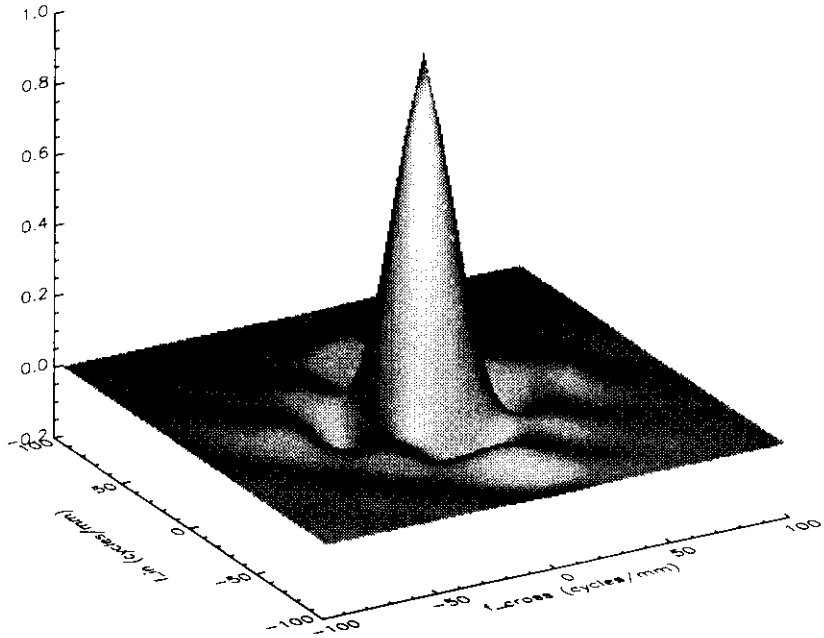

Figure 34. System MTF of band 1' near the center of the detector array.

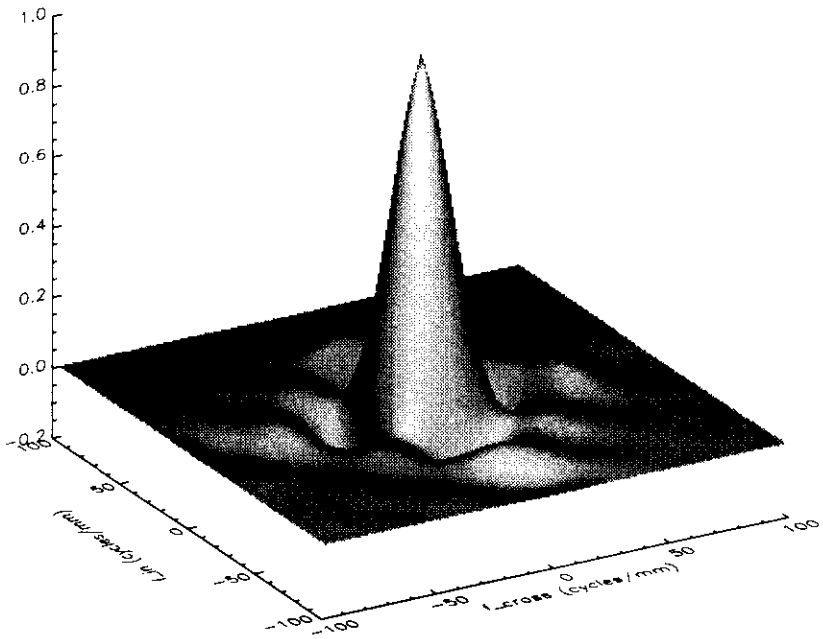

Figure 35. System MTF of band 4' near the center of the detector array.

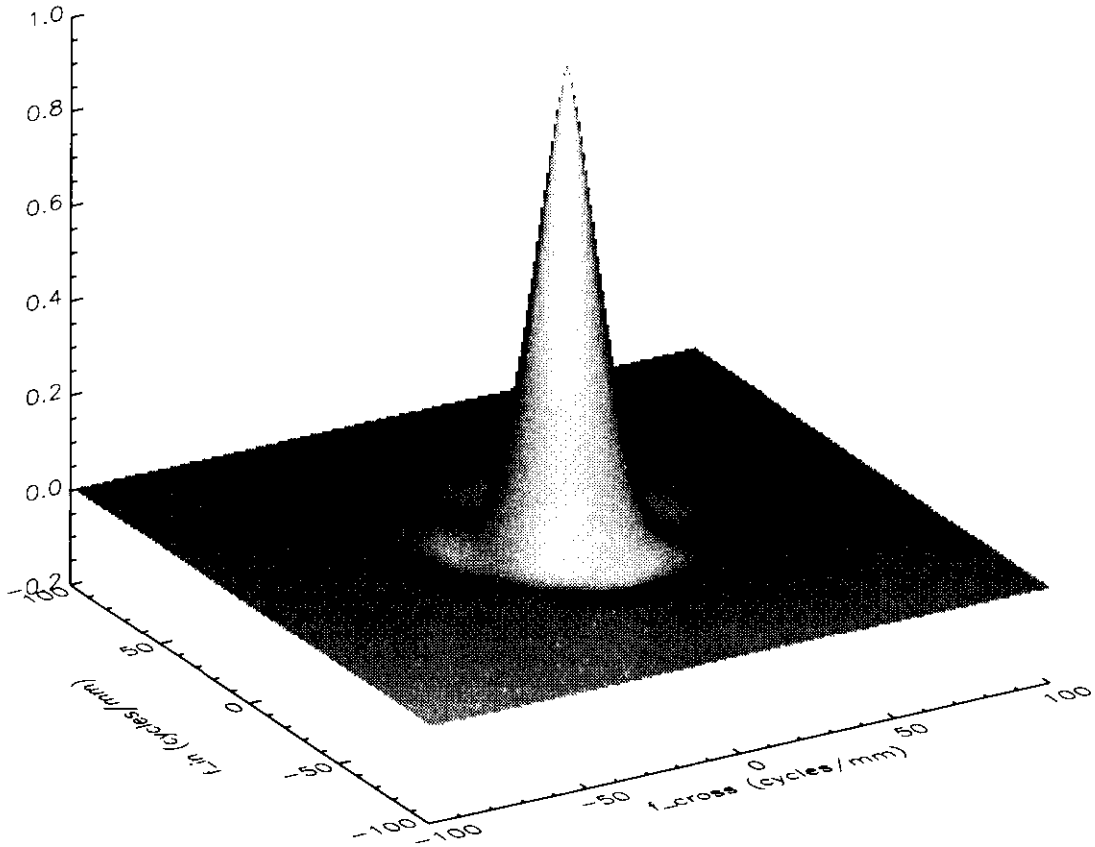

Figure 36. System MTF of band 7 near the center of the detector array.

5.4 POINT-SPREAD FUNCTIONS

Representative point-spread functions computed from the model MTFs are shown in Figures 37 to 45. The in-track spreading caused by scan motion is not included in these PSFs.

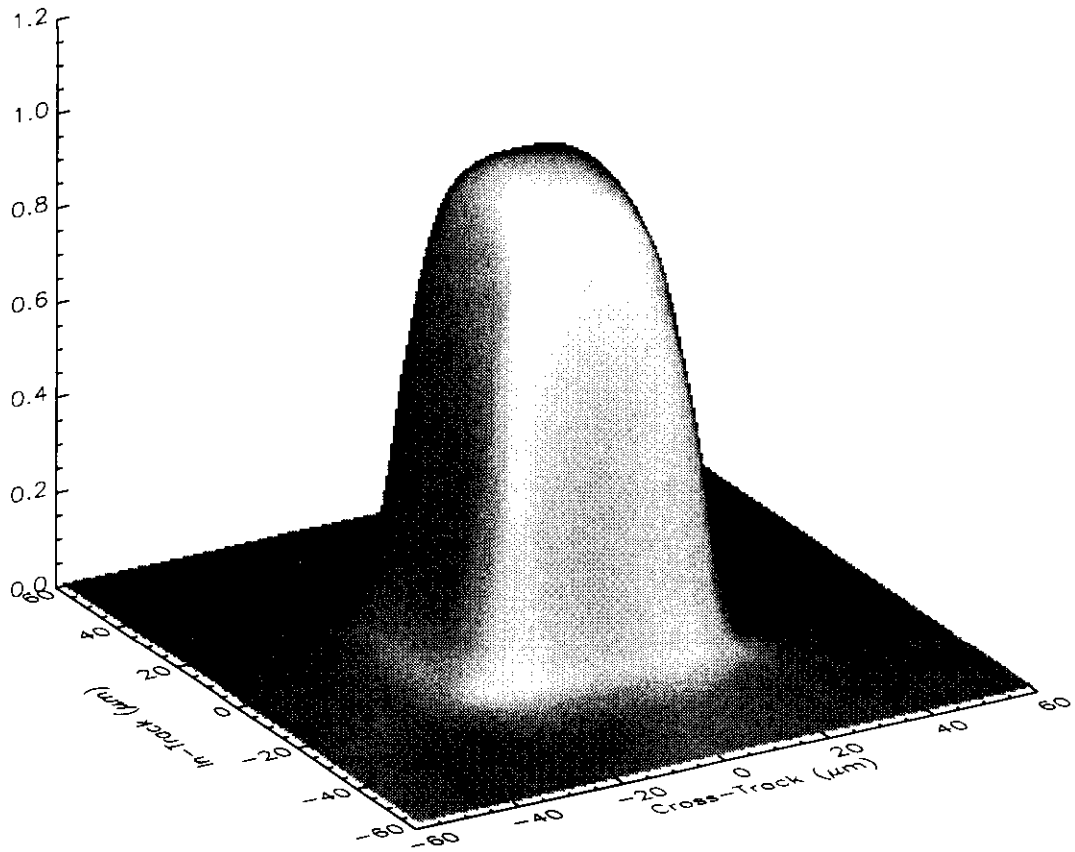

Figure 37. System PSF of band 1' (443 nm) near the center of the detector array.

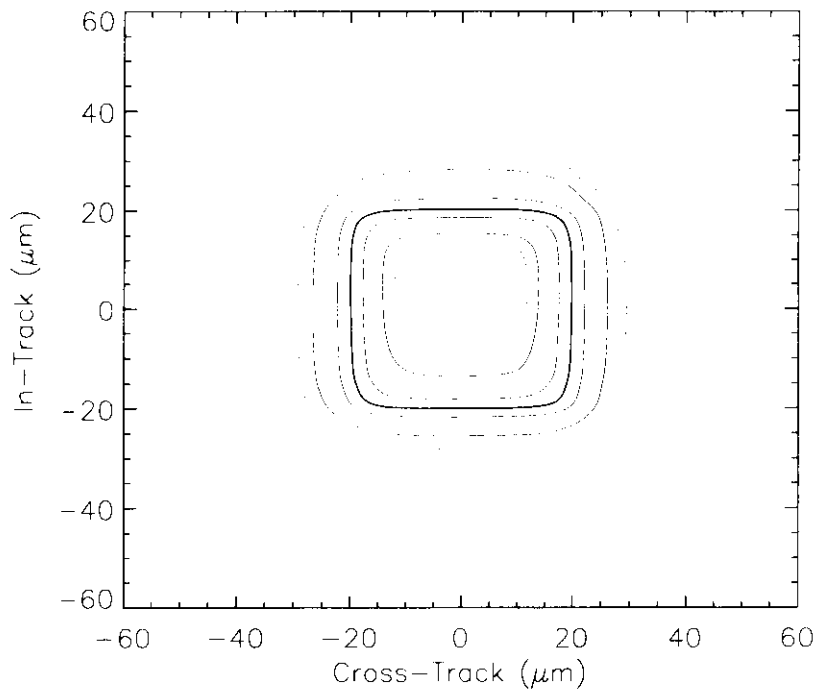

Figure 38. System PSF of band 1' near the center of the detector array. The contour levels are at 5, 10, 30, 50, 70, 90 and 95% of the peak.

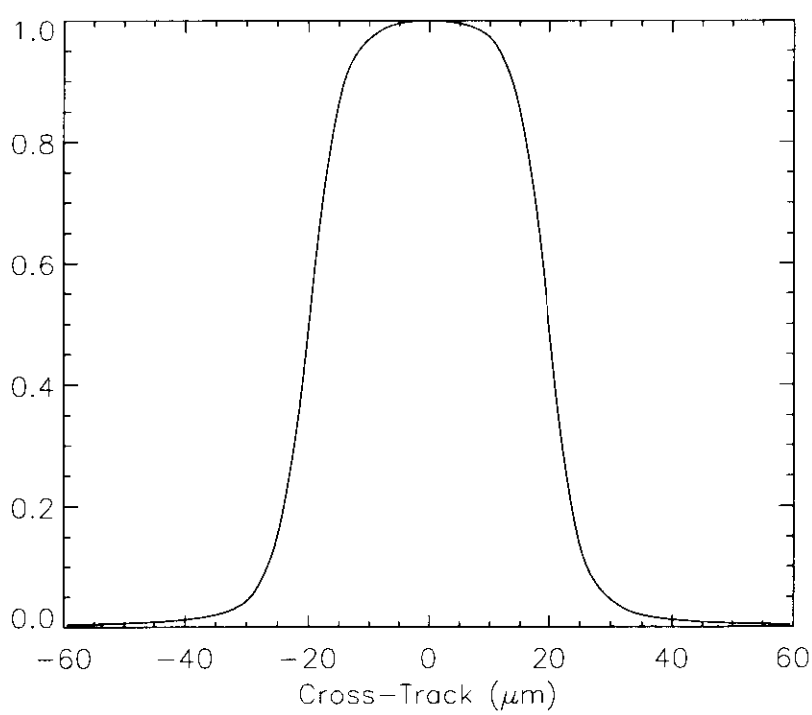

Figure 39. System PSF of band 1' near the center of the detector array. This cross-section is through center in the cross-track direction.

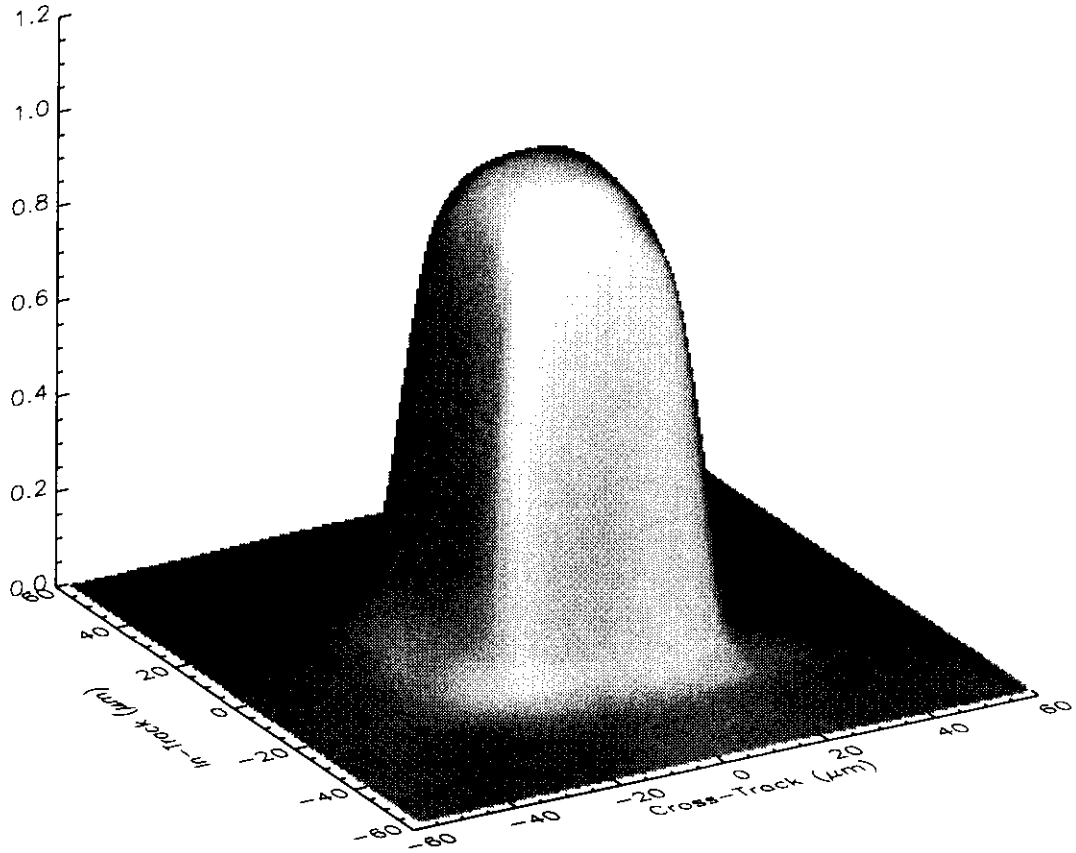

Figure 40. System PSF of band 4' (868 nm) near the center of the detector array.

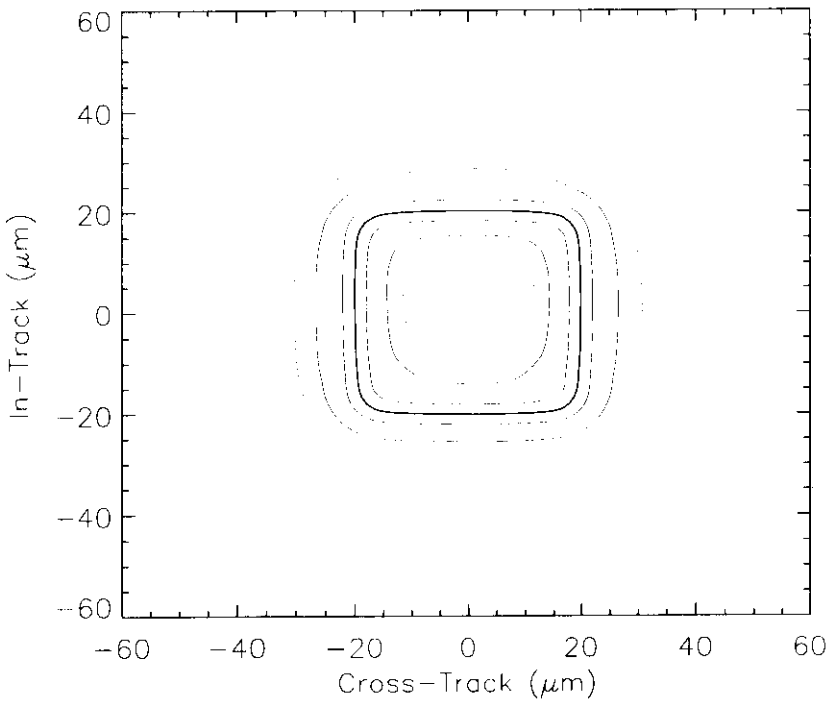

Figure 41. System PSF of band 4' near the center of the detector array. The contour levels are at 5, 10, 30, 50, 70, 90 and 95% of the peak.

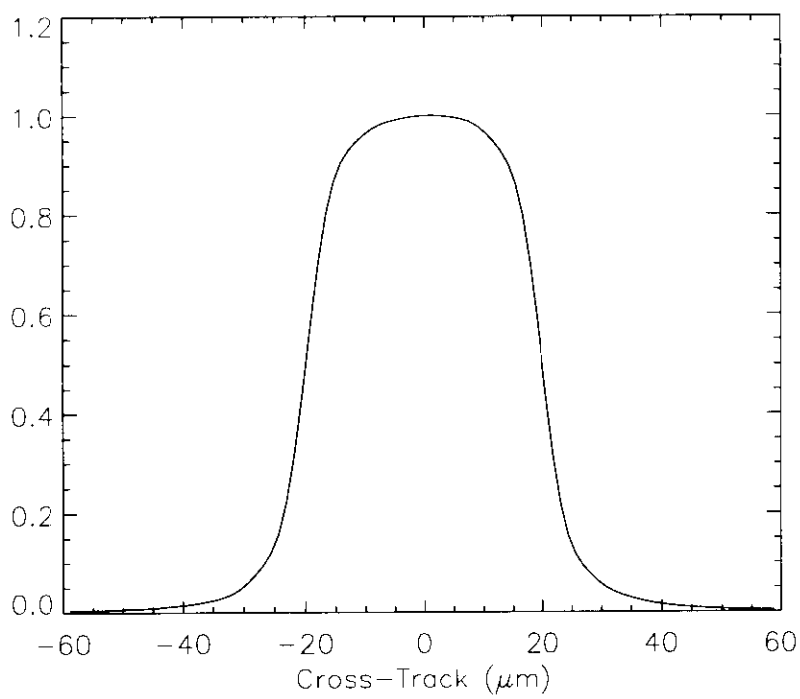

Figure 42. System PSF of band 4' near the center of the detector array. This cross-section is through center in the cross-track direction.

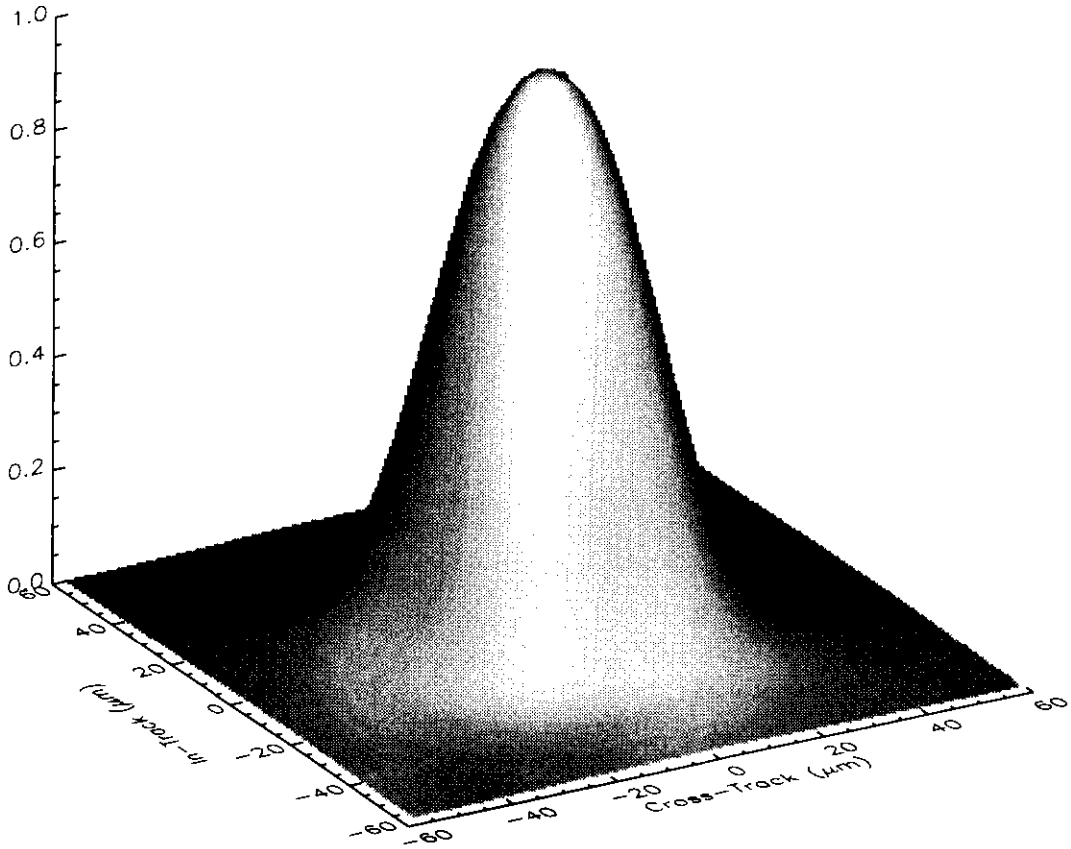

Figure 43. System PSF of band 7 (2.2 μm) near the center of the detector array.

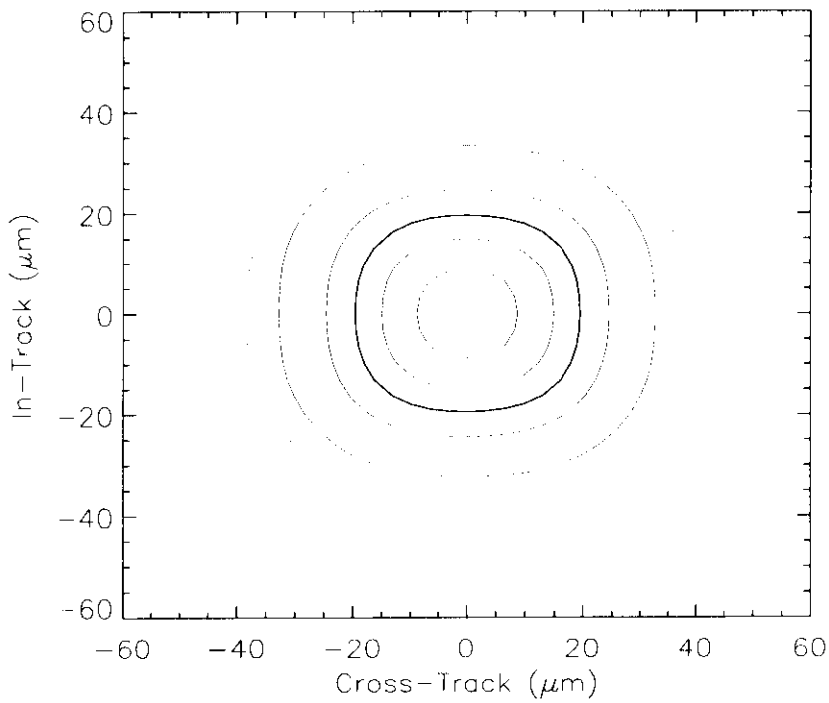

Figure 44. System PSF of band 7 near the center of the detector array. The contour levels are at 5, 10, 30, 50, 70, 90 and 95% of the peak.

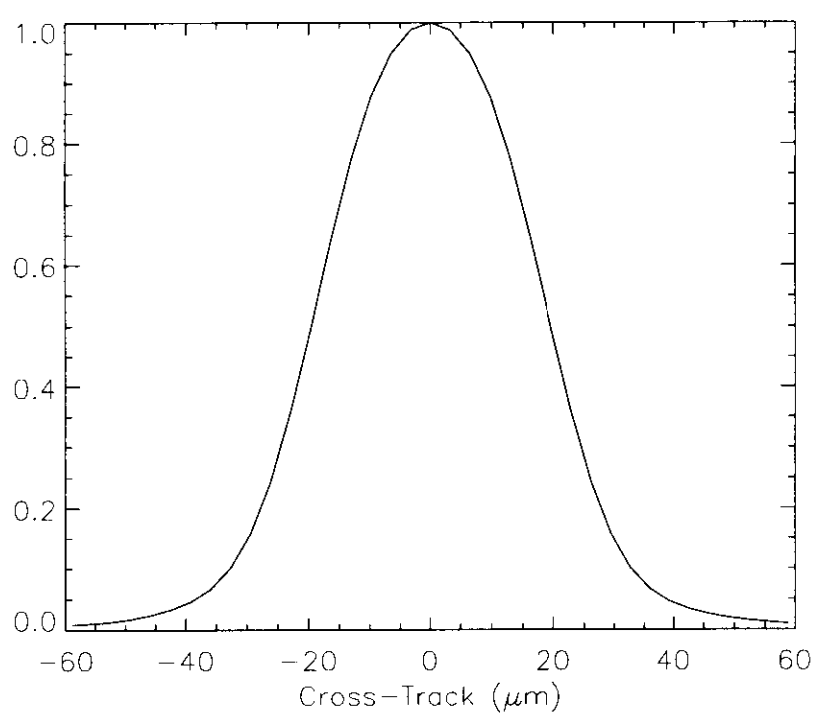

Figure 45. System PSF of band 7 near the center of the detector array. This cross-section is through center in the cross-track direction.

6 REFERENCES

1. Bicknell, W. E., Digenis, C. J., Forman, S. E., and Lencioni, D. E., *EO-1 Advanced Land Imager*, Proc. SPIE, vol. 3750, pp. 80-88, July 1999.

2. Lencioni, D. E., Hearn, D. R., Mendenhall, J. A., and Bicknell, W. E., *EO-1 Advanced Land Imager Calibration and Performance Overview*, Proc. SPIE, vol. 3750, pp. 89-96, July 1999.

3. Hearn, D. R., Mendenhall, J. A., and Willard, B. C., *Spatial Calibration of the EO-1 Advanced Land Imager*, Proc. SPIE, vol. 3750, pp. 97-108, July 1999.

4. Willard, B. C., *Wide field-of-view Schmidt-sphere imaging collimator*, Proc. SPIE, vol. 3750, pp 286-296, July 1999.

5. Lambda Research Corporation, *EO-1 Stray Light Analysis Report No. 2*, Feb. 20, 1998.

6. Tarnowski, G. J., and Maschhoff, K. R., *FPA/Dewar MTF Component Analysis*, Proc. IRIS Detectors, pp. 69-94, 1996.

7. Hearn, D. R., *Vacuum window optical power induced by temperature gradients*, Proc. SPIE, vol. 3750, pp 297-308, July 1999.

APPENDIX A

SPATIAL TRANSFER FUNCTIONS OF THE EO-1 ADVANCED LAND IMAGER

The spatial transfer functions (STFs) of the ALI are tabulated on the following pages. These numerical values are obtained with our analytical model, as described in Section 4 of this report. The location on the focal plane that was used for these calculations is SCA 2, pixel 635, which is in the center of the cross-track extent of the populated part of the focal plane. The STF varies only slightly over the field, so the values given here can be considered fully representative.

Tables A-1 to A-10 list the STFs of each of the bands. The complex STF is given for one quadrant of frequency space. The real part is symmetric, the imaginary part anti-symmetric in both axes. The frequencies listed in the top rows and left columns of the tables are first, spatial frequency at the focal plane (in cycles/millimeter), and second, angular frequency in object space (in cycles/milliradian). (They are related by the focal length of the instrument, 0.946 meters.) The frequency intervals are one-fourth of the Nyquist frequency in each case.

In the main body of each table, the STF value is listed with the real part above, and the imaginary part below in the same cell.

TABLE A-1

Spatial Transfer Function of the Panchromatic Band

Frequency	mm^{-1}	0.000	9.470	18.939	28.409	37.879	47.348	56.818	66.288	75.758	85.227	94.697	104.16	113.63	123.10	132.57	142.04	151.51
	$mrad^{-1}$	0.000	10.031	20.063	30.094	40.126	50.157	60.189	70.220	80.252	90.283	100.31	110.34	120.37	130.40	140.44	150.47	160.50
mm^{-1}	$mrad^{-1}$																	
0.000	0.000	1.000	0.816	0.592	0.376	0.214	0.109	0.047	0.015	0.000	-0.006	-0.008	-0.008	-0.008	-0.006	-0.005	-0.002	0.000
		0.000	-0.009	-0.011	-0.009	-0.003	0.003	0.006	0.003	0.000	-0.001	-0.001	0.000	0.000	-0.001	-0.001	0.000	0.000
9.470	10.031	0.800	0.716	0.534	0.345	0.198	0.101	0.044	0.014	0.000	-0.006	-0.008	-0.008	-0.007	-0.006	-0.004	-0.002	0.000
		0.040	0.034	0.024	0.015	0.013	0.012	0.010	0.005	0.000	-0.002	-0.002	-0.001	-0.001	-0.001	-0.001	0.000	0.000
18.939	20.063	0.594	0.549	0.426	0.282	0.164	0.084	0.036	0.012	0.000	-0.005	-0.006	-0.007	-0.007	-0.006	-0.004	-0.002	0.000
		0.018	0.010	0.007	0.003	0.005	0.007	0.006	0.003	0.000	-0.001	-0.001	-0.001	0.000	0.000	0.000	0.000	0.000
28.409	30.094	0.414	0.392	0.316	0.219	0.132	0.070	0.031	0.010	0.000	-0.004	-0.006	-0.006	-0.006	-0.005	-0.004	-0.002	0.000
		-0.003	-0.010	-0.009	-0.006	-0.003	0.000	0.001	0.001	0.000	0.000	0.000	0.000	0.000	0.000	0.000	0.000	0.000
37.879	40.126	0.265	0.254	0.212	0.153	0.097	0.053	0.025	0.008	0.000	-0.004	-0.005	-0.005	-0.005	-0.004	-0.003	-0.001	0.000
		-0.012	-0.017	-0.014	-0.008	-0.004	-0.002	-0.001	0.000	0.000	0.001	0.001	0.001	0.001	0.001	0.000	0.000	0.000
47.348	50.157	0.153	0.148	0.126	0.095	0.062	0.035	0.017	0.006	0.000	-0.003	-0.004	-0.004	-0.003	-0.003	-0.002	-0.001	0.000
		-0.014	-0.016	-0.013	-0.007	-0.003	-0.002	-0.001	-0.001	0.000	0.001	0.002	0.002	0.001	0.001	0.001	0.000	0.000
56.818	60.189	0.076	0.075	0.065	0.050	0.034	0.020	0.010	0.004	0.000	-0.002	-0.002	-0.002	-0.002	-0.002	-0.001	-0.001	0.000
		-0.011	-0.011	-0.008	-0.005	-0.002	-0.001	-0.001	-0.001	0.000	0.001	0.001	0.001	0.001	0.001	0.000	0.000	0.000
66.288	70.220	0.029	0.028	0.025	0.020	0.014	0.008	0.004	0.002	0.000	-0.001	-0.001	-0.001	-0.001	-0.001	-0.001	0.000	0.000
		-0.006	-0.006	-0.004	-0.002	-0.001	-0.001	-0.001	0.000	0.000	0.000	0.001	0.001	0.001	0.000	0.000	0.000	0.000
75.758	80.252	0.000	0.000	0.000	0.000	0.000	0.000	0.000	0.000	0.000	0.000	0.000	0.000	0.000	0.000	0.000	0.000	0.000
		0.000	0.000	0.000	0.000	0.000	0.000	0.000	0.000	0.000	0.000	0.000	0.000	0.000	0.000	0.000	0.000	0.000
85.227	90.283	-0.017	-0.017	-0.015	-0.012	-0.009	-0.005	-0.003	-0.001	0.000	0.000	0.001	0.001	0.001	0.001	0.000	0.000	0.000
		0.005	0.004	0.003	0.002	0.001	0.001	0.001	0.000	0.000	0.000	0.000	0.000	0.000	0.000	0.000	0.000	0.000
94.697	100.315	-0.026	-0.026	-0.023	-0.019	-0.013	-0.008	-0.004	-0.002	0.000	0.001	0.001	0.001	0.001	0.001	0.000	0.000	0.000
		0.007	0.006	0.004	0.003	0.001	0.001	0.001	0.001	0.000	0.000	-0.001	-0.001	0.000	0.000	0.000	0.000	0.000
104.167	110.346	-0.029	-0.029	-0.026	-0.020	-0.014	-0.009	-0.004	-0.002	0.000	0.001	0.001	0.001	0.001	0.001	0.000	0.000	0.000
		0.007	0.006	0.004	0.002	0.001	0.001	0.001	0.001	0.000	0.000	-0.001	-0.001	0.000	0.000	0.000	0.000	0.000
113.636	120.378	-0.028	-0.026	-0.023	-0.018	-0.012	-0.007	-0.004	-0.001	0.000	0.001	0.001	0.001	0.001	0.001	0.000	0.000	0.000
		0.004	0.003	0.002	0.001	0.001	0.001	0.001	0.000	0.000	0.000	0.000	0.000	0.000	0.000	0.000	0.000	0.000
123.106	130.409	-0.019	-0.019	-0.016	-0.012	-0.008	-0.005	-0.003	-0.001	0.000	0.000	0.001	0.001	0.000	0.000	0.000	0.000	0.000
		0.001	0.001	0.000	0.000	0.001	0.001	0.001	0.000	0.000	0.000	0.000	0.000	0.000	0.000	0.000	0.000	0.000
132.576	140.440	-0.011	-0.010	-0.009	-0.007	-0.004	-0.003	-0.001	0.000	0.000	0.000	0.000	0.000	0.000	0.000	0.000	0.000	0.000
		0.000	-0.001	-0.001	0.000	0.000	0.001	0.000	0.000	0.000	0.000	0.000	0.000	0.000	0.000	0.000	0.000	0.000
142.045	150.472	-0.004	-0.004	-0.003	-0.002	-0.002	-0.001	0.000	0.000	0.000	0.000	0.000	0.000	0.000	0.000	0.000	0.000	0.000
		-0.001	-0.001	-0.001	0.000	0.000	0.000	0.000	0.000	0.000	0.000	0.000	0.000	0.000	0.000	0.000	0.000	0.000
151.515	160.503	0.000	0.000	0.000	0.000	0.000	0.000	0.000	0.000	0.000	0.000	0.000	0.000	0.000	0.000	0.000	0.000	0.000
		0.000	0.000	0.000	0.000	0.000	0.000	0.000	0.000	0.000	0.000	0.000	0.000	0.000	0.000	0.000	0.000	0.000

TABLE A-2

Spatial Transfer Function of Band 1'

Frequency	mm^{-1}	0.000	3.157	6.313	9.470	12.626	15.783	18.939	22.096	25.253	28.409	31.566	34.722	37.879	41.035	44.192	47.348	50.505
	$mrad^{-1}$	0.000	3.344	6.688	10.031	13.375	16.719	20.063	23.407	26.751	30.094	33.438	36.782	40.126	43.470	46.813	50.157	53.501
mm^{-1}	$mrad^{-1}$																	
0.000	0.000	1.000	0.900	0.792	0.659	0.511	0.360	0.218	0.097	0.003	-0.061	-0.096	-0.107	-0.098	-0.077	-0.050	-0.023	0.000
		0.000	-0.003	-0.005	-0.006	-0.006	-0.005	-0.003	-0.002	0.000	0.001	0.003	0.003	0.003	0.003	0.002	0.001	0.000
3.157	3.344	0.896	0.853	0.759	0.634	0.493	0.348	0.211	0.094	0.003	-0.059	-0.094	-0.104	-0.096	-0.075	-0.049	-0.023	0.000
		0.014	0.012	0.009	0.006	0.004	0.002	0.001	0.000	0.000	0.000	0.001	0.001	0.001	0.001	0.001	0.000	0.000
6.313	6.688	0.783	0.753	0.677	0.570	0.444	0.314	0.191	0.085	0.003	-0.054	-0.085	-0.095	-0.087	-0.069	-0.045	-0.021	0.000
		0.024	0.022	0.020	0.016	0.012	0.008	0.004	0.002	0.000	-0.001	-0.001	-0.001	-0.001	-0.001	0.000	0.000	0.000
9.470	10.031	0.645	0.622	0.563	0.476	0.372	0.264	0.161	0.072	0.002	-0.045	-0.072	-0.080	-0.074	-0.058	-0.038	-0.018	0.000
		0.027	0.025	0.023	0.020	0.015	0.011	0.006	0.003	0.000	-0.001	-0.002	-0.002	-0.002	-0.002	-0.001	-0.001	0.000
12.626	13.375	0.493	0.477	0.433	0.367	0.288	0.205	0.125	0.056	0.002	-0.036	-0.056	-0.063	-0.058	-0.046	-0.030	-0.014	0.000
		0.024	0.023	0.021	0.018	0.014	0.010	0.006	0.003	0.000	-0.001	-0.002	-0.002	-0.002	-0.002	-0.001	-0.001	0.000
15.783	16.719	0.342	0.331	0.301	0.256	0.202	0.144	0.088	0.040	0.001	-0.025	-0.040	-0.044	-0.041	-0.032	-0.021	-0.010	0.000
		0.017	0.016	0.015	0.013	0.010	0.007	0.004	0.002	0.000	-0.001	-0.002	-0.002	-0.002	-0.001	-0.001	0.000	0.000
18.939	20.063	0.204	0.198	0.180	0.154	0.121	0.087	0.053	0.024	0.001	-0.015	-0.024	-0.027	-0.025	-0.020	-0.013	-0.006	0.000
		0.009	0.009	0.008	0.007	0.006	0.004	0.002	0.001	0.000	-0.001	-0.001	-0.001	-0.001	-0.001	-0.001	0.000	0.000
22.096	23.407	0.087	0.085	0.077	0.066	0.052	0.037	0.023	0.010	0.000	-0.007	-0.010	-0.012	-0.011	-0.009	-0.006	-0.003	0.000
		0.004	0.003	0.003	0.003	0.002	0.001	0.001	0.000	0.000	0.000	0.000	0.000	0.000	0.000	0.000	0.000	0.000
25.253	26.751	-0.003	-0.003	-0.003	-0.002	-0.002	-0.001	-0.001	0.000	0.000	0.000	0.000	0.000	0.000	0.000	0.000	0.000	0.000
		0.000	0.000	0.000	0.000	0.000	0.000	0.000	0.000	0.000	0.000	0.000	0.000	0.000	0.000	0.000	0.000	0.000
28.409	30.094	-0.065	-0.063	-0.058	-0.050	-0.039	-0.028	-0.018	-0.008	0.000	0.005	0.008	0.009	0.008	0.007	0.004	0.002	0.000
		-0.001	-0.001	-0.001	-0.001	-0.001	0.000	0.000	0.000	0.000	0.000	0.000	0.000	0.000	0.000	0.000	0.000	0.000
31.566	33.438	-0.100	-0.097	-0.089	-0.076	-0.061	-0.044	-0.027	-0.012	0.000	0.008	0.013	0.014	0.013	0.011	0.007	0.003	0.000
		-0.001	-0.001	-0.001	0.000	0.000	0.000	0.000	0.000	0.000	0.000	0.000	0.000	0.000	0.000	0.000	0.000	0.000
34.722	36.782	-0.111	-0.108	-0.099	-0.085	-0.067	-0.049	-0.030	-0.014	0.000	0.009	0.014	0.016	0.015	0.012	0.008	0.004	0.000
		-0.001	0.000	0.000	0.000	0.000	0.000	0.000	0.000	0.000	0.000	0.000	0.000	0.000	0.000	0.000	0.000	0.000
37.879	40.126	-0.102	-0.099	-0.091	-0.078	-0.063	-0.045	-0.028	-0.013	0.000	0.008	0.013	0.015	0.014	0.011	0.007	0.004	0.000
		0.000	0.001	0.001	0.001	0.001	0.001	0.001	0.000	0.000	0.000	0.000	-0.001	-0.001	0.000	0.000	0.000	0.000
41.035	43.470	-0.081	-0.078	-0.072	-0.062	-0.049	-0.036	-0.022	-0.010	0.000	0.007	0.011	0.012	0.011	0.009	0.006	0.003	0.000
		0.001	0.001	0.001	0.001	0.001	0.001	0.001	0.000	0.000	0.000	0.000	-0.001	-0.001	0.000	0.000	0.000	0.000
44.192	46.813	-0.052	-0.051	-0.047	-0.040	-0.032	-0.023	-0.015	-0.007	0.000	0.004	0.007	0.008	0.008	0.006	0.004	0.002	0.000
		0.001	0.001	0.001	0.001	0.001	0.001	0.001	0.000	0.000	0.000	0.000	0.000	0.000	0.000	0.000	0.000	0.000
47.348	50.157	-0.023	-0.022	-0.020	-0.017	-0.014	-0.010	-0.006	-0.003	0.000	0.002	0.003	0.004	0.003	0.003	0.002	0.001	0.000
		0.001	0.001	0.001	0.001	0.001	0.000	0.000	0.000	0.000	0.000	0.000	0.000	0.000	0.000	0.000	0.000	0.000
50.505	53.501	0.004	0.003	0.003	0.003	0.002	0.002	0.001	0.000	0.000	0.000	-0.001	-0.001	-0.001	0.000	0.000	0.000	0.000
		0.000	0.000	0.000	0.000	0.000	0.000	0.000	0.000	0.000	0.000	0.000	0.000	0.000	0.000	0.000	0.000	0.000

TABLE A-3

Spatial Transfer Function of Band 1

Frequency	mm⁻¹	0.000	3.157	6.313	9.470	12.626	15.783	18.939	22.096	25.253	28.409	31.566	34.722	37.879	41.035	44.192	47.348	50.505
	mrad⁻¹	0.000	3.344	6.688	10.031	13.375	16.719	20.063	23.407	26.751	30.094	33.438	36.782	40.126	43.470	46.813	50.157	53.501
mm⁻¹	mrad⁻¹																	
0.000	0.000	1.000	0.909	0.801	0.667	0.518	0.365	0.220	0.097	0.002	-0.063	-0.099	-0.110	-0.102	-0.081	-0.053	-0.025	-0.001
		0.000	-0.003	-0.004	-0.005	-0.005	-0.004	-0.003	-0.002	0.000	0.001	0.002	0.003	0.003	0.003	0.002	0.001	0.000
3.157	3.344	0.903	0.860	0.766	0.641	0.499	0.352	0.213	0.094	0.002	-0.061	-0.097	-0.108	-0.100	-0.079	-0.052	-0.024	-0.001
		0.015	0.013	0.011	0.008	0.005	0.003	0.001	0.000	0.000	0.000	0.000	0.001	0.001	0.001	0.001	0.000	0.000
6.313	6.688	0.791	0.759	0.683	0.575	0.449	0.317	0.192	0.085	0.002	-0.056	-0.088	-0.098	-0.091	-0.072	-0.047	-0.022	-0.001
		0.024	0.023	0.021	0.018	0.013	0.009	0.005	0.002	0.000	-0.001	-0.001	-0.001	-0.001	-0.001	0.000	0.000	0.000
9.470	10.031	0.652	0.628	0.568	0.480	0.376	0.267	0.162	0.071	0.001	-0.047	-0.074	-0.083	-0.077	-0.061	-0.040	-0.019	0.000
		0.026	0.025	0.023	0.020	0.016	0.011	0.007	0.003	0.000	-0.002	-0.002	-0.002	-0.002	-0.001	-0.001	0.000	0.000
12.626	13.375	0.499	0.481	0.437	0.371	0.291	0.207	0.126	0.056	0.001	-0.037	-0.058	-0.065	-0.060	-0.048	-0.032	-0.015	0.000
		0.023	0.022	0.020	0.018	0.014	0.010	0.006	0.003	0.000	-0.002	-0.002	-0.002	-0.002	-0.002	-0.001	-0.001	0.000
15.783	16.719	0.346	0.334	0.304	0.259	0.204	0.145	0.089	0.039	0.001	-0.026	-0.041	-0.046	-0.043	-0.034	-0.022	-0.011	0.000
		0.016	0.015	0.014	0.012	0.010	0.007	0.004	0.002	0.000	-0.001	-0.002	-0.002	-0.002	-0.001	-0.001	0.000	0.000
18.939	20.063	0.205	0.199	0.181	0.155	0.122	0.087	0.053	0.024	0.000	-0.016	-0.025	-0.028	-0.026	-0.021	-0.014	-0.006	0.000
		0.008	0.008	0.007	0.006	0.005	0.004	0.002	0.001	0.000	-0.001	-0.001	-0.001	-0.001	-0.001	0.000	0.000	0.000
22.096	23.407	0.087	0.084	0.076	0.065	0.052	0.037	0.023	0.010	0.000	-0.007	-0.011	-0.012	-0.011	-0.009	-0.006	-0.003	0.000
		0.003	0.003	0.002	0.002	0.002	0.001	0.001	0.000	0.000	0.000	0.000	0.000	0.000	0.000	0.000	0.000	0.000
25.253	26.751	-0.005	-0.004	-0.004	-0.003	-0.003	-0.002	-0.001	-0.001	0.000	0.000	0.001	0.001	0.001	0.000	0.000	0.000	0.000
		0.000	0.000	0.000	0.000	0.000	0.000	0.000	0.000	0.000	0.000	0.000	0.000	0.000	0.000	0.000	0.000	0.000
28.409	30.094	-0.067	-0.065	-0.060	-0.051	-0.041	-0.029	-0.018	-0.008	0.000	0.005	0.009	0.010	0.009	0.007	0.005	0.002	0.000
		-0.001	-0.001	-0.001	-0.001	0.000	0.000	0.000	0.000	0.000	0.000	0.000	0.000	0.000	0.000	0.000	0.000	0.000
31.566	33.438	-0.103	-0.100	-0.091	-0.078	-0.062	-0.045	-0.028	-0.012	0.000	0.008	0.013	0.015	0.014	0.011	0.007	0.004	0.000
		-0.001	-0.001	0.000	0.000	0.000	0.000	0.000	0.000	0.000	0.000	0.000	0.000	0.000	0.000	0.000	0.000	0.000
34.722	36.782	-0.114	-0.111	-0.101	-0.087	-0.070	-0.050	-0.031	-0.014	0.000	0.009	0.015	0.017	0.016	0.013	0.008	0.004	0.000
		0.000	0.000	0.001	0.001	0.001	0.001	0.000	0.000	0.000	0.000	0.000	0.000	0.000	0.000	0.000	0.000	0.000
37.879	40.126	-0.106	-0.103	-0.094	-0.081	-0.065	-0.047	-0.029	-0.013	0.000	0.009	0.014	0.016	0.015	0.012	0.008	0.004	0.000
		0.001	0.001	0.001	0.001	0.001	0.001	0.001	0.000	0.000	0.000	0.000	-0.001	-0.001	-0.001	0.000	0.000	0.000
41.035	43.470	-0.084	-0.082	-0.075	-0.064	-0.051	-0.037	-0.023	-0.010	0.000	0.007	0.011	0.013	0.012	0.010	0.007	0.003	0.000
		0.001	0.002	0.002	0.002	0.001	0.001	0.001	0.000	0.000	0.000	0.000	-0.001	-0.001	0.000	0.000	0.000	0.000
44.192	46.813	-0.054	-0.053	-0.048	-0.042	-0.033	-0.024	-0.015	-0.007	0.000	0.005	0.007	0.008	0.008	0.006	0.004	0.002	0.000
		0.001	0.001	0.001	0.001	0.001	0.001	0.001	0.000	0.000	0.000	0.000	0.000	0.000	0.000	0.000	0.000	0.000
47.348	50.157	-0.024	-0.023	-0.021	-0.018	-0.015	-0.011	-0.007	-0.003	0.000	0.002	0.003	0.004	0.004	0.003	0.002	0.001	0.000
		0.001	0.001	0.001	0.001	0.001	0.000	0.000	0.000	0.000	0.000	0.000	0.000	0.000	0.000	0.000	0.000	0.000
50.505	53.501	0.003	0.003	0.003	0.003	0.002	0.002	0.001	0.000	0.000	0.000	0.000	-0.001	-0.001	0.000	0.000	0.000	0.000
		0.000	0.000	0.000	0.000	0.000	0.000	0.000	0.000	0.000	0.000	0.000	0.000	0.000	0.000	0.000	0.000	0.000

TABLE A-4

Spatial Transfer Function of Band 2

Frequency	mm⁻¹	0.000	3.157	6.313	9.470	12.626	15.783	18.939	22.096	25.253	28.409	31.566	34.722	37.879	41.035	44.192	47.348	50.505
	mrad⁻¹	0.000	3.344	6.688	10.031	13.375	16.719	20.063	23.407	26.751	30.094	33.438	36.782	40.126	43.470	46.813	50.157	53.501
mm⁻¹	mrad⁻¹																	
0.000	0.000	1.000	0.918	0.811	0.677	0.524	0.368	0.223	0.099	0.001	-0.066	-0.101	-0.113	-0.105	-0.083	-0.055	-0.026	0.000
		0.000	-0.003	-0.004	-0.004	-0.004	-0.004	-0.003	-0.001	0.000	0.001	0.002	0.003	0.003	0.002	0.002	0.001	0.000
3.157	3.344	0.911	0.868	0.775	0.649	0.504	0.355	0.215	0.096	0.001	-0.064	-0.099	-0.110	-0.102	-0.081	-0.054	-0.025	0.000
		0.016	0.015	0.013	0.010	0.007	0.004	0.002	0.001	0.000	0.000	0.000	0.001	0.001	0.001	0.001	0.000	0.000
6.313	6.688	0.800	0.768	0.692	0.583	0.454	0.320	0.194	0.087	0.001	-0.058	-0.090	-0.100	-0.093	-0.074	-0.049	-0.023	0.000
		0.024	0.024	0.022	0.019	0.014	0.010	0.005	0.002	0.000	-0.001	-0.001	-0.001	-0.001	0.000	0.000	0.000	0.000
9.470	10.031	0.660	0.635	0.576	0.488	0.381	0.270	0.164	0.073	0.001	-0.049	-0.076	-0.085	-0.079	-0.063	-0.042	-0.020	0.000
		0.026	0.025	0.023	0.021	0.016	0.012	0.007	0.003	0.000	-0.002	-0.002	-0.002	-0.002	-0.001	-0.001	0.000	0.000
12.626	13.375	0.504	0.486	0.442	0.376	0.295	0.209	0.127	0.057	0.001	-0.038	-0.059	-0.067	-0.062	-0.049	-0.033	-0.016	0.000
		0.021	0.020	0.019	0.017	0.014	0.010	0.006	0.003	0.000	-0.001	-0.002	-0.002	-0.002	-0.001	-0.001	0.000	0.000
15.783	16.719	0.350	0.338	0.308	0.263	0.207	0.147	0.090	0.040	0.001	-0.027	-0.042	-0.047	-0.044	-0.035	-0.023	-0.011	0.000
		0.014	0.013	0.012	0.011	0.009	0.007	0.004	0.002	0.000	-0.001	-0.001	-0.001	-0.001	-0.001	-0.001	0.000	0.000
18.939	20.063	0.208	0.201	0.184	0.157	0.124	0.088	0.054	0.024	0.000	-0.016	-0.025	-0.029	-0.027	-0.021	-0.014	-0.007	0.000
		0.007	0.007	0.006	0.006	0.005	0.003	0.002	0.001	0.000	-0.001	-0.001	-0.001	-0.001	0.000	0.000	0.000	0.000
22.096	23.407	0.089	0.086	0.079	0.068	0.053	0.038	0.023	0.011	0.000	-0.007	-0.011	-0.012	-0.012	-0.009	-0.006	-0.003	0.000
		0.003	0.002	0.002	0.002	0.002	0.001	0.001	0.000	0.000	0.000	0.000	0.000	0.000	0.000	0.000	0.000	0.000
25.253	26.751	-0.005	-0.005	-0.004	-0.004	-0.003	-0.002	-0.001	-0.001	0.000	0.000	0.001	0.001	0.001	0.001	0.000	0.000	0.000
		0.000	0.000	0.000	0.000	0.000	0.000	0.000	0.000	0.000	0.000	0.000	0.000	0.000	0.000	0.000	0.000	0.000
28.409	30.094	-0.070	-0.068	-0.062	-0.054	-0.043	-0.031	-0.019	-0.009	0.000	0.006	0.009	0.010	0.010	0.008	0.005	0.002	0.000
		-0.001	-0.001	-0.001	0.000	0.000	0.000	0.000	0.000	0.000	0.000	0.000	0.000	0.000	0.000	0.000	0.000	0.000
31.566	33.438	-0.106	-0.102	-0.094	-0.081	-0.064	-0.046	-0.029	-0.013	0.000	0.009	0.014	0.016	0.015	0.012	0.008	0.004	0.000
		0.000	0.000	0.000	0.000	0.000	0.000	0.000	0.000	0.000	0.000	0.000	0.000	0.000	0.000	0.000	0.000	0.000
34.722	36.782	-0.117	-0.114	-0.105	-0.090	-0.072	-0.052	-0.032	-0.014	0.000	0.010	0.016	0.018	0.017	0.013	0.009	0.004	0.000
		0.000	0.001	0.001	0.001	0.001	0.001	0.000	0.000	0.000	0.000	0.000	0.000	0.000	0.000	0.000	0.000	0.000
37.879	40.126	-0.109	-0.105	-0.097	-0.083	-0.066	-0.048	-0.030	-0.014	0.000	0.009	0.015	0.017	0.016	0.013	0.008	0.004	0.000
		0.001	0.001	0.002	0.001	0.001	0.001	0.001	0.000	0.000	0.000	0.000	0.000	-0.001	0.000	0.000	0.000	0.000
41.035	43.470	-0.086	-0.083	-0.076	-0.066	-0.052	-0.038	-0.024	-0.011	0.000	0.007	0.012	0.013	0.013	0.010	0.007	0.003	0.000
		0.002	0.002	0.002	0.002	0.001	0.001	0.001	0.000	0.000	0.000	0.000	0.000	-0.001	0.000	0.000	0.000	0.000
44.192	46.813	-0.056	-0.054	-0.050	-0.043	-0.034	-0.025	-0.015	-0.007	0.000	0.005	0.008	0.009	0.008	0.007	0.005	0.002	0.000
		0.002	0.002	0.002	0.002	0.001	0.001	0.001	0.000	0.000	0.000	0.000	0.000	0.000	0.000	0.000	0.000	0.000
47.348	50.157	-0.024	-0.024	-0.022	-0.019	-0.015	-0.011	-0.007	-0.003	0.000	0.002	0.003	0.004	0.004	0.003	0.002	0.001	0.000
		0.001	0.001	0.001	0.001	0.001	0.001	0.000	0.000	0.000	0.000	0.000	0.000	0.000	0.000	0.000	0.000	0.000
50.505	53.501	0.004	0.004	0.003	0.003	0.002	0.002	0.001	0.000	0.000	0.000	-0.001	-0.001	-0.001	0.000	0.000	0.000	0.000
		0.000	0.000	0.000	0.000	0.000	0.000	0.000	0.000	0.000	0.000	0.000	0.000	0.000	0.000	0.000	0.000	0.000

TABLE A-5

Spatial Transfer Function of Band 3

Frequency	mm⁻¹	0.000	3.157	6.313	9.470	12.626	15.783	18.939	22.096	25.253	28.409	31.566	34.722	37.879	41.035	44.192	47.348	50.505
	mrad⁻¹	0.000	3.344	6.688	10.031	13.375	16.719	20.063	23.407	26.751	30.094	33.438	36.782	40.126	43.470	46.813	50.157	53.501
mm⁻¹	mrad⁻¹																	
0.000	0.000	1.000	0.923	0.816	0.678	0.525	0.368	0.223	0.097	0.002	-0.066	-0.102	-0.114	-0.106	-0.084	-0.056	-0.027	0.000
		0.000	-0.002	-0.003	-0.004	-0.004	-0.003	-0.002	-0.001	0.000	0.001	0.002	0.003	0.003	0.002	0.002	0.001	0.000
3.157	3.344	0.916	0.873	0.779	0.651	0.504	0.355	0.215	0.094	0.001	-0.064	-0.099	-0.111	-0.103	-0.082	-0.055	-0.026	0.000
		0.016	0.015	0.013	0.011	0.007	0.004	0.002	0.001	0.000	0.000	0.001	0.001	0.001	0.001	0.001	0.000	0.000
6.313	6.688	0.804	0.772	0.696	0.584	0.455	0.320	0.195	0.085	0.001	-0.058	-0.091	-0.101	-0.094	-0.075	-0.050	-0.024	0.000
		0.023	0.023	0.022	0.019	0.015	0.010	0.005	0.002	0.000	-0.001	-0.001	-0.001	0.000	0.000	0.000	0.000	0.000
9.470	10.031	0.661	0.637	0.578	0.487	0.381	0.269	0.164	0.072	0.001	-0.049	-0.077	-0.086	-0.080	-0.064	-0.043	-0.020	0.000
		0.023	0.023	0.022	0.019	0.016	0.011	0.006	0.002	0.000	-0.001	-0.002	-0.001	-0.001	-0.001	0.000	0.000	0.000
12.626	13.375	0.506	0.488	0.444	0.377	0.295	0.209	0.128	0.056	0.001	-0.038	-0.060	-0.067	-0.063	-0.050	-0.034	-0.016	0.000
		0.018	0.018	0.017	0.015	0.013	0.009	0.005	0.002	0.000	-0.001	-0.002	-0.001	-0.001	-0.001	0.000	0.000	0.000
15.783	16.719	0.351	0.340	0.310	0.263	0.207	0.147	0.090	0.040	0.001	-0.027	-0.043	-0.048	-0.045	-0.036	-0.024	-0.011	0.000
		0.012	0.012	0.011	0.010	0.008	0.006	0.004	0.001	0.000	-0.001	-0.001	-0.001	-0.001	-0.001	0.000	0.000	0.000
18.939	20.063	0.210	0.203	0.186	0.158	0.125	0.089	0.054	0.024	0.000	-0.016	-0.026	-0.029	-0.027	-0.022	-0.015	-0.007	0.000
		0.006	0.006	0.005	0.005	0.004	0.003	0.002	0.001	0.000	0.000	-0.001	0.000	0.000	0.000	0.000	0.000	0.000
22.096	23.407	0.088	0.085	0.078	0.067	0.053	0.038	0.023	0.010	0.000	-0.007	-0.011	-0.012	-0.012	-0.009	-0.006	-0.003	0.000
		0.002	0.002	0.002	0.002	0.001	0.001	0.001	0.000	0.000	0.000	0.000	0.000	0.000	0.000	0.000	0.000	0.000
25.253	26.751	-0.005	-0.005	-0.004	-0.004	-0.003	-0.002	-0.001	-0.001	0.000	0.000	0.001	0.001	0.001	0.001	0.000	0.000	0.000
		0.000	0.000	0.000	0.000	0.000	0.000	0.000	0.000	0.000	0.000	0.000	0.000	0.000	0.000	0.000	0.000	0.000
28.409	30.094	-0.071	-0.069	-0.063	-0.054	-0.043	-0.031	-0.019	-0.008	0.000	0.008	0.009	0.010	0.010	0.008	0.005	0.002	0.000
		0.000	0.000	0.000	0.000	0.000	0.000	0.000	0.000	0.000	0.000	0.000	0.000	0.000	0.000	0.000	0.000	0.000
31.566	33.438	-0.107	-0.104	-0.095	-0.082	-0.065	-0.047	-0.029	-0.013	0.000	0.009	0.014	0.016	0.015	0.012	0.008	0.004	0.000
		0.000	0.000	0.000	0.000	0.000	0.000	0.000	0.000	0.000	0.000	0.000	0.000	0.000	0.000	0.000	0.000	0.000
34.722	36.782	-0.118	-0.115	-0.105	-0.090	-0.072	-0.052	-0.032	-0.014	0.000	0.010	0.016	0.018	0.017	0.014	0.009	0.004	0.000
		0.001	0.001	0.001	0.001	0.001	0.001	0.000	0.000	0.000	0.000	0.000	0.000	0.000	0.000	0.000	0.000	0.000
37.879	40.126	-0.109	-0.106	-0.098	-0.084	-0.067	-0.048	-0.030	-0.013	0.000	0.009	0.015	0.017	0.016	0.013	0.009	0.004	0.000
		0.002	0.002	0.002	0.002	0.002	0.001	0.001	0.000	0.000	0.000	0.000	0.000	-0.001	0.000	0.000	0.000	0.000
41.035	43.470	-0.086	-0.084	-0.077	-0.066	-0.053	-0.038	-0.024	-0.011	0.000	0.008	0.012	0.013	0.013	0.010	0.007	0.003	0.000
		0.002	0.002	0.002	0.002	0.002	0.001	0.001	0.000	0.000	0.000	0.000	0.000	0.000	0.000	0.000	0.000	0.000
44.192	46.813	-0.056	-0.054	-0.050	-0.043	-0.034	-0.025	-0.016	-0.007	0.000	0.005	0.008	0.009	0.008	0.007	0.005	0.002	0.000
		0.002	0.002	0.002	0.002	0.001	0.001	0.001	0.000	0.000	0.000	0.000	0.000	0.000	0.000	0.000	0.000	0.000
47.348	50.157	-0.024	-0.024	-0.022	-0.019	-0.015	-0.011	-0.007	-0.003	0.000	0.002	0.003	0.004	0.004	0.003	0.002	0.001	0.000
		0.001	0.001	0.001	0.001	0.001	0.001	0.000	0.000	0.000	0.000	0.000	0.000	0.000	0.000	0.000	0.000	0.000
50.505	53.501	0.004	0.004	0.004	0.003	0.002	0.002	0.001	0.000	0.000	0.000	-0.001	-0.001	-0.001	0.000	0.000	0.000	0.000
		0.000	0.000	0.000	0.000	0.000	0.000	0.000	0.000	0.000	0.000	0.000	0.000	0.000	0.000	0.000	0.000	0.000

TABLE A-6

Spatial Transfer Function of Band 4

Frequency	mm⁻¹	0.000	3.157	6.313	9.470	12.626	15.783	18.939	22.096	25.253	28.409	31.566	34.722	37.879	41.035	44.192	47.348	50.505
	mrad⁻¹	0.000	3.344	6.688	10.031	13.375	16.719	20.063	23.407	26.751	30.094	33.438	36.782	40.126	43.470	46.813	50.157	53.501
mm⁻¹	mrad⁻¹																	
0.000	0.000	1.000	0.926	0.815	0.676	0.521	0.365	0.220	0.096	0.000	-0.065	-0.101	-0.113	-0.105	-0.084	-0.056	-0.026	0.000
		0.000	-0.002	-0.002	-0.003	-0.003	-0.003	-0.002	-0.001	0.000	0.001	0.002	0.003	0.003	0.002	0.001	0.001	0.000
3.157	3.344	0.919	0.877	0.781	0.649	0.502	0.352	0.213	0.093	0.000	-0.063	-0.099	-0.110	-0.102	-0.081	-0.054	-0.026	0.000
		0.015	0.014	0.014	0.011	0.007	0.004	0.002	0.000	0.000	0.000	0.001	0.001	0.002	0.001	0.001	0.000	0.000
6.313	6.688	0.804	0.774	0.694	0.582	0.451	0.317	0.192	0.084	0.000	-0.058	-0.090	-0.100	-0.093	-0.074	-0.050	-0.024	0.000
		0.021	0.021	0.020	0.018	0.014	0.009	0.005	0.002	0.000	0.000	0.000	0.000	0.000	0.001	0.000	0.000	0.000
9.470	10.031	0.660	0.638	0.576	0.485	0.378	0.267	0.162	0.071	0.000	-0.049	-0.076	-0.085	-0.079	-0.063	-0.042	-0.020	0.000
		0.020	0.021	0.020	0.018	0.014	0.010	0.005	0.002	0.000	-0.001	-0.001	-0.001	0.000	0.000	0.000	0.000	0.000
12.626	13.375	0.505	0.488	0.443	0.375	0.293	0.207	0.126	0.056	0.000	-0.038	-0.060	-0.067	-0.062	-0.050	-0.033	-0.016	0.000
		0.016	0.016	0.015	0.014	0.011	0.008	0.004	0.002	0.000	-0.001	-0.001	-0.001	0.000	0.000	0.000	0.000	0.000
15.783	16.719	0.350	0.339	0.309	0.262	0.206	0.146	0.089	0.039	0.000	-0.027	-0.042	-0.047	-0.044	-0.035	-0.024	-0.011	0.000
		0.010	0.010	0.009	0.009	0.007	0.005	0.003	0.001	0.000	-0.001	-0.001	0.000	0.000	0.000	0.000	0.000	0.000
18.939	20.063	0.209	0.202	0.184	0.157	0.124	0.088	0.054	0.024	0.000	-0.016	-0.026	-0.029	-0.027	-0.022	-0.014	-0.007	0.000
		0.005	0.005	0.004	0.004	0.003	0.002	0.001	0.001	0.000	0.000	0.000	0.000	0.000	0.000	0.000	0.000	0.000
22.096	23.407	0.088	0.085	0.078	0.066	0.052	0.037	0.023	0.010	0.000	-0.007	-0.011	-0.012	-0.012	-0.009	-0.006	-0.003	0.000
		0.001	0.001	0.001	0.001	0.001	0.001	0.000	0.000	0.000	0.000	0.000	0.000	0.000	0.000	0.000	0.000	0.000
25.253	26.751	-0.006	-0.006	-0.005	-0.005	-0.004	-0.003	-0.002	-0.001	0.000	0.001	0.001	0.001	0.001	0.001	0.000	0.000	0.000
		0.000	0.000	0.000	0.000	0.000	0.000	0.000	0.000	0.000	0.000	0.000	0.000	0.000	0.000	0.000	0.000	0.000
28.409	30.094	-0.071	-0.069	-0.063	-0.054	-0.043	-0.031	-0.019	-0.008	0.000	0.006	0.009	0.010	0.010	0.008	0.005	0.002	0.000
		0.000	0.000	0.000	0.000	0.000	0.000	0.000	0.000	0.000	0.000	0.000	0.000	0.000	0.000	0.000	0.000	0.000
31.566	33.438	-0.106	-0.103	-0.094	-0.081	-0.064	-0.046	-0.028	-0.013	0.000	0.009	0.014	0.016	0.015	0.012	0.008	0.004	0.000
		0.001	0.001	0.001	0.001	0.001	0.000	0.000	0.000	0.000	0.000	0.000	0.000	0.000	0.000	0.000	0.000	0.000
34.722	36.782	-0.117	-0.113	-0.104	-0.089	-0.071	-0.051	-0.032	-0.014	0.000	0.010	0.016	0.018	0.016	0.013	0.009	0.004	0.000
		0.002	0.002	0.002	0.002	0.001	0.001	0.001	0.000	0.000	0.000	0.000	0.000	-0.001	0.000	0.000	0.000	0.000
37.879	40.126	-0.107	-0.104	-0.096	-0.082	-0.065	-0.047	-0.029	-0.013	0.000	0.009	0.015	0.016	0.015	0.012	0.008	0.004	0.000
		0.003	0.003	0.003	0.002	0.002	0.001	0.001	0.000	0.000	0.000	0.000	-0.001	-0.001	-0.001	0.000	0.000	0.000
41.035	43.470	-0.085	-0.082	-0.075	-0.065	-0.052	-0.037	-0.023	-0.010	0.000	0.007	0.012	0.013	0.012	0.010	0.007	0.003	0.000
		0.003	0.003	0.003	0.003	0.002	0.001	0.001	0.000	0.000	0.000	0.000	0.000	-0.001	0.000	0.000	0.000	0.000
44.192	46.813	-0.055	-0.053	-0.049	-0.042	-0.034	-0.024	-0.015	-0.007	0.000	0.005	0.008	0.009	0.008	0.007	0.004	0.002	0.000
		0.002	0.003	0.002	0.002	0.002	0.001	0.001	0.000	0.000	0.000	0.000	0.000	0.000	0.000	0.000	0.000	0.000
47.348	50.157	-0.024	-0.023	-0.021	-0.018	-0.015	-0.011	-0.007	-0.003	0.000	0.002	0.003	0.004	0.004	0.003	0.002	0.001	0.000
		0.001	0.001	0.001	0.001	0.001	0.001	0.000	0.000	0.000	0.000	0.000	0.000	0.000	0.000	0.000	0.000	0.000
50.505	53.501	0.004	0.004	0.004	0.003	0.002	0.002	0.001	0.000	0.000	0.000	-0.001	-0.001	-0.001	0.000	0.000	0.000	0.000
		0.000	0.000	0.000	0.000	0.000	0.000	0.000	0.000	0.000	0.000	0.000	0.000	0.000	0.000	0.000	0.000	0.000

TABLE A-7

Spatial Transfer Function of Band 4'

Frequency	mm⁻¹	0.000	3.157	6.313	9.470	12.626	15.783	18.939	22.096	25.253	28.409	31.566	34.722	37.879	41.035	44.192	47.348	50.505
	mrad⁻¹	0.000	3.344	6.688	10.031	13.375	16.719	20.063	23.407	26.751	30.094	33.438	36.782	40.126	43.470	46.813	50.157	53.501
mm⁻¹	mrad⁻¹																	
0.000	0.000	1.000	0.926	0.814	0.674	0.519	0.363	0.218	0.096	0.001	-0.064	-0.101	-0.112	-0.104	-0.083	-0.055	-0.026	0.000
		0.000	-0.001	-0.002	-0.002	-0.002	-0.002	-0.002	-0.001	0.000	0.001	0.002	0.003	0.003	0.002	0.001	0.001	0.000
3.157	3.344	0.920	0.878	0.780	0.648	0.500	0.350	0.211	0.093	0.001	-0.062	-0.098	-0.109	-0.101	-0.081	-0.054	-0.025	0.000
		0.014	0.014	0.014	0.011	0.008	0.004	0.002	0.000	0.000	0.000	0.001	0.002	0.002	0.001	0.001	0.000	0.000
6.313	6.688	0.803	0.773	0.693	0.580	0.449	0.315	0.191	0.084	0.001	-0.057	-0.089	-0.099	-0.092	-0.074	-0.049	-0.023	0.000
		0.020	0.020	0.020	0.018	0.013	0.008	0.004	0.001	0.000	0.000	0.000	0.001	0.001	0.001	0.001	0.000	0.000
9.470	10.031	0.659	0.636	0.574	0.483	0.376	0.265	0.160	0.071	0.001	-0.048	-0.075	-0.084	-0.079	-0.063	-0.042	-0.020	0.000
		0.019	0.019	0.019	0.017	0.014	0.009	0.005	0.002	0.000	-0.001	-0.001	0.000	0.000	0.000	0.000	0.000	0.000
12.626	13.375	0.503	0.486	0.441	0.373	0.291	0.206	0.125	0.055	0.000	-0.037	-0.059	-0.066	-0.062	-0.050	-0.033	-0.016	0.000
		0.014	0.014	0.014	0.013	0.011	0.007	0.004	0.002	0.000	-0.001	-0.001	0.000	0.000	0.000	0.000	0.000	0.000
15.783	16.719	0.349	0.338	0.307	0.261	0.204	0.145	0.088	0.039	0.000	-0.027	-0.042	-0.047	-0.044	-0.035	-0.024	-0.011	0.000
		0.008	0.008	0.008	0.008	0.007	0.005	0.003	0.001	0.000	0.000	0.000	0.000	0.000	0.000	0.000	0.000	0.000
18.939	20.063	0.207	0.201	0.183	0.156	0.123	0.087	0.053	0.024	0.000	-0.016	-0.025	-0.029	-0.027	-0.021	-0.014	-0.007	0.000
		0.004	0.004	0.004	0.004	0.003	0.002	0.001	0.000	0.000	0.000	0.000	0.000	0.000	0.000	0.000	0.000	0.000
22.096	23.407	0.088	0.085	0.078	0.066	0.052	0.037	0.023	0.010	0.000	-0.007	-0.011	-0.012	-0.011	-0.009	-0.006	-0.003	0.000
		0.001	0.001	0.001	0.001	0.001	0.001	0.000	0.000	0.000	0.000	0.000	0.000	0.000	0.000	0.000	0.000	0.000
25.253	26.751	-0.006	-0.005	-0.005	-0.004	-0.003	-0.002	-0.001	-0.001	0.000	0.000	0.001	0.001	0.001	0.001	0.000	0.000	0.000
		0.000	0.000	0.000	0.000	0.000	0.000	0.000	0.000	0.000	0.000	0.000	0.000	0.000	0.000	0.000	0.000	0.000
28.409	30.094	-0.069	-0.067	-0.062	-0.053	-0.042	-0.030	-0.018	-0.008	0.000	0.006	0.009	0.010	0.009	0.008	0.005	0.002	0.000
		0.000	0.001	0.000	0.000	0.000	0.000	0.000	0.000	0.000	0.000	0.000	0.000	0.000	0.000	0.000	0.000	0.000
31.566	33.438	-0.105	-0.102	-0.093	-0.080	-0.063	-0.045	-0.028	-0.013	0.000	0.009	0.014	0.015	0.015	0.012	0.008	0.004	0.000
		0.002	0.002	0.002	0.001	0.001	0.001	0.000	0.000	0.000	0.000	0.000	0.000	0.000	0.000	0.000	0.000	0.000
34.722	36.782	-0.115	-0.112	-0.103	-0.088	-0.070	-0.050	-0.031	-0.014	0.000	0.010	0.015	0.017	0.016	0.013	0.009	0.004	0.000
		0.003	0.003	0.003	0.002	0.002	0.001	0.001	0.000	0.000	0.000	0.000	-0.001	-0.001	-0.001	0.000	0.000	0.000
37.879	40.126	-0.106	-0.103	-0.094	-0.081	-0.064	-0.046	-0.029	-0.013	0.000	0.009	0.014	0.016	0.015	0.012	0.008	0.004	0.000
		0.004	0.004	0.003	0.003	0.002	0.001	0.001	0.000	0.000	0.000	0.000	-0.001	-0.001	-0.001	0.000	0.000	0.000
41.035	43.470	-0.083	-0.081	-0.074	-0.064	-0.051	-0.037	-0.023	-0.010	0.000	0.007	0.011	0.013	0.012	0.010	0.007	0.003	0.000
		0.004	0.004	0.003	0.003	0.002	0.001	0.001	0.000	0.000	0.000	0.000	-0.001	-0.001	-0.001	0.000	0.000	0.000
44.192	46.813	-0.054	-0.052	-0.048	-0.041	-0.033	-0.024	-0.015	-0.007	0.000	0.005	0.007	0.008	0.008	0.006	0.004	0.002	0.000
		0.003	0.003	0.003	0.002	0.002	0.001	0.001	0.000	0.000	0.000	0.000	0.000	0.000	0.000	0.000	0.000	0.000
47.348	50.157	-0.023	-0.023	-0.021	-0.018	-0.014	-0.010	-0.006	-0.003	0.000	0.002	0.003	0.004	0.003	0.003	0.002	0.001	0.000
		0.001	0.001	0.001	0.001	0.001	0.001	0.000	0.000	0.000	0.000	0.000	0.000	0.000	0.000	0.000	0.000	0.000
50.505	53.501	0.004	0.004	0.003	0.003	0.002	0.002	0.001	0.000	0.000	0.000	-0.001	-0.001	-0.001	0.000	0.000	0.000	0.000
		0.000	0.000	0.000	0.000	0.000	0.000	0.000	0.000	0.000	0.000	0.000	0.000	0.000	0.000	0.000	0.000	0.000

TABLE A-8

Spatial Transfer Function of Band 5'

Frequency	mm^{-1}	0.000	3.157	6.313	9.470	12.626	15.783	18.939	22.096	25.253	28.409	31.566	34.722	37.879	41.035	44.192	47.348	50.505
	$mrad^{-1}$	0.000	3.344	6.688	10.031	13.375	16.719	20.063	23.407	26.751	30.094	33.438	36.782	40.126	43.470	46.813	50.157	53.501
mm^{-1}	$mrad^{-1}$																	
0.000	0.000	1.000	0.913	0.777	0.618	0.456	0.309	0.186	0.092	0.027	-0.013	-0.033	-0.039	-0.036	-0.028	-0.019	-0.011	-0.005
		0.000	0.000	-0.001	-0.001	-0.002	-0.003	-0.002	-0.001	-0.001	0.000	0.001	0.001	0.000	0.000	0.000	0.000	0.000
3.157	3.344	0.910	0.858	0.739	0.590	0.438	0.298	0.180	0.089	0.026	-0.013	-0.032	-0.038	-0.035	-0.028	-0.019	-0.011	-0.005
		0.011	0.012	0.012	0.009	0.005	0.002	0.000	-0.001	0.000	0.000	0.000	0.000	0.000	0.000	0.000	0.000	0.000
6.313	6.688	0.770	0.735	0.643	0.519	0.388	0.265	0.161	0.080	0.024	-0.011	-0.029	-0.034	-0.032	-0.025	-0.017	-0.010	-0.004
		0.016	0.017	0.017	0.014	0.009	0.004	0.002	0.000	0.000	0.000	0.000	0.000	0.000	0.000	0.000	0.000	0.000
9.470	10.031	0.610	0.586	0.518	0.423	0.318	0.219	0.133	0.067	0.020	-0.009	-0.024	-0.029	-0.027	-0.021	-0.015	-0.009	-0.004
		0.014	0.014	0.014	0.012	0.009	0.005	0.002	0.001	0.000	0.000	0.000	0.000	0.000	0.000	0.000	0.000	0.000
12.626	13.375	0.451	0.434	0.387	0.319	0.242	0.167	0.103	0.052	0.015	-0.007	-0.019	-0.023	-0.021	-0.017	-0.012	-0.007	-0.003
		0.009	0.009	0.009	0.008	0.006	0.004	0.002	0.001	0.000	0.000	0.000	0.000	0.000	0.000	0.000	0.000	0.000
15.783	16.719	0.307	0.296	0.265	0.220	0.168	0.117	0.072	0.036	0.011	-0.005	-0.014	-0.016	-0.015	-0.012	-0.008	-0.005	-0.002
		0.004	0.004	0.004	0.004	0.003	0.002	0.001	0.000	0.000	0.000	0.000	0.000	0.000	0.000	0.000	0.000	0.000
18.939	20.063	0.186	0.178	0.161	0.135	0.104	0.073	0.045	0.023	0.007	-0.003	-0.009	-0.010	-0.010	-0.008	-0.005	-0.003	-0.001
		0.001	0.001	0.001	0.001	0.001	0.001	0.000	0.000	0.000	0.000	0.000	0.000	0.000	0.000	0.000	0.000	0.000
22.096	23.407	0.093	0.090	0.081	0.068	0.052	0.037	0.023	0.012	0.004	-0.002	-0.004	-0.005	-0.005	-0.004	-0.003	-0.002	-0.001
		0.000	-0.001	0.000	0.000	0.000	0.000	0.000	0.000	0.000	0.000	0.000	0.000	0.000	0.000	0.000	0.000	0.000
25.253	26.751	0.027	0.026	0.024	0.020	0.016	0.011	0.007	0.004	0.001	-0.001	-0.001	-0.002	-0.002	-0.001	-0.001	-0.001	0.000
		0.000	0.000	0.000	0.000	0.000	0.000	0.000	0.000	0.000	0.000	0.000	0.000	0.000	0.000	0.000	0.000	0.000
28.409	30.094	-0.013	-0.013	-0.011	-0.010	-0.008	-0.005	-0.003	-0.002	-0.001	0.000	0.001	0.001	0.001	0.001	0.000	0.000	0.000
		0.000	0.000	0.000	0.000	0.000	0.000	0.000	0.000	0.000	0.000	0.000	0.000	0.000	0.000	0.000	0.000	0.000
31.566	33.438	-0.033	-0.032	-0.029	-0.025	-0.020	-0.014	-0.009	-0.005	-0.001	0.001	0.002	0.002	0.002	0.002	0.001	0.001	0.000
		0.001	0.001	0.001	0.001	0.001	0.000	0.000	0.000	0.000	0.000	0.000	0.000	0.000	0.000	0.000	0.000	0.000
34.722	36.782	-0.040	-0.038	-0.035	-0.030	-0.023	-0.017	-0.011	-0.005	-0.002	0.001	0.002	0.003	0.003	0.002	0.001	0.001	0.000
		0.002	0.002	0.001	0.001	0.001	0.001	0.000	0.000	0.000	0.000	0.000	0.000	0.000	0.000	0.000	0.000	0.000
37.879	40.126	-0.037	-0.035	-0.032	-0.027	-0.022	-0.016	-0.010	-0.005	-0.002	0.001	0.002	0.003	0.002	0.002	0.001	0.001	0.000
		0.002	0.002	0.002	0.001	0.001	0.001	0.000	0.000	0.000	0.000	0.000	0.000	0.000	0.000	0.000	0.000	0.000
41.035	43.470	-0.029	-0.028	-0.026	-0.022	-0.017	-0.012	-0.008	-0.004	-0.001	0.001	0.002	0.002	0.002	0.002	0.001	0.001	0.000
		0.002	0.002	0.001	0.001	0.001	0.001	0.000	0.000	0.000	0.000	0.000	0.000	0.000	0.000	0.000	0.000	0.000
44.192	46.813	-0.020	-0.019	-0.018	-0.015	-0.012	-0.009	-0.006	-0.003	-0.001	0.000	0.001	0.001	0.001	0.001	0.001	0.000	0.000
		0.001	0.001	0.001	0.001	0.001	0.000	0.000	0.000	0.000	0.000	0.000	0.000	0.000	0.000	0.000	0.000	0.000
47.348	50.157	-0.012	-0.011	-0.010	-0.009	-0.007	-0.005	-0.003	-0.002	-0.001	0.000	0.001	0.001	0.001	0.001	0.000	0.000	0.000
		0.001	0.001	0.001	0.001	0.000	0.000	0.000	0.000	0.000	0.000	0.000	0.000	0.000	0.000	0.000	0.000	0.000
50.505	53.501	-0.005	-0.005	-0.005	-0.004	-0.003	-0.002	-0.001	-0.001	0.000	0.000	0.000	0.000	0.000	0.000	0.000	0.000	0.000
		0.000	0.000	0.000	0.000	0.000	0.000	0.000	0.000	0.000	0.000	0.000	0.000	0.000	0.000	0.000	0.000	0.000

TABLE A-9

Spatial Transfer Function of Band 5

Frequency	mm^{-1}	0.000	3.157	6.313	9.470	12.626	15.783	18.939	22.096	25.253	28.409	31.566	34.722	37.879	41.035	44.192	47.348	50.505
	$mrad^{-1}$	0.000	3.344	6.688	10.031	13.375	16.719	20.063	23.407	26.751	30.094	33.438	36.782	40.126	43.470	46.813	50.157	53.501
mm^{-1}	$mrad^{-1}$																	
0.000	0.000	1.000	0.905	0.760	0.595	0.433	0.289	0.172	0.084	0.024	-0.011	-0.028	-0.032	-0.029	-0.022	-0.014	-0.008	-0.003
		0.000	0.000	0.000	-0.002	-0.003	-0.003	-0.002	-0.001	0.000	0.000	0.000	0.000	0.000	0.000	0.000	0.000	0.000
3.157	3.344	0.902	0.846	0.720	0.568	0.416	0.278	0.165	0.081	0.023	-0.011	-0.027	-0.031	-0.028	-0.021	-0.014	-0.008	-0.003
		0.010	0.012	0.011	0.007	0.002	0.000	-0.001	-0.001	0.000	0.000	0.000	0.000	0.000	0.000	0.000	0.000	0.000
6.313	6.688	0.754	0.718	0.622	0.497	0.366	0.247	0.147	0.072	0.021	-0.010	-0.024	-0.028	-0.025	-0.019	-0.013	-0.007	-0.003
		0.013	0.015	0.015	0.011	0.006	0.002	0.000	0.000	0.000	0.000	0.000	0.000	0.000	0.000	0.000	0.000	0.000
9.470	10.031	0.591	0.566	0.497	0.401	0.299	0.202	0.122	0.060	0.017	-0.008	-0.020	-0.024	-0.021	-0.016	-0.011	-0.006	-0.002
		0.010	0.010	0.011	0.009	0.005	0.002	0.001	0.000	0.000	0.000	0.000	0.000	0.000	0.000	0.000	0.000	0.000
12.626	13.375	0.431	0.414	0.367	0.299	0.224	0.153	0.093	0.046	0.013	-0.006	-0.016	-0.018	-0.016	-0.013	-0.008	-0.005	-0.002
		0.004	0.004	0.005	0.005	0.003	0.002	0.000	0.000	0.000	0.000	0.000	0.000	0.000	0.000	0.000	0.000	0.000
15.783	16.719	0.289	0.278	0.247	0.204	0.154	0.106	0.064	0.032	0.009	-0.004	-0.011	-0.013	-0.012	-0.009	-0.006	-0.003	-0.001
		0.000	0.000	0.001	0.001	0.001	0.001	0.000	0.000	0.000	0.000	0.000	0.000	0.000	0.000	0.000	0.000	0.000
18.939	20.063	0.172	0.166	0.148	0.123	0.093	0.065	0.039	0.020	0.006	-0.003	-0.007	-0.008	-0.007	-0.006	-0.004	-0.002	-0.001
		-0.001	-0.001	-0.001	0.000	0.000	0.000	0.000	0.000	0.000	0.000	0.000	0.000	0.000	0.000	0.000	0.000	0.000
22.096	23.407	0.084	0.081	0.073	0.061	0.046	0.032	0.020	0.010	0.003	-0.001	-0.004	-0.004	-0.004	-0.003	-0.002	-0.001	0.000
		-0.001	-0.001	-0.001	-0.001	0.000	0.000	0.000	0.000	0.000	0.000	0.000	0.000	0.000	0.000	0.000	0.000	0.000
25.253	26.751	0.024	0.023	0.021	0.018	0.014	0.009	0.006	0.003	0.001	0.000	-0.001	-0.001	-0.001	-0.001	-0.001	0.000	0.000
		-0.001	-0.001	-0.001	0.000	0.000	0.000	0.000	0.000	0.000	0.000	0.000	0.000	0.000	0.000	0.000	0.000	0.000
28.409	30.094	-0.011	-0.011	-0.010	-0.008	-0.006	-0.004	-0.003	-0.001	0.000	0.000	0.001	0.001	0.001	0.000	0.000	0.000	0.000
		0.000	0.000	0.000	0.000	0.000	0.000	0.000	0.000	0.000	0.000	0.000	0.000	0.000	0.000	0.000	0.000	0.000
31.566	33.438	-0.028	-0.027	-0.025	-0.021	-0.016	-0.011	-0.007	-0.004	-0.001	0.001	0.001	0.002	0.001	0.001	0.001	0.000	0.000
		0.001	0.001	0.001	0.001	0.001	0.000	0.000	0.000	0.000	0.000	0.000	0.000	0.000	0.000	0.000	0.000	0.000
34.722	36.782	-0.032	-0.031	-0.028	-0.024	-0.019	-0.013	-0.008	-0.004	-0.001	0.001	0.002	0.002	0.002	0.001	0.001	0.000	0.000
		0.002	0.001	0.001	0.001	0.001	0.001	0.000	0.000	0.000	0.000	0.000	0.000	0.000	0.000	0.000	0.000	0.000
37.879	40.126	-0.029	-0.028	-0.025	-0.021	-0.017	-0.012	-0.007	-0.004	-0.001	0.001	0.001	0.002	0.001	0.001	0.001	0.000	0.000
		0.002	0.001	0.001	0.001	0.001	0.001	0.000	0.000	0.000	0.000	0.000	0.000	0.000	0.000	0.000	0.000	0.000
41.035	43.470	-0.022	-0.021	-0.019	-0.016	-0.013	-0.009	-0.006	-0.003	-0.001	0.000	0.001	0.001	0.001	0.001	0.001	0.000	0.000
		0.001	0.001	0.001	0.001	0.001	0.000	0.000	0.000	0.000	0.000	0.000	0.000	0.000	0.000	0.000	0.000	0.000
44.192	46.813	-0.015	-0.014	-0.013	-0.011	-0.008	-0.006	-0.004	-0.002	-0.001	0.000	0.001	0.001	0.001	0.001	0.000	0.000	0.000
		0.001	0.001	0.001	0.000	0.000	0.000	0.000	0.000	0.000	0.000	0.000	0.000	0.000	0.000	0.000	0.000	0.000
47.348	50.157	-0.008	-0.008	-0.007	-0.006	-0.005	-0.003	-0.002	-0.001	0.000	0.000	0.000	0.000	0.000	0.000	0.000	0.000	0.000
		0.000	0.000	0.000	0.000	0.000	0.000	0.000	0.000	0.000	0.000	0.000	0.000	0.000	0.000	0.000	0.000	0.000
50.505	53.501	-0.003	-0.003	-0.003	-0.002	-0.002	-0.001	-0.001	0.000	0.000	0.000	0.000	0.000	0.000	0.000	0.000	0.000	0.000
		0.000	0.000	0.000	0.000	0.000	0.000	0.000	0.000	0.000	0.000	0.000	0.000	0.000	0.000	0.000	0.000	0.000

TABLE A-10

Spatial Transfer Function of Band 7

Frequency	mm^{-1}	0.000	3.157	6.313	9.470	12.626	15.783	18.939	22.096	25.253	28.409	31.566	34.722	37.879	41.035	44.192	47.348	50.505
	$mrad^{-1}$	0.000	3.344	6.688	10.031	13.375	16.719	20.063	23.407	26.751	30.094	33.438	36.782	40.126	43.470	46.813	50.157	53.501
mm^{-1}	$mrad^{-1}$																	
0.000	0.000	1.000	0.890	0.733	0.562	0.400	0.260	0.149	0.070	0.019	-0.009	-0.020	-0.022	-0.018	-0.012	-0.007	-0.003	-0.001
		0.000	0.000	-0.001	-0.003	-0.004	-0.003	-0.002	0.000	0.000	0.000	0.000	0.000	0.000	0.000	0.000	0.000	0.000
3.157	3.344	0.888	0.826	0.692	0.535	0.382	0.249	0.144	0.068	0.019	-0.008	-0.020	-0.021	-0.017	-0.012	-0.007	-0.003	-0.001
		0.010	0.012	0.009	0.004	0.000	-0.001	-0.001	0.000	0.000	0.000	0.000	0.000	0.000	0.000	0.000	0.000	0.000
6.313	6.688	0.730	0.690	0.591	0.463	0.334	0.219	0.127	0.060	0.017	-0.007	-0.018	-0.019	-0.015	-0.010	-0.006	-0.003	-0.001
		0.010	0.012	0.011	0.007	0.002	0.000	0.000	0.000	0.000	0.000	0.000	0.000	0.000	0.000	0.000	0.000	0.000
9.470	10.031	0.560	0.534	0.464	0.368	0.268	0.177	0.103	0.049	0.014	-0.006	-0.015	-0.016	-0.013	-0.009	-0.005	-0.002	-0.001
		0.004	0.005	0.006	0.005	0.002	0.000	0.000	0.000	0.000	0.000	0.000	0.000	0.000	0.000	0.000	0.000	0.000
12.626	13.375	0.399	0.382	0.335	0.269	0.198	0.132	0.077	0.037	0.010	-0.005	-0.011	-0.012	-0.010	-0.006	-0.004	-0.002	0.000
		0.000	0.000	0.001	0.001	0.001	0.000	0.000	0.000	0.000	0.000	0.000	0.000	0.000	0.000	0.000	0.000	0.000
15.783	16.719	0.260	0.249	0.220	0.178	0.132	0.089	0.052	0.025	0.007	-0.003	-0.008	-0.008	-0.007	-0.004	-0.002	-0.001	0.000
		-0.003	-0.002	-0.002	-0.001	-0.001	-0.001	-0.001	0.000	0.000	0.000	0.000	0.000	0.000	0.000	0.000	0.000	0.000
18.939	20.063	0.150	0.144	0.128	0.104	0.078	0.053	0.031	0.015	0.004	-0.002	-0.005	-0.005	-0.004	-0.003	-0.001	-0.001	0.000
		-0.003	-0.003	-0.002	-0.001	-0.001	-0.001	-0.001	0.000	0.000	0.000	0.000	0.000	0.000	0.000	0.000	0.000	0.000
22.096	23.407	0.070	0.068	0.060	0.049	0.037	0.025	0.015	0.007	0.002	-0.001	-0.002	-0.002	-0.002	-0.001	-0.001	0.000	0.000
		-0.002	-0.002	-0.001	-0.001	-0.001	-0.001	0.000	0.000	0.000	0.000	0.000	0.000	0.000	0.000	0.000	0.000	0.000
25.253	26.751	0.019	0.019	0.017	0.014	0.010	0.007	0.004	0.002	0.001	0.000	-0.001	-0.001	-0.001	0.000	0.000	0.000	0.000
		-0.001	-0.001	-0.001	0.000	0.000	0.000	0.000	0.000	0.000	0.000	0.000	0.000	0.000	0.000	0.000	0.000	0.000
28.409	30.094	-0.009	-0.008	-0.007	-0.006	-0.005	-0.003	-0.002	-0.001	0.000	0.000	0.000	0.000	0.000	0.000	0.000	0.000	0.000
		0.000	0.000	0.000	0.000	0.000	0.000	0.000	0.000	0.000	0.000	0.000	0.000	0.000	0.000	0.000	0.000	0.000
31.566	33.438	-0.020	-0.020	-0.018	-0.015	-0.011	-0.008	-0.004	-0.002	-0.001	0.000	0.001	0.001	0.000	0.000	0.000	0.000	0.000
		0.001	0.001	0.001	0.000	0.000	0.000	0.000	0.000	0.000	0.000	0.000	0.000	0.000	0.000	0.000	0.000	0.000
34.722	36.782	-0.022	-0.021	-0.019	-0.015	-0.012	-0.008	-0.005	-0.002	-0.001	0.000	0.001	0.001	0.000	0.000	0.000	0.000	0.000
		0.001	0.001	0.000	0.000	0.000	0.000	0.000	0.000	0.000	0.000	0.000	0.000	0.000	0.000	0.000	0.000	0.000
37.879	40.126	-0.018	-0.017	-0.015	-0.013	-0.009	-0.006	-0.004	-0.002	0.000	0.000	0.000	0.000	0.000	0.000	0.000	0.000	0.000
		0.000	0.000	0.000	0.000	0.000	0.000	0.000	0.000	0.000	0.000	0.000	0.000	0.000	0.000	0.000	0.000	0.000
41.035	43.470	-0.012	-0.012	-0.010	-0.008	-0.006	-0.004	-0.002	-0.001	0.000	0.000	0.000	0.000	0.000	0.000	0.000	0.000	0.000
		0.000	0.000	0.000	0.000	0.000	0.000	0.000	0.000	0.000	0.000	0.000	0.000	0.000	0.000	0.000	0.000	0.000
44.192	46.813	-0.007	-0.006	-0.006	-0.005	-0.003	-0.002	-0.001	-0.001	0.000	0.000	0.000	0.000	0.000	0.000	0.000	0.000	0.000
		0.000	0.000	0.000	0.000	0.000	0.000	0.000	0.000	0.000	0.000	0.000	0.000	0.000	0.000	0.000	0.000	0.000
47.348	50.157	-0.003	-0.003	-0.003	-0.002	-0.002	-0.001	-0.001	0.000	0.000	0.000	0.000	0.000	0.000	0.000	0.000	0.000	0.000
		0.000	0.000	0.000	0.000	0.000	0.000	0.000	0.000	0.000	0.000	0.000	0.000	0.000	0.000	0.000	0.000	0.000
50.505	53.501	-0.001	-0.001	-0.001	-0.001	0.000	0.000	0.000	0.000	0.000	0.000	0.000	0.000	0.000	0.000	0.000	0.000	0.000
		0.000	0.000	0.000	0.000	0.000	0.000	0.000	0.000	0.000	0.000	0.000	0.000	0.000	0.000	0.000	0.000	0.000

APPENDIX B

ESTIMATED ZERNIKE POLYNOMIAL COEFFICIENTS OF WAVEFRONT ERRORS

SSG, Inc. used a laser unequal-path interferometer (LUPI) to characterize the WFE of the ALI after final alignment of the optical system. They obtained interferograms at eleven points distributed over the 1.26°x15° field of view of the optical system. The interferograms were referenced to a fixture representing the focal plane. The WFE derived from each interferogram was fitted with a set of 37 Zernike polynomials.

The coordinates on the focal plane where the interferograms were made are given in Table B-1. Those positions are referred to the center of the 15°x1.26° field, with X_{SC} the in-track direction, and the SCAs at the $+Y_{SC}$ end of the focal plane. Table B-2 lists the Zernike polynomial definitions used here. The derived coefficients for Zernike terms 4 through 37 are shown in Table B-3. (Terms 1, 2, and 3 are set to zero, since they only represent average phase and tilt of the wavefront.)

TABLE B-1

Measurement Positions in the Focal Plane

Position	X_{SC} (mm)	Y_{SC} (mm)
FP 1	-10.16	127.00
FP 2	0.00	127.00
FP 3	10.16	127.00
FP 4	-10.16	63.50
FP 5	0.00	63.50
FP 6	10.16	63.50
FP 7	-10.16	0.00
FP 8	0.00	0.00
FP 9	10.16	0.00
FP 10	-10.16	-127.00
FP 12	10.16	-127.00

TABLE B-2

Zernike Polynomial Definitions

Term	Polynomial	Term	Polynomial
1	1		
2	$r\cos(\theta)$	14	$\left(10r^5 - 12r^3 + 3r\right)\cos(\theta)$
3	$r\sin(\theta)$	15	$\left(10r^5 - 12r^3 + 3r\right)\sin(\theta)$
4	$2r^2 - 1$	16	$20r^6 - 30r^4 + 12r^2 - 1$
5	$r^2\cos(2\theta)$	17	$r^4\cos(4\theta)$
6	$r^2\sin(2\theta)$	18	$r^4\sin(4\theta)$
7	$\left(3r^3 - 2r\right)\cos(\theta)$	19	$\left(5r^5 - 4r^3\right)\cos(3\theta)$
8	$\left(3r^3 - 2r\right)\sin(\theta)$	20	$\left(5r^5 - 4r^3\right)\sin(3\theta)$
9	$6r^4 - 6r^2 + 1$	21	$\left(15r^6 - 20r^4 + 6r^2\right)\cos(2\theta)$
10	$r^3\cos(3\theta)$	22	$\left(15r^6 - 20r^4 + 6r^2\right)\sin(2\theta)$
11	$r^3\sin(3\theta)$	23	$\left(35r^7 - 60r^5 + 30r^3 - 4r\right)\cos(\theta)$
12	$\left(4r^4 - 3r^2\right)\cos(2\theta)$	24	$\left(35r^7 - 60r^5 + 30r^3 - 4r\right)\sin(\theta)$
13	$\left(4r^4 - 3r^2\right)\sin(2\theta)$	25	$70r^8 - 140r^6 + 90r^4 - 20r^2 + 1$
26	$r^5\cos(5\theta)$		
27	$r^5\sin(5\theta)$		
28	$\left(6r^6 - 5r^4\right)\cos(4\theta)$		
29	$\left(6r^6 - 5r^4\right)\sin(4\theta)$		
30	$\left(21r^7 - 30r^5 + 10r^3\right)\cos(3\theta)$		
31	$\left(21r^7 - 30r^5 + 10r^3\right)\sin(3\theta)$		
32	$\left(56r^8 - 105r^6 + 60r^4 - 10r^2\right)\cos(2\theta)$		
33	$\left(56r^8 - 105r^6 + 60r^4 - 10r^2\right)\sin(2\theta)$		
34	$\left(126r^9 - 280r^7 + 210r^5 - 60r^3 + 5r\right)\cos(\theta)$		
35	$\left(126r^9 - 280r^7 + 210r^5 - 60r^3 + 5r\right)\sin(\theta)$		
36	$252r^{10} - 630r^8 + 560r^6 - 210r^4 + 30r^2 - 1$		
37	$924r^{12} - 2772r^{10} + 3150r^8 - 1680r^6 + 420r^4 - 42r^2 + 1$		

TABLE B-3

Estimated Zernike Polynomial Coefficients

Term	Position					
	FP 1	FP 2	FP 3	FP 4	FP 5	FP 6
4	-0.7885	-0.7765	-0.7463	-0.7080	-0.7567	-0.7572
5	0.1889	0.1747	0.1559	-0.0811	-0.0642	-0.0721
6	-0.0999	-0.0197	0.0176	0.0962	0.1117	0.0993
7	0.1275	0.1197	0.1179	0.0164	-0.0023	-0.0269
8	0.0573	0.0019	-0.0002	0.0284	0.0150	-0.0228
9	0.0639	0.0769	0.0746	-0.0022	0.0126	0.0197
10	0.1184	0.1021	0.0615	-0.0934	-0.1030	-0.0813
11	-0.0217	0.0163	0.0093	0.0373	0.0470	0.0696
12	0.1367	0.1438	0.1448	0.0472	0.0201	-0.0010
13	-0.0247	0.0110	0.0593	0.0188	0.0466	0.0701
14	0.0468	0.0174	0.0176	-0.0322	-0.0406	-0.0376
15	-0.0093	-0.0454	0.0176	0.0189	0.0218	0.0175
16	0.0373	0.0023	-0.0049	0.0287	0.0282	0.0335
17	0.1495	0.1184	0.0712	-0.0075	0.0520	0.0986
18	0.0055	0.0098	-0.0339	0.0323	0.0095	0.0049
19	-0.0355	0.0649	0.0797	0.0157	0.0205	0.0122
20	-0.0230	0.0202	0.0147	0.0098	0.0269	0.0195
21	-0.0355	0.0190	0.0655	0.0054	-0.0009	-0.0054
22	0.0413	0.0097	0.0018	0.0011	-0.0116	-0.0089
23	-0.0160	-0.0113	0.0133	0.0217	0.0102	0.0102
24	0.0452	0.0400	0.0182	-0.0097	-0.0182	-0.0199
25	-0.0018	0.0012	0.0073	0.0047	-0.0038	-0.0144
26	0.0372	-0.0232	-0.0386	-0.0133	-0.0235	0.0031
27	0.0931	0.0793	0.0476	-0.0287	-0.0592	-0.0445
28	0.0140	0.0506	0.0227	0.0050	-0.0109	-0.0421
29	-0.0397	-0.0083	0.0181	0.0178	0.0104	-0.0058
30	-0.0554	-0.0006	0.0211	-0.0129	-0.0024	-0.0114
31	0.0200	-0.0097	-0.0224	-0.0168	-0.0091	-0.0162
32	-0.0367	-0.0014	0.0226	-0.0167	0.0001	0.0076
33	0.0332	0.0292	-0.0032	0.0288	0.0129	0.0044
34	-0.0710	-0.0423	-0.0120	-0.0204	-0.0049	0.0023
35	-0.0494	-0.0053	-0.0262	-0.0179	-0.0078	-0.0166
36	-0.0103	-0.0279	0.0007	-0.0076	-0.0066	0.0043
37	0.0074	0.0195	0.0058	-0.0001	0.0006	-0.0139

(continued)

TABLE B-3

Estimated Zernike Polynomial Coefficients (continued)

Term	Position				
	FP 7	FP 8	FP 9	FP 10	FP 12
4	-0.5369	-0.5140	-0.5408	-0.3554	-0.3121
5	-0.0484	-0.0134	0.0090	0.1974	0.2517
6	0.0171	0.0186	0.0180	-0.0154	-0.0718
7	-0.0316	-0.0535	-0.0554	-0.1158	-0.1316
8	-0.0264	-0.0469	-0.0925	0.1282	0.0171
9	-0.0489	-0.0443	-0.0328	0.0463	0.0460
10	-0.0442	-0.0369	-0.0184	-0.0219	0.0051
11	-0.0752	-0.0906	-0.0851	0.0581	0.0623
12	0.0198	-0.0164	-0.0507	0.0773	0.0699
13	0.0712	0.0717	0.0587	0.0112	-0.0616
14	0.0290	0.0196	0.0029	0.0400	0.0525
15	-0.0122	-0.0303	-0.0247	0.0097	-0.0134
16	0.0643	0.0630	0.0579	0.0332	0.0272
17	-0.0522	-0.0156	0.0230	0.1109	0.0636
18	0.0376	0.0209	0.0107	-0.0263	-0.0509
19	0.0064	0.0017	0.0001	0.0287	0.0175
20	0.0239	0.0394	0.0433	-0.0266	0.0215
21	0.0042	0.0100	0.0153	-0.0075	0.0171
22	-0.0359	-0.0171	-0.0177	-0.0352	-0.0119
23	-0.0083	-0.0028	0.0053	-0.0102	-0.0205
24	-0.0108	-0.0062	0.0192	-0.0142	0.0208
25	-0.0004	-0.0131	-0.0125	-0.0155	0.0017
26	0.0289	-0.0018	-0.0249	-0.0076	0.0485
27	0.0117	0.0029	0.0021	0.1166	0.0532
28	-0.0165	-0.0078	-0.0006	-0.0726	0.0184
29	0.0059	-0.0179	-0.0240	0.0018	0.0010
30	-0.0103	-0.0081	-0.0131	-0.0208	-0.0107
31	-0.0094	0.0004	-0.0071	-0.0080	-0.0050
32	-0.0239	-0.0039	0.0094	-0.0012	-0.0264
33	0.0079	-0.0104	-0.0158	0.0531	-0.0296
34	-0.0094	-0.0216	-0.0174	0.0026	-0.0003
35	-0.0299	-0.0141	-0.0082	-0.0514	0.0006
36	-0.0045	-0.0173	-0.0114	0.0048	0.0029
37	-0.0013	0.0067	0.0065	0.0268	-0.0044

REPORT DOCUMENTATION PAGE

Form Approved
OMB No. 0704-0188

Public reporting burden for this collection of information is estimated to average 1 hour per response, including the time for reviewing instructions, searching existing data sources, gathering and maintaining the data needed, and completing and reviewing the collection of information. Send comments regarding this burden estimate or any other aspect of this collection of information, including suggestions for reducing this burden, to Washington Headquarters Services, Directorate for Information Operations and Reports, 1215 Jefferson Davis Highway, Suite 1204, Arlington, VA 22202-4302, and to the Office of Management and Budget, Paperwork Reduction Project (0704-0188), Washington, DC 20503.

1. AGENCY USE ONLY (*Leave blank*)

2. REPORT DATE
22 March 2000

3. REPORT TYPE AND DATES COVERED
Technical Report

4. TITLE AND SUBTITLE
EO-1 Advanced Land Imager Modulation Transfer Functions

5. FUNDING NUMBERS
C—F19628-95-C-0002

6. AUTHOR(S)
D.R. Hearn

7. PERFORMING ORGANIZATION NAME(S) AND ADDRESS(ES)
Lincoln Laboratory, MIT
244 Wood Street
Lexington, MA 02420-9108

8. PERFORMING ORGANIZATION REPORT NUMBER
TR-1061

9. SPONSORING/MONITORING AGENCY NAME(S) AND ADDRESS(ES)
NASA/GSFC
Mr. Ralph Welsh
Building 16, Room 21 MS740.3
Greenbelt, MD 20771

10. SPONSORING/MONITORING AGENCY REPORT NUMBER
ESC-TR-99-058

11. SUPPLEMENTARY NOTES
None

12a. DISTRIBUTION/AVAILABILITY STATEMENT
Distribution authorized to U.S. Goverment agencies and their contractors; test and evaluation, 7 March 2000. Other requests for this document shall be referred to NASA/GSFC.

12b. DISTRIBUTION CODE

13. ABSTRACT (*Maximum 200 words*)

This report presents results of laboratory calibrations of the EO-1 Advanced Land Imager (ALI) instrument. Specifically, it is concerned with the estimated spatial modulation transfer function, or MTF. A combination of design data for the detectors, measurements on the optical subsystem, and laboratory measurements of the complete instrument are used to construct a model of the system spatial transfer function (STF) of the ALI. The optical subsystem measurements, done by the telescope builder, SSG, consisted of interferograms, which they analyzed with Zernike polynomials. Those polynomials were used to model the optical transfer function. The system measurements were scans of a knife-edge, viewed through an imaging collimator. The parameters of the STF model, in particular focus error and carrier diffusion in the detectors, were adjusted to obtain the best agreement with the system measurements. The full, two-dimensional STF's for the ten spectral bands of the instrument are presented.

14. SUBJECT TERMS

15. NUMBER OF PAGES
68

16. PRICE CODE

17. SECURITY CLASSIFICATION OF REPORT
Unclassified

18. SECURITY CLASSIFICATION OF THIS PAGE
Unclassified

19. SECURITY CLASSIFICATION OF ABSTRACT
Unclassified

20. LIMITATION OF ABSTRACT
Same as Report